

https://dspace.org/

Dewatering of Coal Mine Tailings Using Electrokinetics

Sekwele, Matome Ludwick

2006-11-14T08:07:04Z
http://hdl.handle.net/10539/1661

Downloaded from a DSpace repository. https://dspace.org/

DECLARATION

I declare that this dissertation is my own, unaided work. It is being submitted for the Degree of Master of Science in the University of the Witwatersrand, Johannesburg. It has not been submitted before for any degree or examination in any other University.

_____
(Signature of candidate)

_____day of _____ (year) _____

ABSTRACT

Increasing quantities of finer wastes often contain reactive sulphide minerals and high water contents that pose stability and environmental concerns. This study investigates how electrokinetic process can be improved, to make it more viable towards dewatering finer coal slurries.

In the electrokinetic process, a direct current induces the movement of water out of a porous material. A wooden test box was filled up to two-thirds with fine coal slurries. Electrokinetic Geotextiles (EKGs) and brass were used as electrodes. The conducting wires were attached to each electrode and connected to a DC source to form an electro-osmosis cell. Current was passed through the cell and water moved to the cathode where it was withdrawn.

The dewatering efficiencies ranged from 13.13 to 109.84 ml/Ah. The energy consumptions ranged from 5.23 to 14.03 kWh/m^3 and are in line with those recorded by Johns (2005). Conductivity and pH measurements were taken. EKGs performed better than brass electrodes.

To my loving and supporting family,

Sekweles

ACKNOWLEDGEMENTS

I would like to express my sincere gratitude to my co-supervisors, Professor Geoffrey Blight and Professor Andy Fourie for their assistance, guidance and motivation in my research work. To Mr. Norman Alexander and Mr. William Mainganye of the soils laboratory for their invaluable advice and suggestions. I would like to thank the National Research Foundation (NRF) and Council for Scientific and Industrial Research (CSIR) whose financial support made this research work possible.

CONTENTS

DECLARATION 2
ABSTRACT 3
ACKNOWLEDGEMENTS 5
CONTENTS 6
LIST OF FIGURES 10
LIST OF TABLES 13
LIST OF SYMBOLS 17

1 INTRODUCTION 18

1.1 Overview 18
1.2 Definition and Principles of Electrokinetics 20
1.3 Background to the Research 21
1.4 Problem Statement 22
1.5 Justification 22
1.6 Objectives 22
1.7 Hypothesis 23

2 LITERATURE REVIEW 24

2.1 Conventional Coal Tailings Dewatering Methods 24
2.1.1 Geotextile-Assisted Dewatering 24
2.1.2 The Dorr-Oliver Electroosmotically-Aided Vacuum Filter 25
2.2 Electrochemical Reactions 25
2.3 Water Quality 26
2.4 Dewatering Efficiency and Effectiveness 26
2.5 Power and Energy Consumption 27
2.6 Intermittent and Constant Current 28

3 METHODOLOGY 30

3.1 Electrokinetic Dewatering using EKGs as Electrodes 30
3.2 Electrokinetic Dewatering using Brass Electrodes 31
3.3 Characterization of Materials 31
3.3.1 Specific Gravity and Atterberg Limits 32
3.3.2 Particle Size Analysis 32
3.3.3 Mineralogy 33
3.4 Treatment of the Findings 36

4 RESULTS 37

4.1 Effects of Electrode Type 38

TEST 1 38
4.1.1 Variation in Moisture Content 38
4.1.2 Changes in pH and Conductivity Measurements 40
4.1.3 Variation in Final Moisture Content 40
4.1.4 Energy Consumption and Dewatering Efficiency 40

TEST 2 43
4.1.5 Variation in Moisture Content 43
4.1.6 Changes in pH and Conductivity Measurements 43
4.1.7 Variation in Final Moisture Content 43
4.1.8 Energy Consumption and Dewatering Efficiency 43
4.2 Effect of Initial Water Content 47
4.3 Comparative Plots 47
4.3.1 Comparing the Final Moisture Contents 48
4.3.2 Comparing the Final pH Measurements 49
4.3.3 Comparing the Final Conductivity Measurements 49
4.3.4 Comparing the Power Consumptions 52
4.3.5 Comparing the Energy Consumptions 52

4.3.6 Comparing the Dewatering Efficiencies 52

5 DISCUSSION 54

5.1 Voltage, Current, Initial Water Content and Volume of Water 54
5.2 Variation in Moisture 55
5.3 pH Measurements 55
5.4 Conductivity Measurements 56
5.5 Dewatering Efficiency, Power and Energy Consumption 57
5.6 Observation during Tests 58
5.6.1 Cracks 58
5.6.2 Effects of Electrochemical Reactions 58
5.7 Final Water Contents 60
5.8 Successes and Failures in Attaining Objectives 61
5.9 Costs and Efficiency 64

6 EXTENDING ELECTROKINETIC DEWATERING TO FULL-SCALE APPLICATIONS 65

6.1 Introduction 65
6.2 Tentative Guidelines 65
6.2.1 Vertical versus Horizontal Electrodes 66
6.2.2 Machine versus Tailings Pond 66
6.3 Containment of Tailings 70

7 CONCLUSION AND RECOMMENDATIONS 71

7.1 Summary 71
7.2 Conclusions 72
7.3 Recommendations for Further Research 73

APPENDIX A CHARACTERIZATION OF MATERIALS: DETAILED RESULTS 74
APPENDIX B MINERALOGICAL INVESTIGATIONS: RESULTS AND EQUIPMENT SETTINGS 83
APPENDIX C EXPERIMENTAL RESULTS: EFFECT OF DIFFERENCE IN INITIAL WATER CONTENT 91
APPENDIX D CUMULATIVE WATER, CONDUCTIVITY, pH, MOISTURE CONTENT DATA 122

8 REFERENCES 147

LIST OF FIGURES

Figure 3.1 Particle Grading Analysis 33
Figure 4.1 Cumulative Water vs. Time 39
Figure 4.2 Variation of Moisture Content with Time 39
Figure 4.3 pH vs. Time 41
Figure 4.4 Conductivity versus Time 41
Figure 4.5 Variation in Moisture Content from Anode to Cathode 42
Figure 4.6 Power versus Time 42
Figure 4.7 Cumulative Water versus Time 44
Figure 4.8 Variation of Moisture Content versus Time 44
Figure 4.9 pH versus Time 45
Figure 4.10 Conductivity versus Time 45
Figure 4.11 Variation in Moisture Content from Anode to Cathode 46
Figure 4.12 Power versus Time 46
Figure 4.13 Comparing the Initial and Final Moisture Contents 49
Figure 4.14 Initial Water Content versus Final Water Content After 100h 50
Figure 4.15 Comparing the Initial and Final pH 51
Figure 4.16 Comparing the Initial and Final Conductivity 51
Figure 4.17 Comparing the Power Consumptions 52
Figure 4.18 Comparing Energy Consumptions for Equivalent 100h Tests 53
Figure 4.19 Comparing Dewatering Efficiencies for Equivalent 100h Tests 53
Figure C1 Cumulative Water versus Time 92
Figure C2 Variation in Moisture Content versus Time 92
Figure C3 pH versus Time 93
Figure C4 Conductivity versus Time 93
Figure C5 Variation in Final moisture content from Anode to Cathode 94
Figure C6 Power versus Time 94
Figure C7 Cumulative Water versus Time 95
Figure C8 Variation in Moisture Content versus Time 95
Figure C9 pH versus Time 96

Figure C10 Conductivity versus Time 96
Figure C11 Variation in final Moisture Content from Anode to Cathode 97
Figure C12 Power versus Time 97
Figure C13 Cumulative Water versus Time 98
Figure C14 Variation of Moisture Content versus Time 98
Figure C15 pH versus Time 99
Figure C16 Conductivity versus Time 99
Figure C17 Variation in Final Moisture Content from Anode to Cathode 100
Figure C18 Power versus Time 100
Figure C19 Cumulative Water vs. Time 101
Figure C20 Variation of Moisture Content with Time 101
Figure C21 pH vs. Time 102
Figure C22 Conductivity vs. Time 102
Figure C23 Variation in Moisture Content from Anode to Cathode 103
Figure C24 Power versus Time 103
Figure C25 Cumulative Water vs. Time 104
Figure C26 Variation of Moisture Content with Time 104
Figure C27 pH vs. Time 105
Figure C28 Conductivity vs. Time 105
Figure C29 Variation in Moisture Content from Anode to Cathode 106
Figure C30 Power versus Time 106
Figure C31 Cumulative Water vs. Time 107
Figure C32 Variation of Moisture Content with Time 107
Figure C33 pH vs. Time 108
Figure C34 Conductivity vs. Time 108
Figure C35 Variation in Moisture Content from Anode to Cathode 109
Figure C36 Power versus Time 109
Figure C37 Cumulative Water vs. Time 110
Figure C38 Variation of Moisture Content with Time 110
Figure C39 Conductivity vs. Time 111
Figure C40 Conductivity vs. Time 111
Figure C41 Variation in Moisture Content from Anode to Cathode 112

Figure C42 Power versus Time 112
Figure C43 Cumulative Water versus Time 113
Figure C44 Variation in Moisture Content versus Time 113
Figure C45 pH versus Time 114
Figure C46 Conductivity versus Time 114
Figure C47 Variation in Final moisture content from Anode to Cathode 115
Figure C48 Power versus Time 115
Figure C49 Cumulative Water versus Time 116
Figure C50 Variation in Moisture Content versus Time 116
Figure C51 pH versus Time 117
Figure C52 Conductivity versus Time 117
Figure C53 Variation in Final moisture content from Anode to Cathode 118
Figure C54 Power versus Time 118
Figure C55 Cumulative Water versus Time 119
Figure C56 Variation in Moisture Content versus Time 119
Figure C57 pH versus Time 120
Figure C58 Conductivity versus Time 120
Figure C59 Variation in Final moisture content from Anode to Cathode 121
Figure C60 Power versus Time 121

LIST OF TABLES

Table 3.1 Specific Gravity and Atterberg Limits 32
Table 3.2 Mineralogy for Delkor 1 34
Table 3.3 Mineralogy for Delkor 2 34
Table 3.4 Mineralogy for GG1 Delkor 35
Table 3.5 Mineralogy for GG2 Delkor 35
Table 3.6 Mineralogy for GG1 Thickener Underflow 36
Table 4.1 Summaries of Entire Test Series 38
Table 4.2 Summary of Test Series for Comparative Plots 48
Table 5.1 Voltage, Current, Initial Water Content and Extracted Water 54
Table 5.2 pH Measurements 55
Table 5.3 Conductivity Measurements 56
Table 5.4 Dewatering Efficiency, Power and Energy Consumptions 57
Table A1 Liquid limit 75
Table A2 Plastic limit 75
Table A3 Specific Gravity 75
Table A4 Particle Size Distribution 76
Table A5 Liquid limit 76
Table A6 Plastic Limit 77
Table A7 Specific Gravity 77
Table A8 Particle Size Distribution 78
Table A9 Liquid limit 78
Table A10 Plastic limit 78
Table A11 Specific Gravity 79
Table A12 Particle Size Distribution 79
Table A13 Liquid limit 80
Table A14 Plastic limit 80
Table A15 Specific Gravity 80
Table A16 Particle Size Distribution 81
Table A17 Liquid limit 81

Table A18 Plastic limit 81
Table A19 Specific Gravity 82
Table A20 Particle Size Distribution 82
Table B1 Quantification of Sample GG 1 DELKOR 85
Table B2 Quantification of Sample GG 1 Thickener Underflow 86
Table B3 Quantification of Sample GG2 Delkor 87
Table B4 Quantification of Sample Delkor 1 89
Table B5 Quantification of Sample Delkor 2 90
Table D1 Initial Water Content 123
Table D2 Amount of Water Removed from Sample 123
Table D3 Variation in Moisture Content 124
Table D4 Changes in pH and Conductivity Measurements during Test 124
Table D5 Variation in Final Moisture Content 124
Table D6 Initial Water Content 125
Table D7 Amount of Water Removed from Sample 125
Table D8 Variation in Moisture Content 125
Table D9 Changes in pH and Conductivity Measurements during Test 126
Table D10 Variation in Final Moisture Content 126
Table D11 Initial Water Content 127
Table D12 Amount Of water Removed from Sample 127
Table D13 Variation in Moisture Content 127
Table D14 Changes in pH and Conductivity Measurements during Test 127
Table D15 Variation in Final Moisture Content 128
Table D16 Initial Water Content 129
Table D17 Amount Of Water Removed from Sample 129
Table D18 Variation in Moisture Content 129
Table D19 Changes in pH and Conductivity Measurements during Test 129
Table D20 Variation in Final Moisture Content 130
Table D21 Initial Water Content 131
Table D22 Amount of Water Removed from Sample 131
Table D23 Variation in Moisture Content 131
Table D24 Changes in pH and Conductivity Measurements during Test 132

Table D25 Variation in Final Moisture Content 132
Table D26 Initial Water Content 133
Table D27 Amount of Water Removed from Sample 133
Table D28 Variation in Moisture Content 133
Table D29 Changes in pH and Conductivity Measurements during Test 134
Table D30 Variation in Final Moisture Content 134
Table D31 Initial Water Content 135
Table D32 Amount of Water Removed from Sample 135
Table D33 Variation in Moisture Content 135
Table D34 Changes in pH and Conductivity Measurements during Test 136
Table D35 Variation in Final Moisture Content 136
Table D36 Initial Water Content 137
Table D37 Amount of Water Removed from Sample 137
Table D38 Variation in Moisture Content 137
Table D39 Changes in pH and Conductivity Measurements during Test 138
Table D40 Variation in Final Moisture Content 138
Table D41 Initial Water Content 139
Table D42 Amount of Water Removed from Sample 139
Table D43 Variation in Moisture Content 139
Table D44 Changes in pH and Conductivity Measurements during Test 140
Table D45 Variation in Final Moisture Content 140
Table D46 Initial Water Content 141
Table D47 Amount of Water Removed from Sample 141
Table D48 Variation in Moisture Content 141
Table D49 Changes in pH and Conductivity Measurements during Test 142
Table D50 Variation in Final Moisture Content 142
Table D51 Initial Water Content 143
Table D52 Amount of Water Removed from Sample 143
Table D53 Variation in Moisture Content 143
Table D54 Changes in pH and Conductivity Measurements during Test 144
Table D55 Variation in Final Moisture Content 144
Table D56 Initial Water Content 145

Table D57 Amount of Water Removed from Sample 145
Table D58 Variation in Moisture Content 145
Table D59 Changes in pH and Conductivity Measurements during Test 146
Table D60 Variation in Final Moisture Content 146

LIST OF SYMBOLS

Dewatering Efficiency (DE)..…….η

Electro-osmotic Permeability……K_e

Total Amount of Water Removed……...Q

Current……...….. I

Voltage……V

Time…….t

Volume of Solids (Tailings)……...V_s

Power Consumption……P

Energy Consumption per Unit Volume of Dry Tailings (EC)...……E_u

Specific Gravity…….G_s

Plastic Limit……..PL

Liquid Limit……..LL

Plastic Index……..PI

Linear Shrinkage……L_s

Water Content……...Wc

Initial Water Content……Wc_i

Final Water Content…….Wc_f

Initial pH……...pH_i

Final pH……pH_f

Initial Conductivity……..Cond.$_i$

Final Conductivity……...Cond.$_f$

Wavelength Alpha ……..Å

Brass Electrodes……..B

Electrokinetic Geotextiles Electrodes……..EKGs

1 INTRODUCTION

1.1 Overview

The mining and processing of raw materials from the ground are the basic building blocks from which all technological advancements and products that we use in our everyday life are made. The quality of our life, our national security, the stability of domestic and world economies, science, industry, and the arts are all based on the minerals we mine from the earth. South Africa's history is intimately related to mining.

The mining method used to extract a specific commodity depends chiefly on the form and location of the deposit. The mineral may be mined by surface or underground mining methods. In many instances, the deposit is relatively flat and continuous over a large area. Examples of flat, or tabular, deposits are coal, potash, salt, and oil shale. These deposits are found in beds, or seams, between layers of rock. The material above the seam is called the overburden (Mineral Policy Institute, 2004).

Mining uses one of a variety of methods to extract these deposits either from the surface or underground. Open-pit (open-cut) mining, strip mining and quarrying are surface mining methods. Underground mining methods include sublevel stoping, block caving, sublevel caving, cut-and-fill mining, borehole mining etc. The method used depends on the geometry, size, and location of the deposit (Mineral Policy Institute, 2004).

Some of the minerals produced, such as coal and salt, are ready to use right after they have been mined. It may be necessary to wash or treat these commodities in different ways to enhance their quality, but their properties remain essentially unchanged.

Metals, on the other hand, usually occur in nature as ores, i.e., combined in complex proportions with other materials. This means that they must be treated physically or with chemicals or heat, to separate the desired metal from its host material. These processing techniques can be very complex and expensive, but they are necessary to recover the metal of interest (Mineral Policy Institute, 2004).

During the operation of a mine, large amounts of tailings are produced which can cause significant environmental impacts. Safe disposal of mine waste, including tailings, is generally recognized as the single largest environmental challenge facing the mining industry worldwide and a major expense for mining companies. The fine waste or tailings pose the greatest structural problem in the disposal process; they have inherently adverse geotechnical properties such as high moisture content, low hydraulic conductivity, low shear strength and poor particle sizing (Mineral Policy Institute, 2004). Mine waste may also pose an environmental threat not only through its volume but sometimes because of its toxicity. The storage of this waste poses significant engineering challenges.

Mine tailings may contain sulfides as well as remaining traces of, for example, cadmium, copper, iron, lead, manganese, mercury, silver, and zinc—that are the reason for mining the ore body. When sulfides in tailings are exposed to air they oxidize and environmentally toxic sulfuric acid is produced. This acid is known as Acid Mine Drainage (AMD). The sulfuric acid also accelerates metal leaching from tailings. AMD can have an adverse impact on ground and surface water around mines. According to the United States Environmental Protection Agency, water contamination from mining poses one of the top three ecological security threats in the world (Mineral Policy Institute, 2004).

Fine tailings produced during mineral processing are relatively difficult to dewater because of the fineness of the particles and hence the interparticle pores. Electrokinetics, being a surface process is relatively insensitive to pore size and is therefore an attractive process for dewatering fine tailings.

Electrokinetic dewatering is by no means a new technology; but has been widely regarded as uneconomic for industrial solid-liquid separations. The practical applications of electro-osmotic dewatering have mostly occurred where other methods were inadequate and/or dewatering costs were a secondary concern, such as in civil engineering construction and the ceramics industry.

This study focuses on applying electrokinetics principles to the dewatering of coal tailings. The study hopes to find measures to improve on the dewatering efficiencies and power consumptions and has two distinct objectives: the physical stabilization and attaining the required mechanical strength of coal tailings for stability and safety.

Results of tests conducted by Yuan, *et al*., (2003) showed that increasing either the potential gradient or the processing time would enhance the tailings dewatering efficiency.

Electrokinetics is an energy intensive process. Cost and efficiency will vary with the treated material, extent of desired dewatering, rate of power application, etc.

1.2 Definition and Principles of Electrokinetics

Electrokinetics uses direct current to induce the movement of tailings suspended in water and further induces the movement of water out of the tailings structure. The two stages are known as sedimentation / electrophoresis and consolidation / electro-osmosis respectively. When pairs of electrodes are installed after sedimentation of the solid particles and electric current is made to flow from one to the other, the soil water migrates from the positive electrode (anode) toward the negative one (cathode) and the water that seeps into it can be removed. This phenomenon is known as electro-osmosis. The long consolidation process after sedimentation is a major challenge in many engineering problems (McVay, *et al.*, 1987; Huerta, *et al*., 1988; Al-Hussaini and Ahmad, 1996) and is the main focus of this research work.

1.3 Background to the Research

Research on electrokinetic dewatering started in the 1960's when the United States Bureau of Mines (USBM) pioneered the research and development of electrokinetic dewatering of wastes derived from mineral processing and coal processing.

Electro-osmotic dewatering of various slimes and sludges has occasionally been reported, particularly for sewage sludge [Sunderland and Dellis, (1976, 1977)], but no industrial applications seem to have developed until the U.S. Bureau of Mines dewatered siliceous tailings that were dumped in mined-out areas of underground metal-ore mines. The Bureau of Mines subsequently applied the technique to coal wastes.

The Australian Commonwealth Scientific and Research Organization (CSIRO) began their research on electrokinetic dewatering of tailings in the late 1970s (Lockhart, 1986). More than 60 tailings from coal preparation plants, sand-washing plants, mineral processing, and water purification plants were tested. Sprute and Kelsh (1975, 1980) reported several successful field applications.

The CSIRO has also been involved in experimental studies on electro-osmotic dewatering. The work at CSIRO involved small- and large-scale laboratory tests, comprising evaluation of electro-osmotic dewatering under standard experimental conditions for a wide variety of fine suspensions from mineral processing, together with optimization of the experimental conditions of electro-osmosis using a limited number of samples, including pure clays [Lockhart (1981, 1982, 1983)]. Following successful trials of electro-osmotic dewatering in coal washery tailings ponds, both CSIRO and the Bureau of Mines are working towards commercial demonstrations.

1.4 Problem Statement

In mining, either during extraction or processing stages, large quantities of wastes are produced. Stringent environmental regulations and legislation are always placed on mining activities with the aim of protecting the natural environment from pollution and eventual degradation.

Water contained in these tailings also poses stability concerns that could have disastrous consequences if not controlled. The mining industry is often required to manage these problems by developing new geo-technologies. For this reason, mining has sometimes been described as a waste management business.

1.5 Justification

Suspensions of fine particles that are produced, for example, in mineral processing or coal preparation, settle slowly to a high water content sediment that is difficult to dewater and consolidate because of the fineness of the pores. Electro-osmotic flow, being a surface process, is relatively insensitive to pore size and is therefore attractive in principle for dewatering suspensions of fine particles (Lockhart and Stickland, 1984).

Stability and pollution potentials of tailings may be governed in part by drainage and control of the water. The removal (and often the recovery) of aqueous phase from the tailings can be a very important and economic aspect in most mines and it becomes very important to utilize the most economic and optimum method for dewatering.

1.6 Objectives

The main objective of the study is to compare the electrokinetic dewatering efficiencies using electrokinetic geotextiles (EKGs) and brass electrodes starting at different water contents.

The specific objectives of this experimental study are as follows:

- To compare electrokinetic dewatering efficiencies of EKGs and brass electrodes.
- To investigate the effect of differences in initial water content in electrokinetic dewatering tests involving both EKGs and Brass electrodes.
- To find ways of improving/increasing the dewatering efficiency and effectiveness.
- To provide useful guidelines that can be used when extending the electrokinetic dewatering technology to full-scale applications.

1.7 Hypothesis

The effectiveness and efficiency of electrokinetic dewatering can be increased/improved by applying various techniques such as increasing processing time, reducing sample volume, and simple/inexpensive procedures such as gravitational sedimentation and drainage.

2 LITERATURE REVIEW

2.1 Conventional Coal Tailings Dewatering Methods

In this part, characteristics of existing and previously used dewatering techniques are described.

2.1.1 Geotextile-Assisted Dewatering

Geotextiles are used in the civil engineering industry for a wide range of applications. For example, in various stages of a modern road construction; reinforcement is provided by geogrids in the foundations of structures; filtration geofabrics are used in the drainage systems; geomembranes may be used to facilitate vegetation growth. The myriads of products continue to increase, driven by low cost, environmental benefits and construction speed.

The use of geotextile tubes and bags started in earnest during the 1970s and was primarily used for structural purposes, mainly associated with coastal engineering projects. Dredged sand was pumped at high rates into high-strength polyester or polypropylene tubes where the sand was retained and the water quickly drained. The resulting tube was then used as part of a structure, either for dam/breakwater development or beach improvements. Since experimentation in the USA, Brazil, Holland and Germany throughout the 1980s, the techniques have been successfully applied worldwide in a number of instances for dewatering, drainage, runoff protection, erosion and scour protection and the containment of contaminated materials (Fowler *et al.*, 1997).

In the UK, geotextile-assisted dewatering has been applied to a wide variety of troublesome slurries with varying degrees of success. The minimal capital investment required to implement a solution is attractive and the possible re-sale of the dewatered product has the potential to turn the waste stream into a revenue stream (Newman, 2003).

This technology is just beginning and the high unit costs associated with it are expected to fall as the method gains acceptance and experience with the use of flocculants and pumping rates improves (Newman *et al.*, 2003).

2.1.2 The Dorr-Oliver Electroosmotically-Aided Vacuum Filter

The Dorr-Oliver Electroosmotically-Aided Vacuum Filter is operating commercially on kaolin clay slurries, but no details of the claimed applications to other mineral slurries seem to be available. It is not known whether this machine can be adapted for tailings dewatering [Adams *et al.*, (1983) and Freeman (1982)].

2.2 Electrochemical Reactions

Electrochemical reactions associated with an electrokinetic process have been identified and summarized as follows. At the anode:

[1] $H_2O \rightarrow O_2\uparrow + H^+$

[2] $M_a \rightarrow M_a^{n+} + ne^-$

where M_a is the anode metal. Equation [1] states that the anode hydrolysis generates oxygen and reduces the solution pH. As a result, a metallic anode will corrode, as shown in [2]. At the cathode:

[3] $H_2O \rightarrow H_2\uparrow + OH^-$

[4] $M_i^{n+} + ne^- \rightarrow M_i\downarrow$

[5] $M_i^{n+} + OH^- \rightarrow M_i(OH)_n\downarrow$

where M_i^{n+} is the dissolved cation species i in solution.

The solution pH will increase rapidly at the cathode and hydrogen will be generated, as shown in [3]. Cations are driven to the cathode by the electric gradient, reducing to element metals, as shown in [4], and (or) more likely forming hydroxides, as shown in [5] (Shang 1996). Most hydroxides are insoluble at pH > 5 with only several exceptions, such as KOH and NaOH (Lindsay, 1979). Shang (1996) states that a pH gradient will be generated across the soil as an overall result of the electrode reactions.

2.3 Water Quality

In an experimental study conducted by Lockhart and Stickland (1984) on dewatering coal washery tailings ponds by electro-osmosis, sodium was by far the dominant cation present in samples of water brought to the surface and of the pore water in the tailings near the surface prior to the power being applied. The sodium increased from 24 to 47 mmol after the power had been on for several days. The concentrations of other cations (K, Ca, Mg, Al) were in the range 0.12 – 0.6 mmol, and electro-osmosis produced only a slight increase (K, Al) or a decrease (Ca, Mg). The common heavy metal cations (Cu, Mn, Zn, Pb, Cd, Ni) were present at lower concentrations in the range < 0.1 to 2 μmol, and none of these increased with electro-osmosis. Iron increased from ~0.04 to 0.08 mmol, presumably as a result of dissolution of the anode material.

Lockhart and Stickland (1984) further found that the concentrations of anions before and after electro-osmosis were as follows: hydroxides 0/2.0 mmol, carbonate 0.15/19 mmol, bicarbonate 8/0 mmol, chlorite 11/4 mmol, sulphate 2.5/1.2 mmol, nitrate 0.92/0.02 mmol. The increased salinity and alkalinity in the water is accompanied by de-salting of the bulk of the sample.

2.4 Dewatering Efficiency and Effectiveness

The dewatering efficiency is a measure of how water is being dewatered under certain electrokinetic conditions over a particular time.

The equation is as follows:

$\eta = Q/It$ (in ml/Ah),

where η represents the dewatering efficiency, Q for total amount of water removed, I for current and t for operational time.

The effectiveness of electrokinetic dewatering is governed by the electro-osmotic permeability K_e (Mitchell, 1993).

In a large field test undertaken by Lockhart and Stickland (1984) it was not possible to measure water from the base of pond, and the water collecting at the surface of the pond could not easily be adjusted to the contributions from sedimentation, natural drainage, rainfall and evaporation. However, the approximate electro-osmotic dewatering rate was measured during the siphoning operations and it corresponded to 400 ml/Ah. This value decreased as the tailings approached the spadeable state and as they continued to dewater.

Comparative data from laboratory tests suggest that the above dewatering efficiencies would be typical for many coal washery tailings. Some coal tailings, sand washing slimes and other samples have been found to give order of magnitude higher values (4 000 ml/Ah), at least in the initial stages of dewatering. This does not necessarily mean lower power consumption (watt hours) for a given degree of dewatering, since the voltage necessary may be higher, but it does not greatly reduce ampere hours and consequently much lower consumption of anode metal (Lockhart and Stickland, 1984).

2.5 Power and Energy Consumption

Energy is transformed to dewater a particular volume of solids. Power consumption is a critical factor for the viability of electrokinetic dewatering of materials.

The power consumption can be calculated from the following equation:

$$P = VI$$

where P is the power consumption (W); V, the voltage (V) and I, the current (A).

The energy consumption can be calculated based on the equation below:

$$E_u = P/V_s = (\int VI\, dt) / V_s$$

where E_u is the energy consumption per unit volume of dry tailings (kWh/m^3); V, the voltage (V); I, the current (A); V_s, the volume of the tailings (m^3) and t, processing time (h).

In the constant-voltage tests, the energy consumption was directly related to the processing time. Higher energy consumption would result in higher water removal efficiency. The same phenomenon was also found for the case of constant-processing time: the higher the potential gradient, the more the power consumption (Yuan *et al.*, 2002).

2.6 Intermittent and Constant Current

A continuous DC electric field has been generally used for fundamental study and practical application of electro-osmotic dewatering. Under DC conditions, however, the electrical contact resistance between the electrode and the dewatered material is excessively increased in the dewatering process, resulting in interruption of the dewatering process.

For efficient performance of electroosmotic dewatering, intermittent power application has been used to reduce excessive increase of the electrical contact resistance with the lapse of time. Rectifying an AC electric field made an intermittent electric field, and it was constituted of half waves. Both rectangular and sine waves were used as the waveform of an AC electric field. Electro-

osmotic dewatering under the rectified half-wave intermittent electric field was investigated experimentally, under both conditions of the same peak-value voltage and the same effective-value voltage as the voltage applied under DC and AC electric fields.

Intermittent power application is suggested to reduce the increase of the electrical contact resistance with time caused by the DC process. In the case of intermittent power application having the same effective voltage as DC and AC, the rate and the amount of removed water were increased compared with DC and AC fields, and the efficiency of electric power consumption for the amount of removed water was much higher (Yoshida, 2000).

3 METHODOLOGY

The experimental study was undertaken using EKGs and brass as electrodes.

3.1 Electrokinetic Dewatering using EKGs as Electrodes

The test facility consisted of a wooden test box, control box and electrokinetic geosynthetics (EKGs) as electrodes. A wooden box is used because of its non-conductivity. The test box measured 300 mm in length, 220 mm in width and 180 mm in depth, which could accommodate 0.011 880 m^3 of sample. The joints were waterproofed.

The cylindrical geosynthetic electrodes were about 200 mm in height and 50 mm in diameter. One of these was used as the anode or cathode respectively. They were rolled to form cylinders and tied in this position using a strong plastic thread. A conducting wire was installed around one end of each electrode. The conducting wire was covered with silicone sealant to prevent corrosion.

A green-coded wire was joined to one electrode and a black-coded wire joined to the other to be used as anode and cathode respectively. The free ends of the wires were connected to a DC source to form an electro-osmosis cell. The cathode was covered with a tube of geosynthetic fabric to allow water to pass, but to exclude solids. Only the part of the conducting wire around the rim of the electrode and colour-coded wire was left uncovered. Other details of the test apparatus were as follows:

- One wooden box was used as test apparatus and a plastic box as a control. All the boxes were two-thirds filled with wet coal slurry. Details of the coal slurries are given in Appendix A. The initial water content was determined before the start of each test.
- The cathode was placed inside the test box before any slurry was poured in. It was placed at least 20 mm away from the edge of the box. After the

2/3 of the slurry had been poured in, the anode was placed directly opposite the cathode at least 20 mm away from the edge of the wooden box. With this arrangement, the electrodes were about 180 mm apart as measured from their centres.

- The programme of electrical current, voltage, treatment times and reversals of the polarity were then applied.
- Suitable time intervals to measure volume of water extracted, pH, conductivity, etc. were chosen.

The essential information gathered before the commencement of the test was the mass of the test box, mass of electrodes, mass of test box + wired electrodes + wet sample, initial pH and conductivity measurements and the starting time, volts and current readings.

3.2 Electrokinetic Dewatering using Brass Electrodes

The two pieces of brass tubing used as electrodes were 253 mm in height and the inside and outside diameters were measured 25 mm and 32 mm respectively. One of these was used as the anode or cathode respectively. The cathode had small holes drilled into and was covered with a geosynthetic filter tube that allowed only water to move into it where it could be collected and withdrawn. The rest of the details are similar to those described in section 3.1.

The important information to gather before the commencement of the test is the mass of the test box, mass of electrodes, mass of test box + wired electrodes + wet sample, initial pH and conductivity measurements and to note the starting times, volts and current reading to observe how they change throughout the experimental study.

3.3 Characterization of Materials

Results of materials characterization tests have been summarized in this section. Detailed results are given in Appendices A and B.

3.3.1 Specific Gravity and Atterberg Limits

The specific gravity of a material is a comparison of its density to that of water. It is a unit-less measure. Specific gravity and Atterberg limit tests were undertaken for the different coal slurries using standard ASTM procedures. Detailed information is documented in Appendix A. However, the materials produced the following results:

Table 3.1 Specific Gravity and Atterberg Limits

Sample Identification	**LL (%)**	**PL (%)**	**PI**	**L_s (%)**	**(G_s)**
Delkor 1	28.9	22.5	6	2.5	1.75
Delkor 2	28.2	22.2	6	2.3	1.68
GG1 Delkor	30.9	22.3	9	2.5	1.70
GG2 Delkor	28.8	22.4	6	2.2	1.58
GG1Thickener underflow	29.5	22.4	7	2.1	1.59

(LL = Liquid limit, PL = Plastic Limit, PI = Plastic Index, L_s = Linear Shrinkage G_s = Specific Gravity)

3.3.2 Particle Size Analysis

The particle size analysis determines the relative proportions of the different particle sizes of a sample representative of a given material. Particle size analysis was undertaken for Delkor 1, Delkor 2, GG1 Delkor, GG2 Delkor and GG1 Thickener Underflow. Particle size analysis was carried out in accordance with ASTM procedures. Detailed information on the relative proportions of the different particle sizes of samples is included in Appendix A. The results for the five different coal slurries are given below:

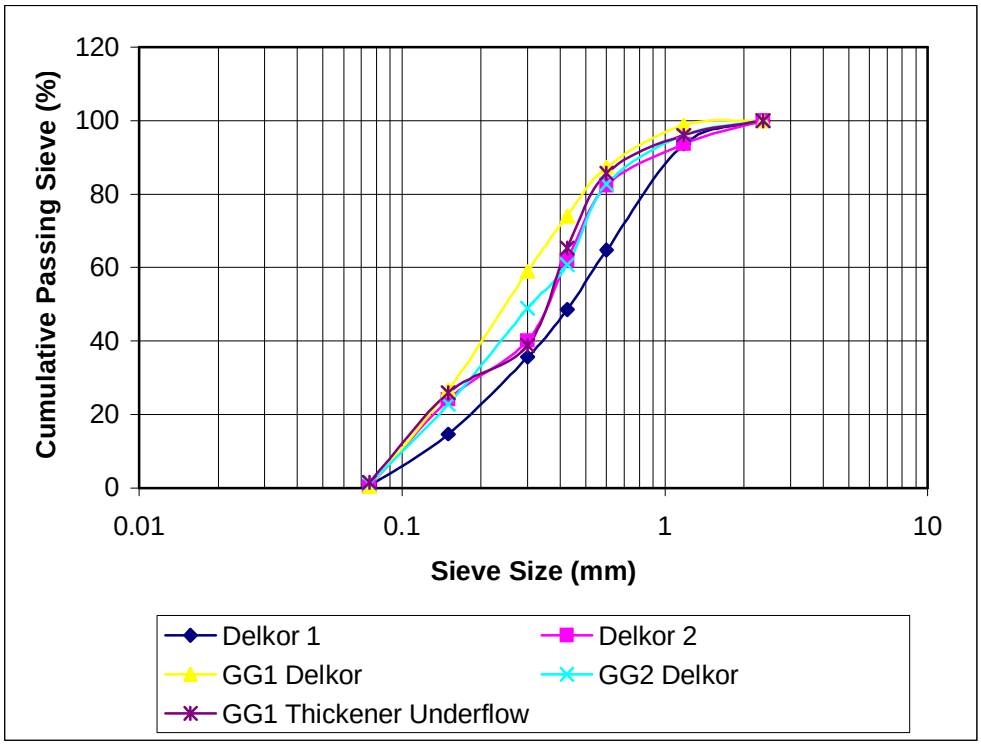


Figure 3.1 Particle Grading Analysis

3.3.3 Mineralogy

The chemical and mineralogical composition can be considered fundamental in understanding geotechnical properties of tailings (Gawu, 2003).

The methodology and equipment settings and calibrations for determining the mineralogical characteristics of the coal samples have been explained extensively in Appendix B. The mineralogical investigations have produced the following results:

Table 3.2 Mineralogy for Delkor 1

Analyte	**Compound Formula**	**Concentration (%)**
Na	Na_2O	0.178
Mg	MgO	1.416
Al	Al_2O_3	23.759
Si	SiO_2	53.163
P	P_2O_5	0.896
K	K_2O	1.333
Ca	CaO	6.314
Ti	TiO_2	2.059
Fe	Fe_2O_3	6.288
S	S	4.213
Sr	Sr	0.065
Zr	Zr	0.078
Ba	Ba	0.237
TOTAL (%)		**99.999**

Table 3.3 Mineralogy for Delkor 2

Analyte	**Compound Formula**	**Concentration (%)**
Mg	MgO	1.190
Al	Al_2O_3	22.467
Si	SiO_2	50.487
P	P_2O_5	0.281
K	K_2O	1.436
Ca	CaO	8.340
Ti	TiO_2	2.241
Fe	Fe_2O_3	6.579
S	S	6.820
Sr	Sr	0.071
Zr	Zr	0.089
TOTAL (%)		**100.000**

Table 3.4 Mineralogy for GG1 Delkor

Analyte	Compound Formula	Concentration (%)
Na	Na_2O	0.203
Mg	MgO	1.235
Al	Al_2O_3	21.922
Si	SiO_2	48.331
P	P_2O_5	1.065
K	K_2O	1.261
Ca	CaO	9.228
Ti	TiO_2	2.769
Fe	Fe_2O_3	5.828
S	S	7.650
Sr	Sr	0.096
Zr	Zr	0.110
Ba	Ba	0.301
TOTAL (%)		**99.999**

Table 3.5 Mineralogy for GG2 Delkor

Analyte	Compound Formula	Concentration (%)
Mg	MgO	1.069
Al	Al_2O_3	21.687
Si	SiO_2	51.810
P	P_2O_5	0.312
K	K_2O	1.612
Ca	CaO	7.074
Ti	TiO_2	2.036
Fe	Fe_2O_3	8.046
S	S	5.924
Sr	Sr	0.081
Zr	Zr	0.090
Ba	Ba	0.260
TOTAL (%)		**100.000**

Table 3.6 Mineralogy for GG1 Thickener Underflow

Analyte	**Compound Formula**	**Concentration (%)**
Mg	MgO	1.347
Al	Al_2O_3	19.617
Si	SiO_2	52.253
P	P_2O_5	0.093
K	K_2O	1.560
Ca	CaO	5.396
Ti	TiO_2	1.828
Fe	Fe_2O_3	12.393
S	S	5.233
Sr	Sr	0.045
Zr	Zr	0.089
Mn	MnO	0.147
TOTAL (%)		**100.000**

3.4 Treatment of the Findings

The results of each test would be grouped together and reported into developed categories. Tables, bar charts and scatter and area diagrams would be used for graphic representation of the data. The bar charts would be used to compare values across categories and the XY Scatter will show data points connected by smooth lines. Some of the results would require area charts to display the trend of values over time. All these graphic representations would be correctly labelled and each briefly explained and referred to in the text. Some of the findings will be reported using the quantitative approach.

Comparative plots would be used to provide easy visual comparison of the parameters measured in the test series.

4 RESULTS

Large proportions of finer particles are being produced during mineral processing. The conventional dewatering methods are less effective with these finer tailings because of the fineness of the pores. The large water contents often associated with finer tailings may cause serious safety and environmental problems.

The results are from tests undertaken using electrokinetic dewatering. Section 4.1 investigates the effect of electrode type on the electrokinetic dewatering process. Test 1 involved brass electrodes while Test 2 involved EKGs as electrodes. Both tests started with the same initial water content and used the same coal tailings material. Section 4.2 investigates the effect of increasing initial water content on the dewatering process. These tests have been taken as typical and are discussed in detail. The results of the remaining tests have been summarized in Table 4.1 and detailed results are recorded in Appendix C and Appendix D.

Descriptions of materials and methods applied are also summarized in Table 4.1. Detailed descriptions are included in Chapter 3, Methodology. The aspects to be covered include comparing variations in moisture contents, final moisture contents, pH, conductivity, dewatering efficiency and energy consumptions between EKG and brass electrodes.

4.1 Effects of Electrode Type

Table 4.1 Summaries of Entire Test Series

Test No.:	Material Type	V_i	pH_i	Cond.$_i$ mS/cm	Wc_i (%)	LL (%)	PL (%)	G_s
1	Delkor 1 (B)	10	12.01	7.54	57.25	28.90	22.50	1.75
2	Delkor 1 (E)	10	12.01	7.55	57.25	28.90	22.50	1.75
3	GG1 Delk (B)	10	12.55	7.59	41.50	30.93	22.26	1.70
4	GG1 Delk (B)	10	12.47	5.55	47.26	28.80	22.40	1.58
5	GG1 T u/f (B)	10	8.00	7.11	53.33	25.20	20.10	1.80
6	GG1 T u/f (B)	10	8.30	7.18	60.26	25.20	20.10	1.80
7	GG1 T u/f (B)	10	8.24	7.19	63.05	25.20	20.10	1.80
8	GG1 T u/f (E)	10	8.25	7.19	42.94	25.20	20.10	1.80
9	GG1 T u/f (E)	10	8.31	7.18	43.24	25.20	20.10	1.80
10	Delkor 2 (E)	10	12.21	7.38	55.60	28.24	22.15	1.68
11	Delkor 2 (E)	10	12.35	7.50	61.47	28.24	22.15	1.68
12	Delkor 1 (E)	10	12.40	7.66	64.91	28.90	22.50	1.75

(B = Brass, E = EKGs, V_i = initial voltage, Wc_i = initial water content, pH_i = initial pH, Cond.$_i$ = initial conductivity, LL = Liquid Limit, PL = Plastic Limit, Gs = Specific Gravity)

TEST 1

4.1.1 Variation in Moisture Content

Water drawn at the cathode at specific times was measured. Detailed information is referred to in Appendix D. Also in the appendices, is a table showing how the water content of the sample varied as a result of the dewatering effect. Figure 4.1 was plotted to show the cumulative water removed at the cathode over time. Figure 4.2 gives a visualization of how the water content varied with time.

The dotted lines on both figures indicate that the data may not be perfectly reliable.

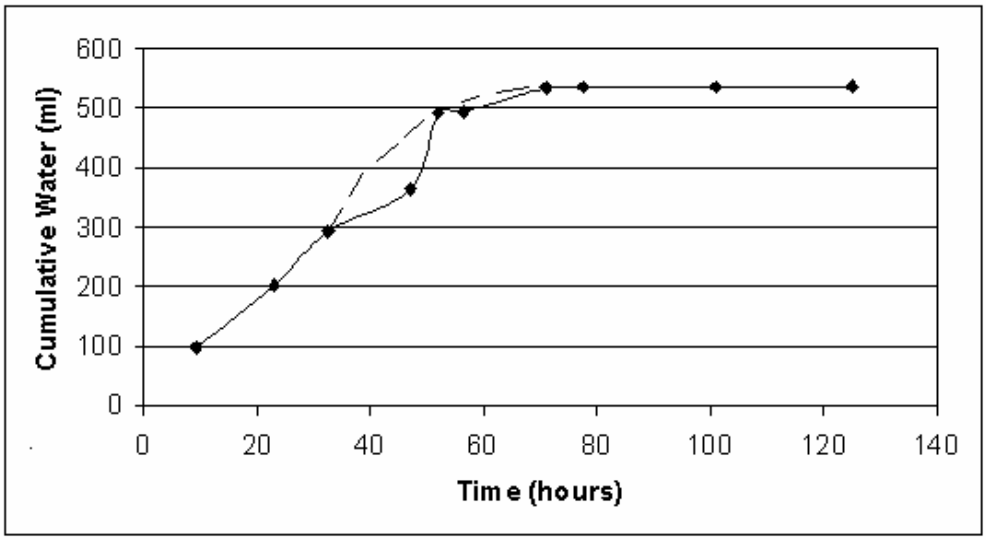


Figure 4.1 Cumulative Water vs. Time

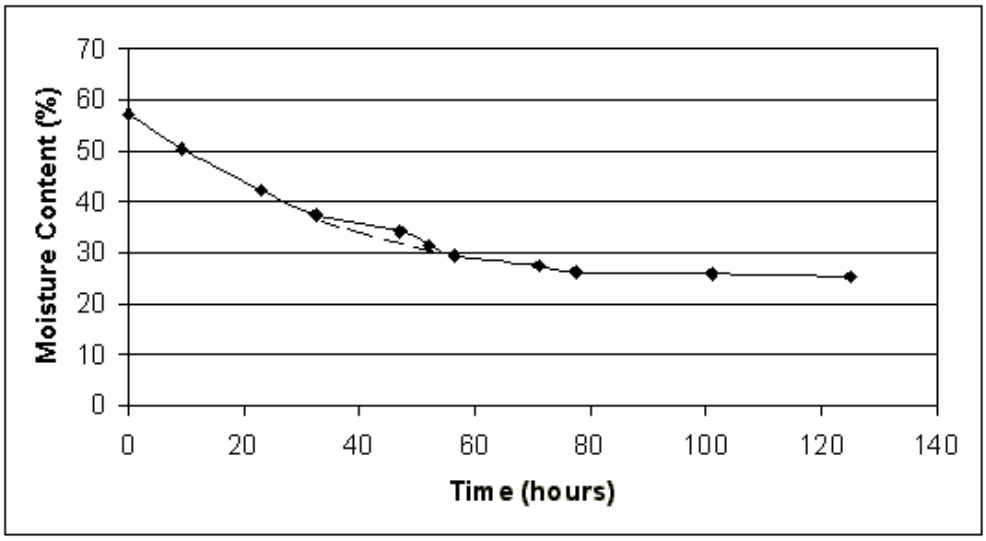


Figure 4.2 Variation of Moisture Content with Time

4.1.2 Changes in pH and Conductivity Measurements

Both the pH and conductivity varied during the test. Two graphs for both pH vs. time and conductivity vs. time are included. Figure 4.3 and Figure 4.4 on page 41 refer.

4.1.3 Variation in Final Moisture Content

At the end of the test two samples were taken at both cathode and anode and another two at the center, i.e. 20 mm, 150 mm and 280 mm lengths. More information on the calculation of the final moisture contents is detailed in Appendix D.

The average of the moisture contents at the anode, center and cathode are 23.91 %, 21.73 % and 26.59 % respectively. The average of the final moisture content is 24.08 % for the sample as a whole. Figure 4.5 on page 42 shows how the moisture content varied from anode to cathode.

4.1.4 Energy Consumption and Dewatering Efficiency

The calculations for energy consumption and dewatering efficiency data for Test 1 are detailed in Appendix D. The power consumption for Test 1 is 8×10^{-4} kW while the energy consumption per unit volume of dry tailings (E_u) is found to be 12.85 kWh/m^3. The dewatering efficiency for the test is 53.60 ml/Ah.

The graph of power consumption versus elapsed time is included on page 42 as Figure 4.6. The voltage and current were maintained constant. The area underneath depicts the energy transformed during the test.

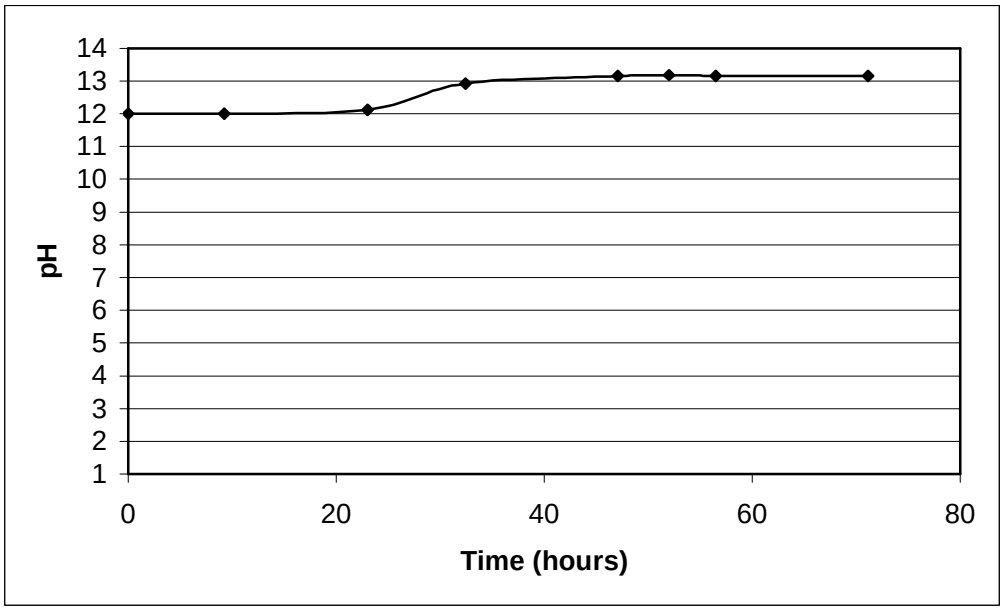


Figure 4.3 pH vs. Time

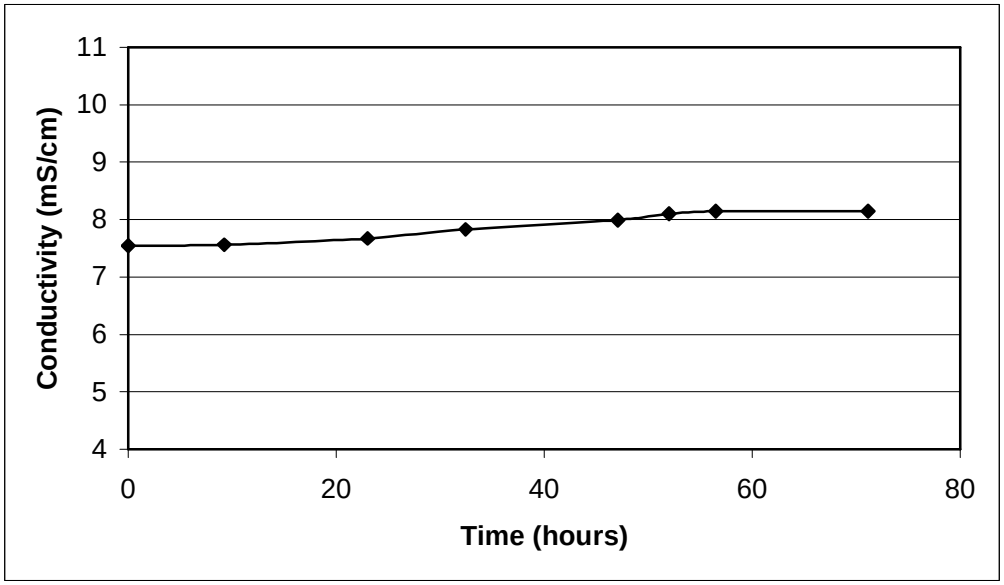


Figure 4.4 Conductivity versus Time

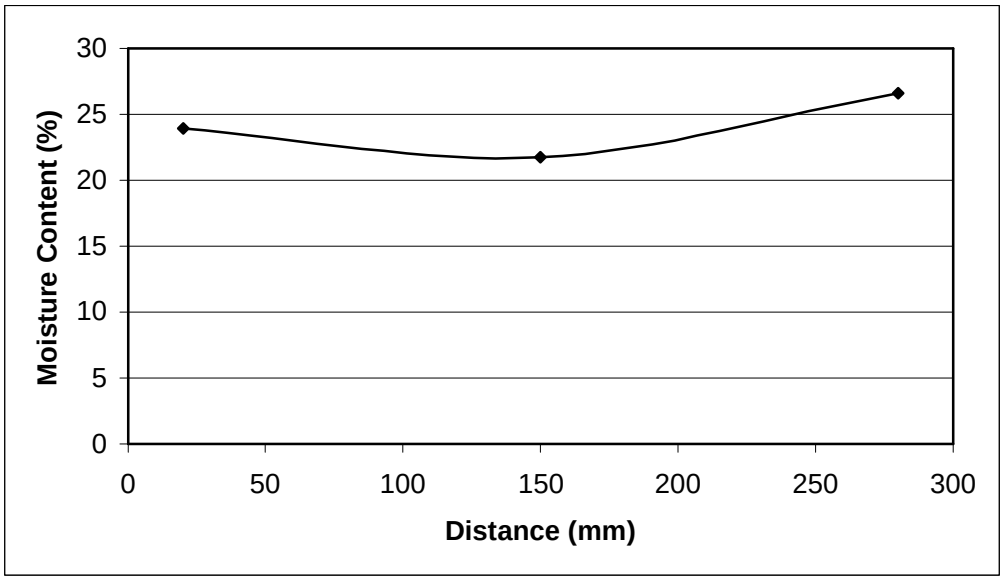


Figure 4.5 Variation in Moisture Content from Anode to Cathode

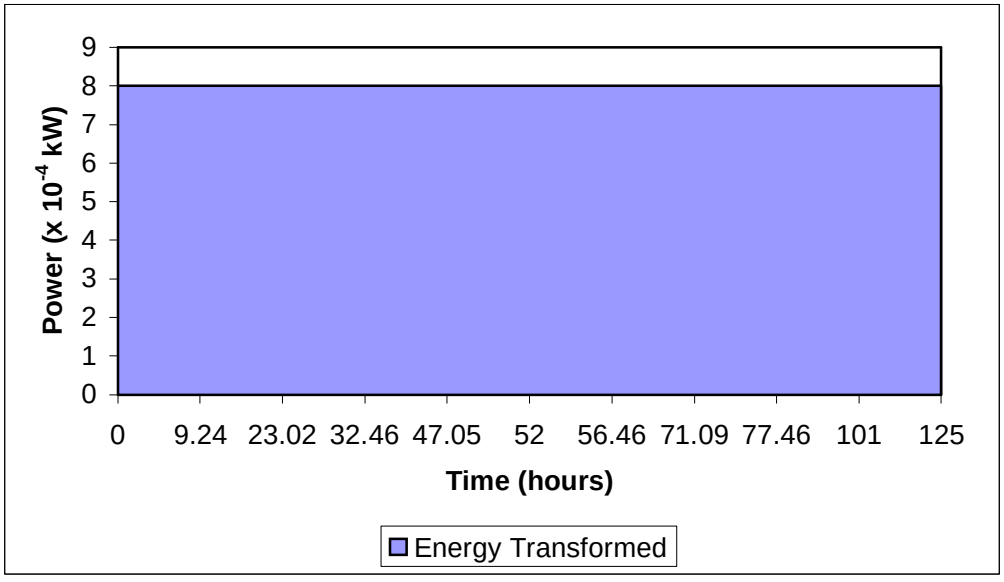


Figure 4.6 Power versus Time

TEST 2

4.1.5 Variation in Moisture Content

The water that was periodically drawn at the cathode was measured. The graph for such data is referred to as Figure 4.7 on page 44. Figure 4.8, also on page 44, allows for visual inspection of how the water content varied with time.

4.1.6 Changes in pH and Conductivity Measurements

The data for pH and conductivity measurements is presented together in the appendices. Two graphs for both pH versus time and conductivity versus time are included on page 45 as Figure 4.9 and Figure 4.10 respectively.

4.1.7 Variation in Final Moisture Content

The averages of the final moisture contents at the anode, center and cathode are 29.06 %, 31.44 % and 29.17 % respectively. The average of the final moisture content is 29.89 % for the sample. On page 46, Figure 4.11 depicts the dewatering effects from anode to cathode.

Figures 4.5 and 4.11 show how the final moisture content varied from anode to cathode for brass and EKG respectively. Figure 4.5 has a concave shape while Figure 4.11 has a convex shape. Possible causes will be discussed in Chapter 5, Discussion.

4.1.8 Energy Consumption and Dewatering Efficiency

The power consumption for Test 2 is 5×10^{-4} kW while the energy consumption per unit volume of dry tailings (E_u) is 5.23 kWh/m^3. Dewatering efficiency for Test 2 is 109.84 ml/Ah. The graph for power consumption versus time is included as Figure 4.12 on page 46. Both the voltage and current were maintained constant.

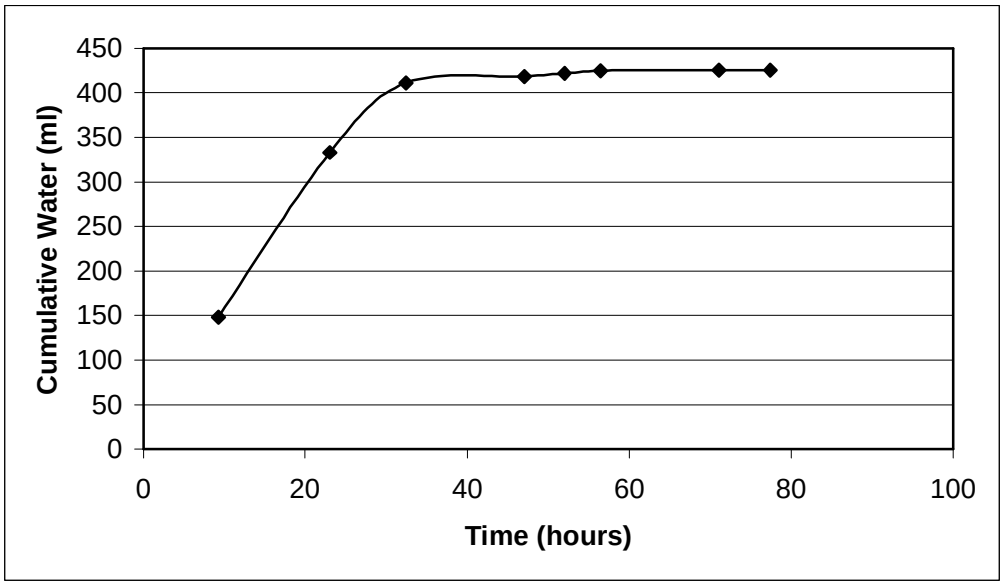


Figure 4.7 Cumulative Water versus Time

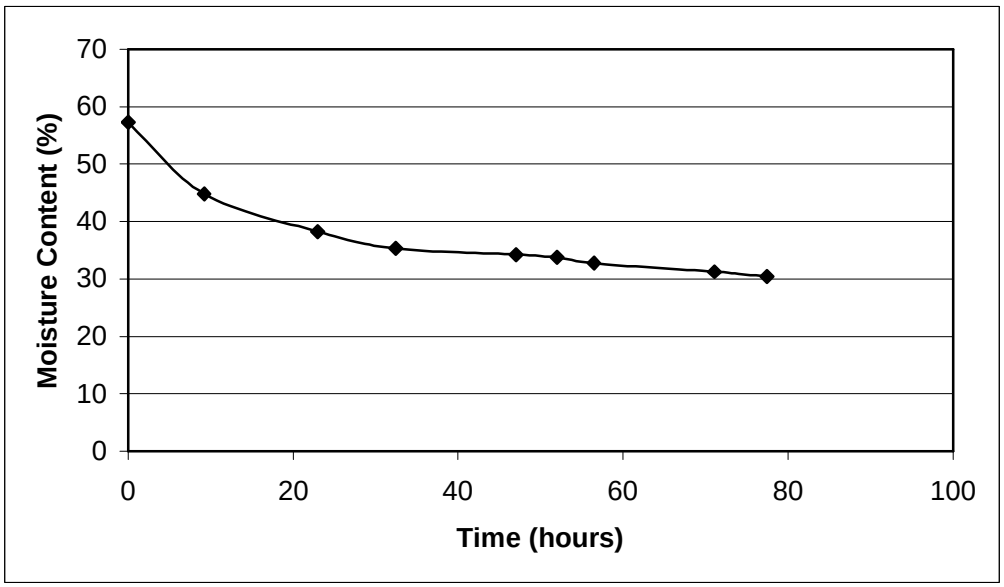


Figure 4.8 Variation of Moisture Content versus Time

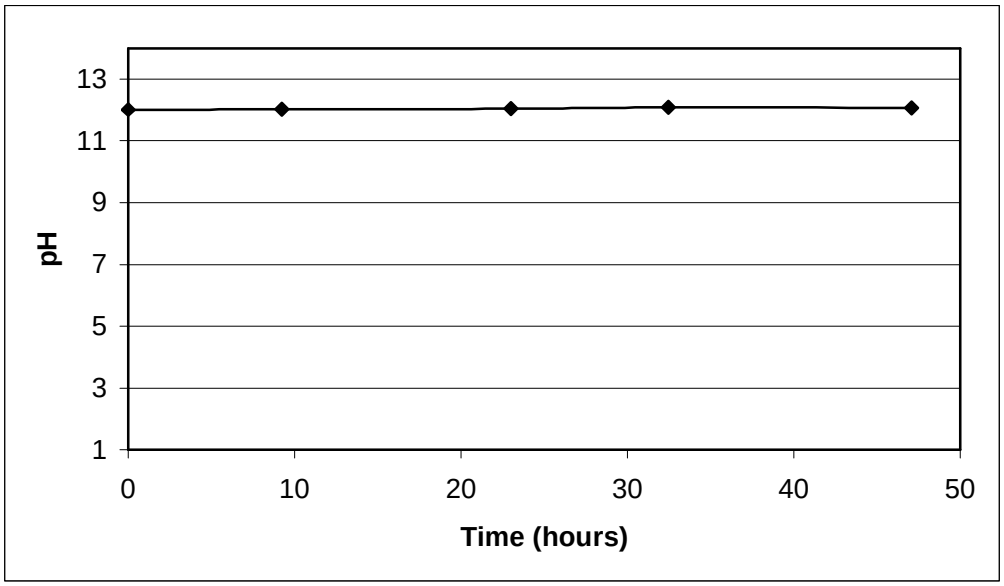


Figure 4.9 pH versus Time

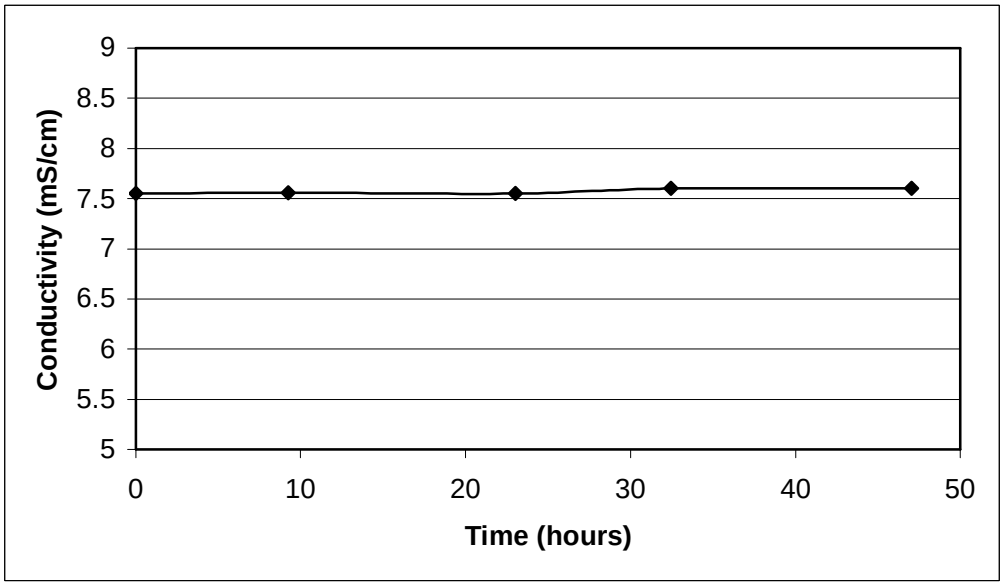


Figure 4.10 Conductivity versus Time

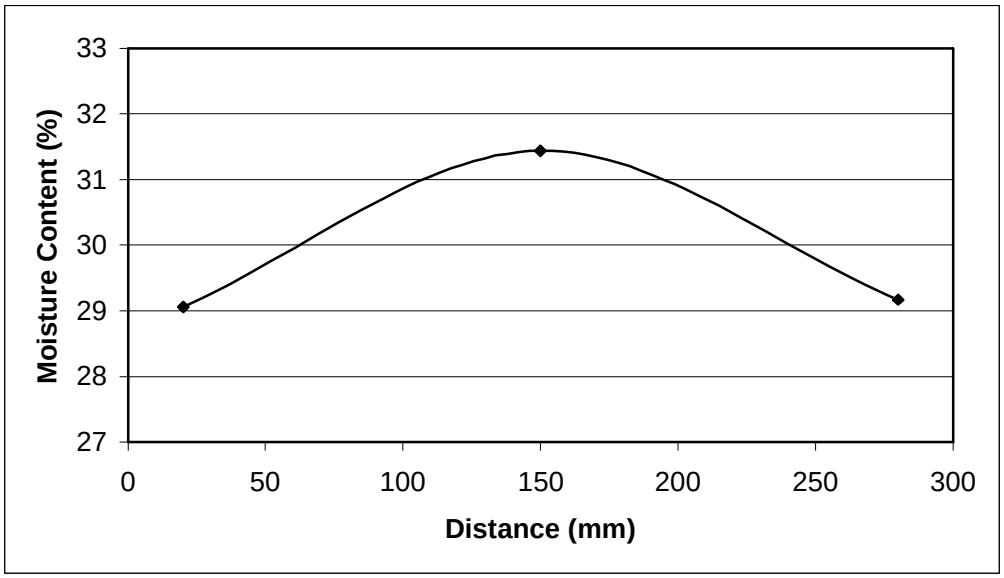


Figure 4.11 Variation in Moisture Content from Anode to Cathode

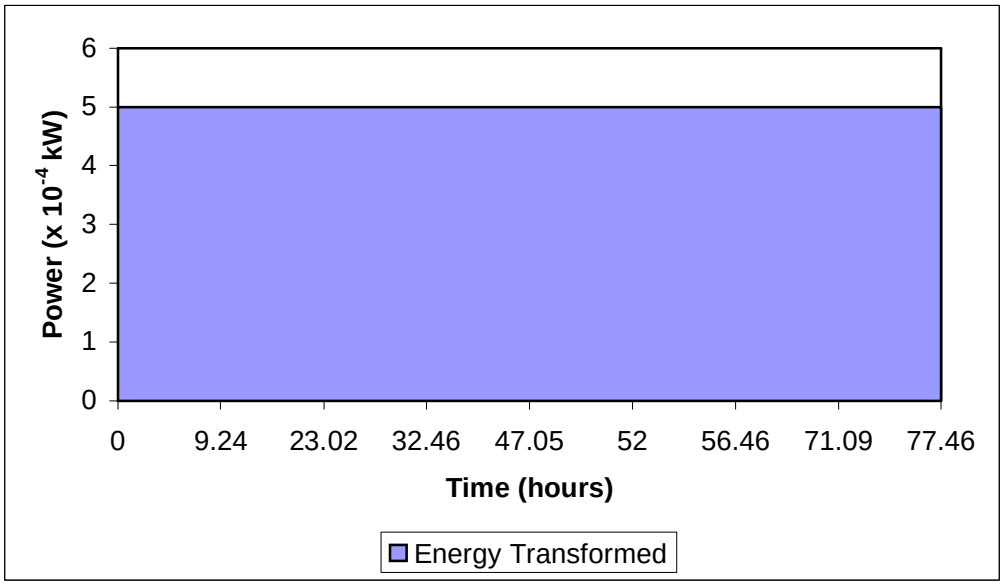


Figure 4.12 Power versus Time

4.2 Effect of Initial Water Content

Tests 3 to 7 were conducted using the same methodology as Test 1 all involving brass electrodes. Tests 8 to 12 were undertaken with the same methodology as in Test 2 but involving EKGs as electrodes.

The results for these tests are also presented under the same categories of variation in moisture content, changes in pH and conductivity measurements, variation in final moisture content, energy consumption and dewatering efficiency as Tests 1 and 2. These results show how the electrokinetic dewatering process is affected, as the initial water contents of tests involving both brass and EKGs are progressively increased.

The test results are lengthy due to their repetitive nature and have been recorded in Appendix C to improve the readability of this section.

Data on pH measurements, conductivity measurements, cumulative water and calculations of initial and final water contents are tabled in Appendix D.

4.3 Comparative Plots

Table 4.2 below contains a summary of information on final moisture content, final pH, final conductivity, power consumption, energy consumption per unit volume of tailing and dewatering efficiency from the entire tests.

The main aim is to plot same parameters from different tests on a single graph to provide easy comparison. These graphs will allow comparison by visual inspection.

Table 4.2 Summary of Test Series for Comparative Plots

Test No.:	Mc at 100 h	Mc_f (%)	pH_f	$Cond._f$ (mS/cm)	Power (x 10^{-4} kW)	EC at 100h (kWh/m^3)	DE at 100h (ml/Ah)
1 (B)	25.00	24.08	13.15	8.14	8	10.28	67.00
2 (E)	30.00	29.89	12.07	7.60	5	6.76	85.00
3 (B)	29.50	29.28	12.44	7.98	8	10.63	37.03
4 (B)	39.50	39.16	12.75	5.91	8	10.18	35.60
5 (B)	33.00	27.64	10.10	5.83	9	11.74	35.24
6 (B)	33.50	30.33	08.33	7.24	8	10.08	43.26
7 (B)	37.50	33.93	08.30	7.24	8	10.05	43.80
8 (E)	29.90	29.33	08.38	7.23	5	06.18	58.10
9 (E)	31.00	30.57	08.36	7.22	5	06.31	61.68
10(E)	34.50	33.58	12.56	7.18	5	07.18	67.62
11(E)	35.00	33.38	12.62	7.40	5	06.71	68.27
12(E)	40.00	35.93	12.56	7.57	6	07.91	59.46

(B = Brass electrodes, E = EKG electrodes, Mc = Moisture content,
Mc_f = Final moisture content, pH_f = Final pH, $Cond._f$ = Final conductivity,
EC = Energy consumption, DE = Dewatering efficiency)

The values for moisture content, energy consumption and dewatering efficiency at 100 hours were determined by means of visual inspection and extrapolation.

The plots that follow below show information from a number of tests on one graph to allow comparison.

4.3.1 Comparing the Final Moisture Contents

The graphs for average of final moisture content for all tests are presented together to give a comparative view. Figure 4.13 on page 49 refers. The final moisture content was taken to be the moisture content at 100 hours since the tests were all at different times.

Figure 4.14 on page 50 is a graph showing comparison of initial water content versus final water content for the test series.

4.3.2 Comparing the Final pH Measurements

The final pH measurements from all the tests are compared together. Figure 4.15 on page 51 refers.

4.3.3 Comparing the Final Conductivity Measurements

The final conductivity measurements for all the tests are compared together in one graph. Figure 4.16 on page 51 refers.

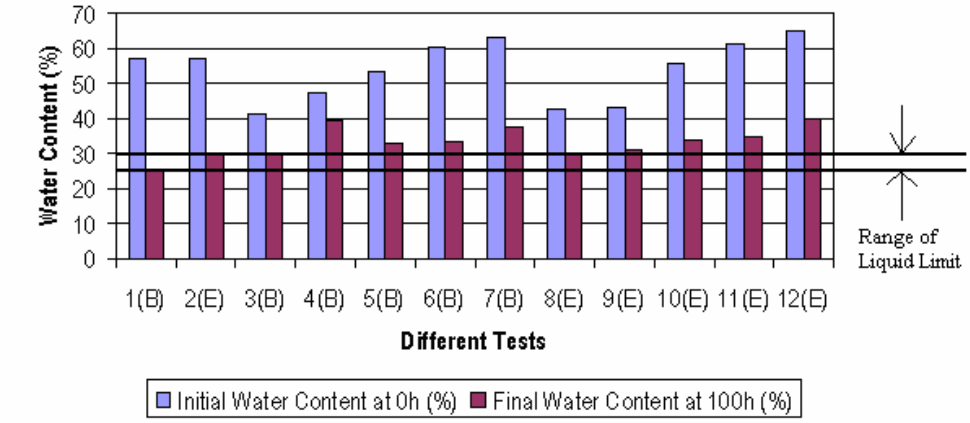


Figure 4.13 Comparing the Initial and Final Moisture Contents

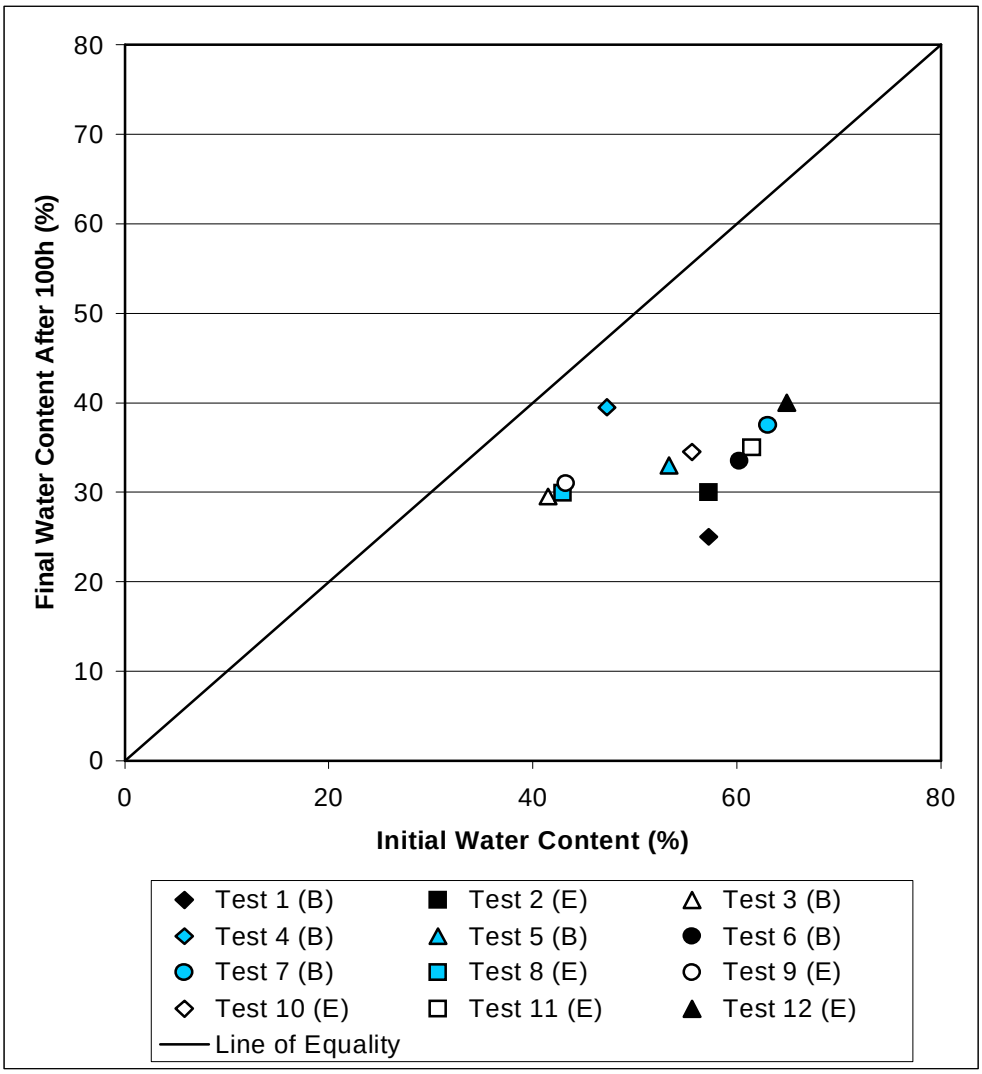


Figure 4.14 Initial Water Content versus Final Water Content After 100h

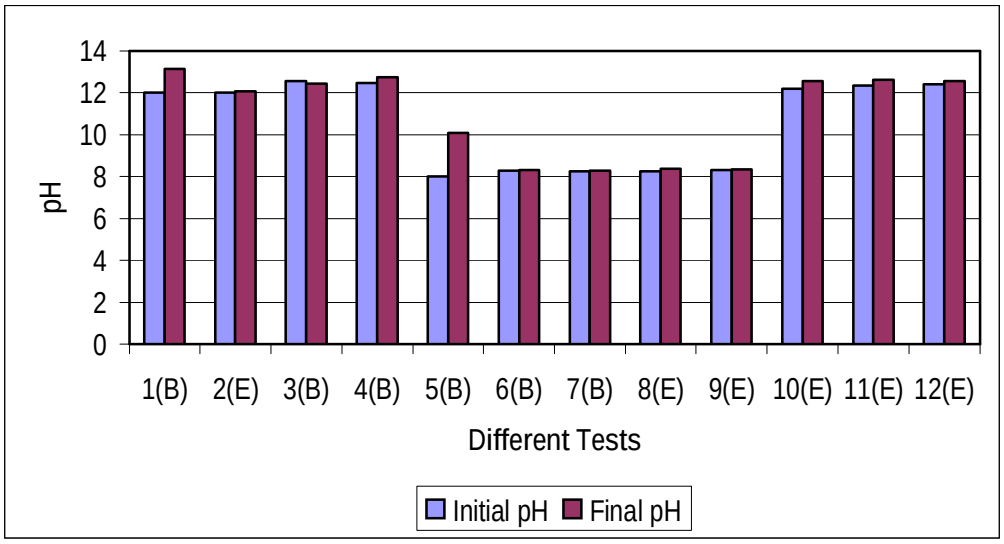


Figure 4.15 Comparing the Initial and Final pH

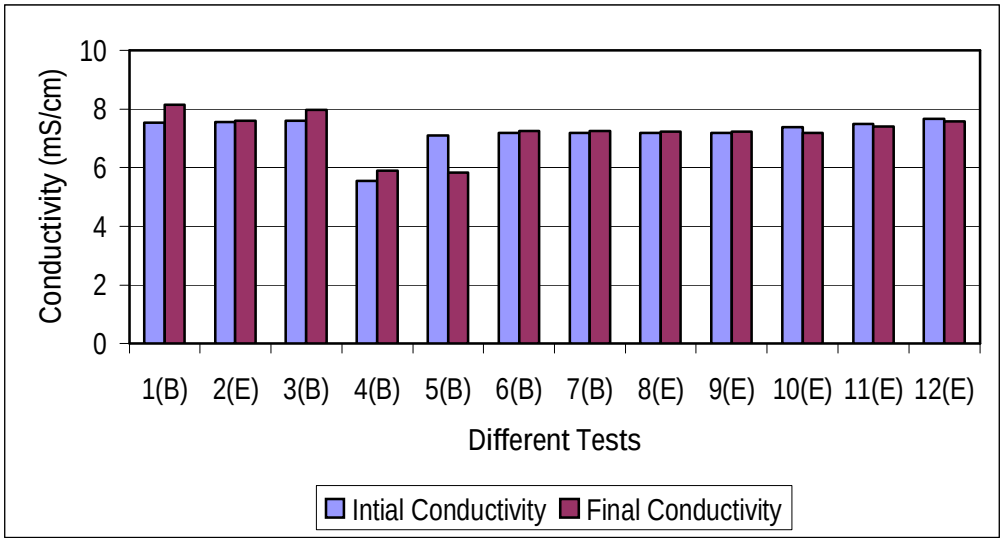


Figure 4.16 Comparing the Initial and Final Conductivity

4.3.4 Comparing the Power Consumptions

The power consumptions for each test are compared together. Figure 4.17 below refers.

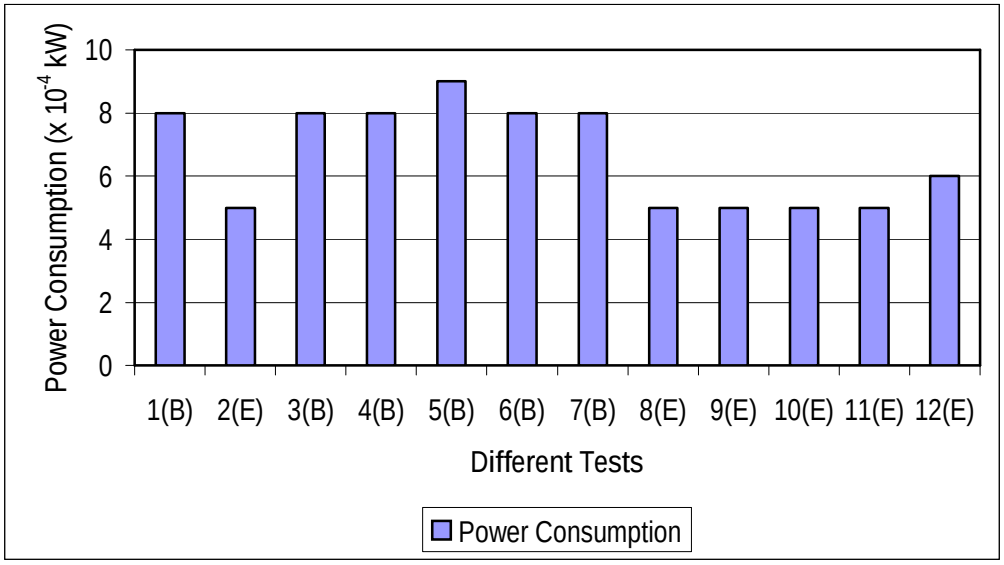


Figure 4.17 Comparing the Power Consumptions

4.3.5 Comparing the Energy Consumptions

The energy consumptions for various tests are compared together. Figure 4.18 on page 53 refers. The tests are compared for an equivalent of 100 hours.

4.3.6 Comparing the Dewatering Efficiencies

The dewatering efficiencies of all the tests are plotted along each other to provide comparison by visual inspection. Figure 4.19 on page 53 refers. The tests are compared for an equivalent of 100 hours.

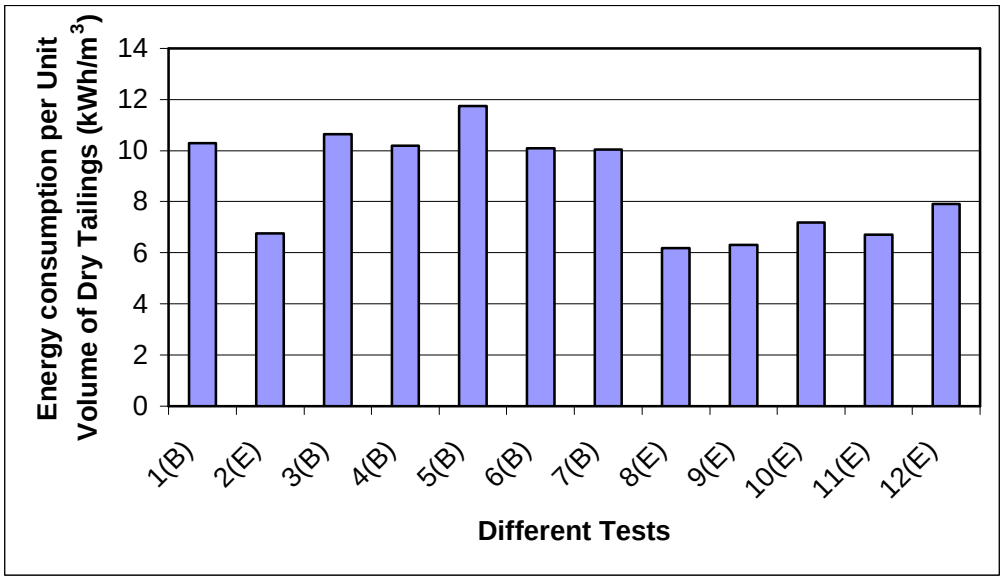


Figure 4.18 Comparing Energy Consumptions for Equivalent 100h Tests

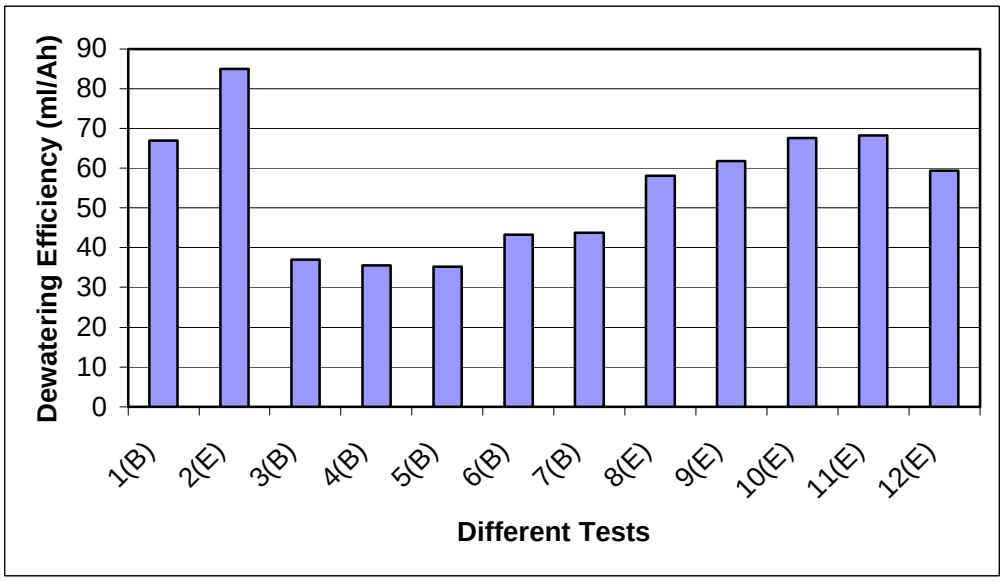


Figure 4.19 Comparing Dewatering Efficiencies for Equivalent 100h Tests

5 DISCUSSION

The voltage, current, initial water content, pH, conductivity, variation in moisture content and dewatering efficiency are discussed in this chapter. Aspects such as power, energy consumption, effect of electrode type, effect of difference in initial water contents, costs and observations made during the tests also formed part of the discussion.

Research objectives and hypothesis are reviewed in terms of whether they have been achieved or not. Findings and conclusions of the research dissertation are discussed.

5.1 Voltage, Current, Initial Water Content and Volume of Water

Table 5.1 Voltage, Current, Initial Water Content and Extracted Water

Test No.:	Voltage (V)	Current (A)	Wc_i (%)	Amount of Water Extracted (ml)	Wc_f (%)
1	10	0.08	57.25	536.00	24.08
2	10	0.05	57.25	425.40	29.89
3	10	0.08	41.50	269.20	29.28
4	10	0.08	47.26	284.77	39.16
5	10	0.09	53.33	317.14	27.64
6	10	0.08	60.26	346.11	30.33
7	10	0.08	63.05	350.41	33.93
8	10	0.05	42.94	290.52	29.33
9	10	0.05	43.24	308.40	30.57
10	10	0.05	55.60	338.09	33.58
11	10	0.05	61.47	341.37	33.38
12	10	0.06	64.91	356.78	35.93

(Wc_i = Initial water content, Wc_f = Final water content)

It is quite evident that most of the water is withdrawn during the first few hours after the tests had started, i.e. during electrophoresis. The graphs have a steep incline during this stage to indicate the above observation clearly.

5.2 Variation in Moisture

Even though the tests had different initial water contents, the decline of water content with time was similar for all the tests. The graphs start as steep declines (indicating electrophoresis) and slowly become flatter towards the end. The trend is also similar between longer tests and those that lasted only a few tens of hours. The graphs though, are relatively variable. Figure 4.13 shows a comparison of the variation in moisture content from all the tests.

Final water contents were variable and seem to correlate with initial water contents. Refer to Figures 4.13 and 4.14. In all cases, initial water contents were all above the liquid limit, but the final water contents appear to be close to the liquid limit, regardless of the starting value.

5.3 pH Measurements

Table 5.2 pH Measurements

Test No.:	Electrode Type	Material Type	Initial pH	Final pH
1	Brass	Delkor 1	12.01	13.15
2	EKG	Delkor 1	12.01	12.07
3	Brass	GG1 Delkor	12.55	12.44
4	Brass	GG1 Delkor	12.47	12.57
5	Brass	GG1 Thickener u/f	8.00	10.10
6	Brass	GG1 Thickener u/f	8.30	08.33
7	Brass	GG1 Thickener u/f	8.24	08.30
8	EKG	GG1 Thickener u/f	8.25	08.38
9	EKG	GG1 Thickener u/f	8.31	08.36
10	EKG	Delkor 2	12.21	12.56
11	EKG	Delkor 2	12.35	12.62
12	EKG	Delkor 1	12.40	12.56

The initial pH depended on the source of the tailings. As shown in Table 4.1 and 5.2, the pH of Delkor 1, 2 and GG1 Delkor tailings were all in the range 12 to 12.5, whereas GG1 Thickener underflow had a pH range of 8.0 to 8.3. In most tests, the pH remained almost unchanged during the test, but in Test 5 (GG1 Thickener underflow) it rose rapidly from 8.0 to just over 10.0. The reason for this different behaviour is not clear.

5.4 Conductivity Measurements

Table 5.3 Conductivity Measurements

Test No.:	Electrode Type	Material Type	Initial Conductivity	Final Conductivity
1	Brass	Delkor 1	7.54	8.14
2	EKG	Delkor 1	7.55	7.60
3	Brass	GG1 Delkor	7.59	7.98
4	Brass	GG1 Delkor	5.55	5.91
5	Brass	GG1 Thickener u/f	7.11	5.83
6	Brass	GG1 Thickener u/f	7.18	7.24
7	Brass	GG1 Thickener u/f	7.19	7.24
8	EKG	GG1 Thickener u/f	7.19	7.23
9	EKG	GG1 Thickener u/f	7.18	7.22
10	EKG	Delkor 2	7.38	7.18
11	EKG	Delkor 2	7.50	7.40
12	EKG	Delkor 1	7.66	7.57

All the initial conductivities varied in the range 7.1 to 7.6 mS/cm except Test 4 (GG1 Delkor) where for unknown reasons, the initial conductivity was only 5.5 mS/cm. Conductivities varied little during the tests.

5.5 Dewatering Efficiency, Power and Energy Consumption

Table 5.4 Dewatering Efficiency, Power and Energy Consumptions

Test No.:	Electrode Type	Power ($x 10^{-4}$ kW)	Energy Consumption (kWh/m^3)	Dewatering Efficiency (ml/Ah)
1	Brass	8	12.85	53.60
2	EKG	5	05.23	109.84
3	Brass	8	11.40	31.38
4	Brass	8	11.49	31.51
5	Brass	9	13.85	29.86
6	Brass	8	14.03	13.13
7	Brass	8	13.82	31.86
8	EKG	5	07.12	50.45
9	EKG	5	07.29	52.15
10	EKG	5	10.57	45.95
11	EKG	5	09.70	47.26
12	EKG	6	12.13	38.76

The energy consumption was in the range of 11.40 kWh/m^3 and 14.03 kWh/m^3 for tests undertaken using brass electrodes. The energy consumption for tests involving EKGs was relatively lower than that of brass electrodes and ranged from 5.23 kWh/m^3 to 12.13 kWh/m^3.

Figure 4.16 shows very clearly that tests using EKG electrodes consistently used only 55 to 67 % of the energy consumed in tests using brass electrodes. EKG electrodes are therefore considerably more energy-efficient than the brass electrodes used in the study. However, it may well be that the design of the brass electrodes was not optimal for this application and that brass electrodes with different configurations would improve their energy efficiency.

The energy consumptions are in line with those that were recorded by Johns (2005) for the same voltage. There's however the effect of overburden to consider in the experimental study conducted by Johns (2005). Johns (2005) used electro-

osmotic cells that are capable of applying pressures to tailings specimen and consequently, the energy consumptions may have been affected.

5.6 Observations during Tests

Below are some of the observations noted during the running and after dismantling of the tests. Some of the observations are common in all tests while others are only seen in some tests.

5.6.1 Cracks

These were very common in all the tests. A number of large cracks developed, radiating outwards away from the electrodes. Cracks forming a ring were formed immediately around the cathode. These cracks increased in depth and length as more water was withdrawn, i.e. as the sample become drier.

The cracks around the anode resembled small fissures and only became wider during the last stages of the test.

5.6.2 Effects of Electrochemical Reactions

These effects were very dominant in tests involving brass electrodes but appeared insignificant in tests involving EKGs. After the experiments were dismantled, the following were observed:

(a) Corrosion on Electrodes

'Surface roughness' was observed on both electrodes. The roughness could be due to electrodeposition processes or corrosion that are similar (albeit reversed) processes. Electrodeposition will be discussed in (b) and focus here will be on corrosion.

In all the tests involving brass electrodes, there was significantly more corrosion on the surface of anodes than on cathode surfaces. The difference was easily seen when both electrodes were gently scraped and thoroughly cleaned and their

masses re-measured. Before all the tests, the anode and cathode weighed 611.0 and 609.5 grams respectively. After Test 1, the brass electrodes were cleaned and weighed 600.4 and 609.7 grams for anode and cathode respectively. Before the test, the anode weighed more than the cathode but now the cathode weighed more than the anode. For Test 1, the anode lost 10.6 grams and the cathode gained 0.2 grams.

Test 3 was started with the anode and cathode weighing 600.4 and 609.7 grams respectively. After it was dismantled and cleaned, the anode and cathode weighed 593.7 and 610.0 grams respectively. The anode lost a further 6.7 grams and the cathode had gained 0.3 grams. Test 4 was started with the anode and cathode weighing 593.7 and 610.0 grams respectively. When measured again after the test, the anode and cathode weighed 591.4 and 610.2 grams respectively. For Test 4, the anode has lost 2.3 grams and the cathode had gained 0.2 grams.

The next test involving brass electrodes was Test 5. The test was started with anode and cathode weighing 591.4 and 610.2 respectively. After the test, the anode had lost 1.2 grams and the cathode had gained 0.2 grams.

The last tests involving brass electrodes were Tests 6 and 7. Both commenced with anode and cathode electrodes weighing 590.2 g & 610.4 g and 589.8 g & 610.5 g respectively. After Test 6, the anode had lost 1.2 grams while its corresponding cathode had gained 0.2 grams. After Test 7, the anode had lost 0.4 grams while the cathode had gained 0.1 grams when the test ceased.

(b) Precipitation on Electrodes

There were significant amounts of greenish precipitates found on the lower parts of the electrodes (the parts covered with coal tailings). Since the electrodes were of brass, it is possible the electrodeposited precipitates were copper.

There was more precipitation on the anode surface than cathode, but large amounts of precipitates found on the geosynthetic material suggests that

electrodeposition was greater at the cathode surface than on the surface of the anode. The changes in electrode mass reported earlier support this suggestion.

It was reported earlier that electrodeposition and corrosion took place simultaneously at both the cathode and anode surfaces. However, it should be noted that electrodeposition was greater at the cathode while corrosion was dominant at the anode. This conclusion is based on the changes in mass of both electrodes and the roughness evident on their surfaces. The anodes consistently lost mass while the cathodes gained mass.

The scraping and cleaning of precipitates was deliberately not 100 percent thorough on both electrodes so as not to damage the electrodes. Although there is evidently variation in the cleanness on surface of both electrodes, obviously due to a lack of a similar cleaning mechanism, but the significant loss in mass by the anode from 611.0 to 589.8 grams and the small gain in mass by the cathode from 609.5 to 610.5 grams support the notion that there was more corrosion on anode than cathode and that the effect of a different cleaning mechanism on each electrode was not significant to render this observation invalid.

There was no precipitation or corrosion observable by visual inspection on the EKGs. There was also no significant change in mass of either electrode. The changes in mass are relatively difficult to document because the cylindrical EKGs are difficult to clean.

5.7 Final Water Contents

Graphs depicting final moisture content against distance for Tests 1, 3, 4, 10, 11 and 12 displayed concave shapes while the rest of the test series displayed convex-shaped graphs. Simply put, these tests had water contents at midway between the anode and cathode that were less than those measured at either the anode or cathode.

Tests 2, 5, 6, 7, 8 and 9 seem to conform to the researcher's expectations. The electrokinetic dewatering effect caused the water to move from the area around the anode through the midway point into the area surrounding the cathode. The greatest dewatering effect should occur nearer to the anode and cathode and be less further away from the electrodes where current is less concentrated. In some of the tests in the series, small depressions developed around the anode. The opening of cracks in the tailings has also been documented and these two factors could have had an effect.

There seem to be small differences between the final water contents measured at the anode, cathode and at midway between with the final water contents calculated from the water removed from the cathode. The average of the water contents measured at the anode, cathode and at midway appear to represent the true final moisture content. This is because the samples were completely dried in the oven to find the final water content which therefore represents the average water content throughout the whole wooden box.

When comparing the moisture contents at 100 hours and the final moisture contents for the entire test series, the results favoured the tests involving brass electrodes. These tests recorded relatively lower water contents when measured at 100 hours and when the tests eventually ceased.

5.8 Successes and Failures in Attaining Objectives

The specific objectives documented in section 1.6 for this research work have all been achieved with varying degrees of success. The first objective aimed at comparing the dewatering efficiencies between brass and EKGs. The comparison was intended to be over the whole range of testing but all the starting parameters were made similar for Tests 1 and 2. Both tests were started at water content of 57.25 %. Brass test (Test 1) lasted 125 hours while Test 2 lasted only 77.46 hours. The dewatering efficiency for Test 1 was 53.60 ml/Ah and for Test 2 was 109.84 ml/Ah. Coal samples in Test 1 were reduced to water content of 24.08 % and those used in Test 2 were reduced to water content of 29.89 %.

The energy consumption was 12.85 kWh/m^3 for Test 1 and 5.23 kWh/m^3 for Test 2. Brass electrodes produced higher current densities than EKGs. This means the dewatering efficiency for brass electrodes is improved but the efficiency is still lower compared to EKGs.

The first objective favoured the EKGs because they have achieved relatively higher dewatering efficiencies when compared to their brass counterpart. The EKGs performed beyond expectations.

Dewatering efficiency is dependent on time. The EKG cathode had relatively larger perforations when compared to brass cathode. The treatment time was stopped earlier when any further time extensions failed to bring further electro-osmotic effects. Consequently, the tests with EKGs had relatively higher dewatering efficiencies than their brass counterparts. But should the degree of perforation have been identical, a different picture might have occurred.

The second objective's main intent was to investigate the effect of difference in initial water content in the test series. The results show that final water contents and the water contents after 100 hours were progressively increasing as the initial water content increased. This progressive increase in the final water contents and power consumption is seen in tests involving both EKGs and brass electrodes. Figure 4.13 shows the correlation between the initial water contents and final water contents. The coal samples were dewatered close to their liquid limits irrespective of the starting water contents.

Figure 4.14 is a scatter diagram comparing pairs of initial water content and final water content. The initial water contents were in the long range from 41.50 to 64.91 %. However, the range of final water contents was shorter, from 25.0 to 40.0 % and this range is close to the liquid limit range for this test series. Figure 4.14 reiterates the argument made earlier that the coal samples were dewatered close to their liquid limits, regardless of the starting water contents.

The power consumption continued to rise for tests that had higher initial water contents. Comparing the initial water contents to final water contents for EKGs and brass, the results seem to favour the tests involving brass electrodes despite the higher dewatering efficiencies experienced with EKGs.

The higher the initial water content, the more time it would take to dewater the sample. It would generally increase the dewatering efficiency. Increased lifespan of the test means increased operational costs. Different initial water contents did not affect the way the samples were being dewatered. The variation in water content with time for all the tests was almost the same. The similar trend between the different tests indicates this.

The third objective and the research hypothesis in the introductory chapter focus on finding ways of increasing or improving the dewatering efficiency and effectiveness. At first Q/t remained constant but then reduced progressively as depicted in Figures 4.1 and 4.7. But after a certain time period in the test, no matter how longer the tests lasted, no more water would be drawn out of the cathode and the dewatering efficiency would start to decrease.

Although specifically not forming part of the research work, it is logical to assume that reducing the volume of the sample allows the electrokinetic dewatering process to be more effective and efficient. Reducing the volume will decrease the electrode spacing but the cost of electrodes is increased.

Increasing the level of perforation on the cathode might result in higher permeability allowing more water to pass through, especially during the earliest periods in the tests, i.e. during electrophoresis. During this first stage in electrokinetics, the solids settle under the combined action of gravitational and other viscous forces. However this aspect need to be researched.

Lastly, the guidelines that may be useful when extending electrokinetic dewatering to full-scale applications are detailed and documented in the next chapter.

5.9 Costs and Efficiency

Initial costs. EKGs are currently manufactured for experimental purposes and their actual market price is unknown. The brass material would be expected to cost much more than electrokinetic geotextile material. This is mostly due to high prices of copper and zinc.

Operating costs. Here the EKGs and brass are compared in terms of their laboratory or operational costs. The EKGs are bought with their inherent large perforations while it would take extra costs to drill applicable holes into the brass electrodes to be able to allow water to pass through.

Table 4.2 shows that in terms of saving energy and power costs, EKGs are much more efficient than brass.

Brass electrodes experienced surface roughness after each test due to electrochemical reactions taking place on their surfaces. There would be more replacement costs associated with brass electrodes due to their relative susceptibility to electrochemical reactions that decrease their durability.

Tests involving EKGs recorded better dewatering efficiencies and lower operating costs than brass electrodes. In the end, EKGs are relatively more cost-effective than brass electrodes and when the initial costs are taken into account, the difference would even be bigger.

Considerations as to which electrode type is the most suitable will depend on the dewatering requirements and the financial implications associated with that desired level of dewatering.

6 EXTENDING ELECTROKINETIC DEWATERING TO FULL-SCALE APPLICATIONS

6.1 Introduction

Quantities of finer tailings are on the increase as milling and mineral extraction processes used to separate the minerals from waste are being perfected. The conventional dewatering methods tend to decrease in their effectiveness and efficiency as tailings fineness increases.

As indicated in the earlier chapters, the dewatering of tailings using electrokinetics is by no means a new technology. The laboratory research was aimed at finding ways to improve the dewatering process to keep up with the increasing tonnage of finer tailings produced by mines.

The laboratory study undertaken has shown that the electrokinetic dewatering technology can be a feasible option in effectively dewatering tailings, especially in the case of fine coal tailings.

The ultimate objective of any laboratory study is to investigate and assess how well a particular laboratory discovery can be applied at full-scale. Below are some tentative guidelines.

6.2 Tentative Guidelines

The research experiment has been undertaken at laboratory scale but some recommendations and suggestions are given as guidelines for consideration if and when electrokinetic dewatering technology appears to provide a solution. These

guidelines are not intended to provide detailed instructions on how to develop this technology at full-scale as they are neither specific, comprehensive nor complete and each mine has its own site and material characteristics.

Every tailing has its own physical, mineralogical and chemical characteristics. Successful implementation of dewatering by electrokinetics will require full understanding of the nature of mine tailings being used.

6.2.1 Vertical versus Horizontal Electrodes

The laboratory work so far has exclusively been on vertical electrodes. This arrangement requires large surface areas and reasonable depths of sample for laboratory testing. This entailed handling and collecting much larger quantities of material, and resulted in fewer experiments over longer time periods. However, the use of vertical electrodes is more practical than horizontal electrodes in many situations, especially for ponds already filled with tailings and can be adjusted to any desired electrode separation. Lockhart *et al.*, (1984) showed that there are many possible vertical configurations both with and without well-points (at which the water is collected and pumped off), or with only a limited number of well-points. Vertical electrodes will more likely be the solution in many circumstances.

6.2.2 Machine versus Tailings Pond

The electrokinetic dewatering technique can be developed into a machine, incorporating electrokinetics or be designed and installed at tailings ponds. Both have their own advantages and disadvantages. It is certainly better in theory to dewater any small depths of sample in one operation, i.e. a machine is fundamentally superior to a tailings pond. Machines will certainly deal with the future trends to finer materials. However, machines can be complicated and very expensive, both to buy and to operate. It is very likely that electrokinetic dewatering in large tailings ponds would be cheaper.

Firstly, the capital cost for a tailings pond holding enough tailings to equal the expected throughput of a machine in its lifetime, should be much less than the cost of the machine. Secondly, the pond situation takes full advantage of the natural sedimentation and drainage such that the 'feed' solids content for the purposes of electrokinetic (specifically electro-osmosis) is much higher than for a machine. Indeed, the coarse fraction from many coal tailings (and mineral tailings generally) settles out naturally at the input end of the pond, leaving only part of the tailings to be dewatered by electrokinetics. Thirdly, the pond operation could be run without needing continuous monitoring or maintenance, it could be switched on or off to average out electrical loads, and it might not break down, as a machine would do (Lockhart, *et al*., 1984).

For some mining houses, a machine might be a more feasible option depending on the washery/ mine-site characteristics. Another advantage will be that the environmental requirements are more likely to be less than that of a tailings pond.

The machine may need to be automated and assembled to run continuously to reduce some of the costs. Effective usage of energy will also be much easier to control and manage (The Energy Conservation Center, 1993). Some guidelines are provided below.

The electrokinetic dewatering unit as a process plant is operated by electric power. Energy conservation is meant not to reduce the energy for operation, but to ensure "waste-saving" and "effective" use of energy, thereby resulting in reduced energy for operation. "Waste-saving" use is provided by continuous operation from the start of operation to the day of shutdown determined by the waste production schedule, without the electrokinetic dewatering process being interrupted by the machine and system failure, electric failure due to accidents.

This continuous operation requires:

1) A quality control system which permits the constant production of stable well-dried tailings, without products being rejected in the inspection, and
2) A preventive maintenance (PM) system that reduces the possibility of machine and equipment troubles or failure due to electric equipment failure (The Energy Conservation Center, 1993).

It is generally felt that there is no remedy for electric failure. Frequent power failure means the company must adopt private power generation equipment to ensure a stable supply of power more free from electric failure. Operation efficiency will be increased, while power cost will be reduced as compared to that of the purchased power (The Energy Conservation Center, 1993).

The electrokinetic dewatering unit, either machine or tailings pond, like most mining processes, cannot enjoy continuous operation without an effective maintenance work force. Preventive maintenance (PM) is to prevent accidents in advance and to repair and improve the equipment by planned equipment maintenance based on the past experience with the equipment failure and by checking the operation through a daily equipment inspection on patrol. It is intended to eliminate the operation shutdown by the maintenance division (The Energy Conservation Center, 1993).

- Economics

Electrokinetic dewatering is a very cost-effective solution for the separation of water from fine coal tailings. Should the unit be used at commercial level, the researcher anticipates the unit to be designed to a comparatively low weight. The civil engineering requirements will be kept to a minimum and indeed the design should be such that the unit will fit into a standard single story building.

Extensive use of geosynthetic membranes as coating on electrodes will result in long life and minimal outlay on replacement parts. The system is designed for low power consumption.

- Efficiency

The dewatering cathodes should be completely permeable all round, allowing rapid dewatering on all sides, especially during electrophoresis.

- Features

Although the study was conducted on a laboratory scale, application of geosynthetic membranes has significantly reduced the rate and amount of corrosion of electrodes.

An auto-feeder unit could be installed to distribute specific amounts of tailings sludge evenly across the dewatering containers ensuring even and efficient dewatering and reduced application time.

The dewatering method should be able to operate at room temperature and low pressure rather than conventional technologies that require high temperature and high pressure for dewatering.

- Configurations

The electrokinetic system can be designed and configured in a tilting position that can provide a gravity dewatering position prior to entering the normal application where electric current is being applied. This configuration can have the effect of increasing efficiency and reducing energy requirements.

Research before implementation is a very important factor to be considered. Research might include characterizing the tailings and investigating the merits and demerits of using either machine or tailings pond; horizontal or vertical electrodes or relevant parameters that can help in designing the most optimal and economic electrokinetic dewatering unit. This will also help in the setting of dewatering

requirements. *Planning* is also a key to successful implementation. This involves setting in place all the logistics, resources, quality control system, preventive maintenance system and time frames, some of which may be pre-requisites of certain legal requirements. Much of the planning should also go into making this dewatering project an integral part of the mining and environmental activities of the mine, thereby reducing costs and time spent.

6.3 Containment of Tailings

The containment of tailings before being dewatered is a very important concept, as any failures in the tailings dams can result in damage to machines and destruction of human life. Significant design input and sufficient factors of safety are required to be put in place in order to ensure the safety of the impoundment (Wagener *et al.*, 1998).

7 CONCLUSION AND RECOMMENDATIONS

The important findings and conclusions of the study are highlighted. Also included are some recommendations and restating of developments on this laboratory research work and related efforts by the U.S. Bureau of Mines and other researchers on electrokinetic dewatering of coal tailings.

7.1 Summary

The work undertaken by Lockhart and Stickland (1984) on dewatering of coal washery tailings ponds and related efforts by the U.S. Bureau of Mines show that larger-scale electro-osmotic dewatering of tailings ponds is a feasible proposition, at least in the case of coal tailings. Much of the cost would be in constructing and dismantling of ponds, followed by the removal of the dewatered material, so that ponds with three permanent walls and one removable wall of coarse refuse are sensible. Electro-osmosis could be especially attractive where large permanent disposal ponds are available, to which thickened tailings could be dumped.

Machines have also been used to dewater and they are found to be fundamentally superior to a tailing pond. However, machines are complicated and very expensive, both to buy and operate, even when only mechanical and not electrical dewatering is involved. Furthermore, centrifuges, vacuum filters, belt press filters, etc., often cannot give good results, and this problem is certain to increase in the future with trends to finer particles. The experimental study, conducted on a laboratory scale, has shown that electrokinetics (electro-osmosis) is effective in dewatering coal tailings. In addition, as noted earlier, electro-osmotic process, being a surface process, is relatively insensitive to pore size and is therefore attractive in principle to the dewatering of fine particles (Lockhart *et al*., 1984).

In this experimental study, vertical electrodes are used instead of horizontal ones. Each electrode arrangement has its own merits and demerits but vertical electrodes are a more desirable solution likely to be used in many circumstances, since they are relatively easy to install after test box is filled with sample coal tailings. This advantage could be achieved at field scale where it would be easy to install vertical electrodes in already filled up ponds and can be adjusted to any desired electrode separation.

The intermittent current and polarity reversal can significantly improve the effectiveness of electrokinetic dewatering and reduce energy consumption and adverse electrode reactions (Shang *et al.*, 1998).

7.2 Conclusions

The end-result of the research work was to create significant contributions to the continuing need for improvement of existing electrokinetic dewatering methods and this has been achieved in the last chapter.

Again it should be emphasized that the tests conducted have been on particular coal tailings with their distinct physical, organic, chemical and mineralogical characteristics and therefore the results obtained from the testing may not hold true for all coal tailings.

This research work and related efforts by the other researchers and by the U. S. Bureau of Mines show that large-scale electrokinetic dewatering of tailings is a feasible proposition, at least in the case of coal tailings. Much of the cost would be in constructing and dismantling of ponds, followed by the removal of dewatered material as stated earlier.

From an environmental point of view, electrokinetic dewatering of tailings is beneficial as it reduces the energy needed for complete evaporation of remaining water. This will reduce time needed for complete evaporation. This can be true especially if the original design location was further away from direct sunlight

that could have evaporated the water for free and much quicker. In this case both the quantity of primary energy sources and the accompanying CO_2 emission for obtaining a certain amount of solid waste are reduced (Raats *et al*., 2002).

In previous discussions, it was mentioned that power consumption is another critical factor in considering the viability of electrokinetic dewatering. It is very much dependent on time. Therefore the operational time is the governing factor. The effective time in the electrokinetic dewatering is dependent on materials properties. The extension of treatment beyond the effective time would not generate appreciable further effects. Since the majority of the dewatering effect takes place during electrophoresis sedimentation, when the water content is still high, the time of electro-osmotic consolidation could be adjusted based on considerations such as the required final water content and project budget.

7.3 Recommendations for Further Research

Research to assess existing/old and new/novel methods of dewatering coal tailings in terms of efficiency, throughput, cost and general optimization using modern technology. The improved dewatering of coal is a continuing basic need. Research should perhaps consider whether it would be achieved better by changes to the dewatering system design as well as improved methods. Would a reduced moisture level be obtained by treating specific sizes separately rather than as a combined whole as is now generally the case? Lower moisture levels would improve thermal value and reduce handling difficulties. The latter although not a major problem, does create a real difficulty of high cost down time when controllable flow cannot be maintained.

APPENDIX A

CHARACTERIZATION OF MATERIALS - DETAILED RESULTS

The following appendix has been grouped according to coal sample names in no particular order.

A. Sample Identification: DELKOR 1

1. Atterberg Limits

The coal samples in containers no. 25, 23 and 15 were subjected to 10, 25 and 48 number of blows respectively.

Table A1 Liquid limit

Container no.	25	23	15
No. Of Blows	10	25	48
Moisture Content (%)	31.6	28.6	26.5
Average Moisture Content Of Sample	28.9		

Table A2 Plastic limit

Container no.	3	20
Moisture Content (%)	23.5	21.5
Average Moisture Content (%)	22.5	

Plasticity Index

The plastic index is calculated as the difference between the liquid and plastic limits.
PI = LL – PL
= 28.9 – 22.5
= 6.4 ~ 6

Trough no. A was used to determine linear shrinkage:

Length of dry sample = 146.3
Total shrinkage = 3.7
Linear shrinkage = 2.5

2. Specific Gravity

The standard test was undertaken using two sample bottles to obtain the average specific gravity. The parameters measured and the specific gravity are noted below in the table below:

Table A3 Specific Gravity

Bottle Number	9	10
Mass of Bottle, w1	39.078	39.985
Mass of Bottle & Dry Sample, w2	49.326	50.190
Mass of Bottle, Sample & Water, w3	96.236	95.590
Mass of Bottle & Water, w4	91.924	91.163
Specific Gravity, Gs	1.726	1.766
Average Specific Gravity, Gs	1.75	

3. Grain-size Analysis- Mechanical Method

The grain-size distribution data of the coal sample was obtained using standard soil classification methods and procedure.

The mass of pan & dry material before washing= 382.8 g
The mass of pan & dry material after washing= 291.7g
Mass of pan= 189.4 g

Full data concerning the sieving process is presented in the table below:

Table A4 Particle Size Distribution

Sieve No.	Sieve Size (mm)	Retained by Sieve			Cumulative (%) Passing Sieve
		Mass (g)	% Of Total Mass	Cumulative % of Total Mass	
8	2.360	0	0	0	100.0
16	1.180	6.50	1.44	1.44	93.65
28	0.600	36.10	7.98	9.27	64.71
40	0.425	52.60	11.63	21.05	48.58
50	0.300	65.90	14.57	35.62	35.58
100	0.150	87.30	19.30	54.92	14.66
200	0.075	101.80	22.51	77.43	0.49
Pan	--	102.10	22.57	100.0	--
TOTAL	--	452.3	100.0	--	--

To detect any loss of coal tailings in the mechanical sieving operation:

Total $\sum$ weight retained= 102.1 g
Original weight of sample + weight of pan – weight of pan= 291.7 – 189.4= 102.3 g
102.1 / 102.3 x 100= 99.80 %. Therefore 0.2 % of sample is lost. Less than 2 % of sample is lost and sieving process is validated. More than 2 % of sample loss is unacceptable and the test should be repeated.

Less than 10% passes the # 200 sieve, a hydrometer analysis will not be performed. Since less than 10% is -#200 material, this completes the particle size analysis.

B. Sample Identification: DELKOR 2

1. Atterberg Limits

The coal samples in containers no. 15, 18 and 21 were subjected to 10, 25 and 48 number of blows respectively.

Table A5 Liquid limit

Container no.	15	18	21
No. Of Blows	10	25	48
Moisture Content (%)	30.53	28.30	25.90
Average Moisture Content Of Sample (%)	28.24		

Table A6 Plastic Limit

Container no.	5	13
Moisture Content (%)	23.5	21.1
Average Moisture Content (%)	22.15	

Plasticity Index

The plastic index is calculated as the difference between the liquid and plastic limits.
PI = LL – PL
= 28.24 – 22.15
= 6.09 ~ 6

Trough no. A was used to determine linear shrinkage:

Length of dry sample = 146.5
Total shrinkage = 3.5
Linear shrinkage (%) = 2.3

2. Specific Gravity

The standard test was undertaken using two sample bottles to obtain the average specific gravity.

Table A7 Specific Gravity

Bottle Number	9	10
Mass of Bottle, w1	39.078	39.985
Mass of Bottle & Dry Sample, w2	50.234	50.998
Mass of Bottle, Sample & Water, w3	96.347	96.416
Mass of Bottle & Water, w4	91.835	91.979
Specific Gravity, Gs	1.678	1.675
Average Specific Gravity, Gs	1.68	

3. Grain-size Analysis- Mechanical Method

The grain-size distribution data of the coal sample was obtained using standard soil classification methods and procedure.

The mass of pan & dry material before washing= 387.5 g
The mass of pan & dry material after washing= 197.9 g
Mass of pan= 189.6 g

Table A8 Particle Size Distribution

Sieve No.	Sieve Size (mm)	Retained by Sieve			Cumulative (%) Passing Sieve
		Mass (g)	% Of Total Mass	Cumulative % of Total Mass	
8	2.360	0	0	0	100.0
16	1.180	12.50	1.59	1.59	93.68
28	0.600	35.00	4.47	6.05	82.31
40	0.425	75.10	9.58	15.63	62.05
50	0.300	118.50	15.12	30.74	40.12
100	0.150	150.30	19.18	49.91	24.05
200	0.075	195.10	24.90	74.80	0.35
Pan	--	197.20	25.16	100.0	--
TOTAL	--	783.7	100.0	--	--

To detect any loss of coal tailings in the mechanical sieving operation:

Total $\sum$ weight retained= 197.2 g
Original weight of sample + weight of pan – weight of pan= 387.5 – 189.6= 197.9 g
197.2 / 197.9 * 100= 99.65 %
Therefore 0.35 % of sample is lost. Less than 2 % of sample is lost and sieving process is validated. More than 2 % of sample loss is unacceptable and the test should be repeated.

Less than 10% passes the # 200 sieve, a hydrometer analysis will not be performed. Since less than 10% is -#200 material, this completes the particle size analysis.

C. Sample Identification: GG1 DELKOR

1. Atterberg Limits

The coal samples in containers no. 25, 23 and 15 were subjected to 10, 25 and 48 number of blows respectively.

Table A9 Liquid limit

Container no.	10	20	23
No. Of Blows	10	25	48
Moisture Content (%)	34.52	30.45	27.83
Average Moisture Content Of Sample (%)	30.93		

Table A10 Plastic limit

Container no.	9	11
Moisture Content (%)	21.87	22.71
Average Moisture Content Of Sample (%)	22.26	

Plasticity Index:

PI = LL – PL
= 30.93 – 22.26
= 8.7 ~ 9

Trough no. B was used to determine linear shrinkage:

Length of dry sample = 148.3
Total shrinkage = 1.7
Linear shrinkage = 2.5

2. Specific Gravity

The experiment was undertaken using two sample bottles to obtain the average specific gravity.

Table A11 Specific Gravity

Bottle Number	4	6
Mass of Bottle, w1	29.701	28.609
Mass of Bottle & Dry Sample, w2	39.530	38.560
Mass of Bottle, Sample & Water, w3	81.694	82.178
Mass of Bottle & Water, w4	79.670	78.088
Specific Gravity, Gs	1.693	1.680
Average Specific Gravity, Gs	1.70	

3. Grain-size Analysis- Mechanical Method

The mass of pan & dry material before washing= 543.8 g. The mass of pan & dry material after washing= 338.1 g. Mass of pan= 190.2 g.

Table A12 Particle Size Distribution

Sieve No.	**Sieve Size (mm)**	**Retained by Sieve**			**Cumulative (%) Passing Sieve**
		Mass (g)	**% Of Total Mass**	**Cumulative % of Total Mass**	
8	2.360	0	0	0	100.0
16	1.180	1.7	0.22	0.22	98.85
28	0.600	18.7	3.81	3.81	87.36
40	0.425	38.3	7.32	11.13	74.10
50	0.300	60.7	11.60	22.73	58.96
100	0.150	108.4	20.72	43.45	26.71
200	0.075	147.4	28.20	71.65	0.22
Pan	--	148.7	28.25	100.0	--
TOTAL	--	523.1	100.0	--	--

To detect any loss of coal tailings in the mechanical sieving operation:

Total $\sum$ weight retained= 147.8 g
Original weight of sample – weight of pan= 338.1 – 190.2= 147.9 g
147.8 / 147.9 * 100= 99.93 %
Therefore 0.07 % of sample is lost. Less than 2 % of sample is lost and sieving process is validated. More than 2 % of sample loss is unacceptable and the test should be repeated.

Less than 10% passes the # 200 sieve, a hydrometer analysis will not be performed. Since less than 10% is -#200 material, this completes the particle size analysis.

D. Sample Identification: GG2 DELKOR

1. Atterberg Limits

The coal samples in containers no. 8, 10 and 11 were subjected to 10, 25 and 48 number of blows respectively.

Table A13 Liquid limit

Container no.	8	10	11
No. Of Blows	10	25	48
Moisture Content (%)	31.8	28.3	26.4
Average Moisture Content Of Sample (%)	28.8		

Table A14 Plastic limit

Container no.	15	21
Moisture Content (%)	22.9	21.8
Average Moisture Content Of Sample (%)	22.4	

Plasticity Index

The plastic index is calculated as the difference between the liquid and plastic limits.

PI = LL – PL
= 28.8 – 22.4
= 6.4 ~ 6
Trough no. A was used to determine linear shrinkage:

Length of dry sample = 146.7
Total shrinkage = 3.3
Linear shrinkage = 2.2

2. Specific Gravity

The standard test was undertaken using two sample bottles to obtain the average specific gravity.

Table A15 Specific Gravity

Bottle Number	10	11
Mass of Bottle, w1	39.985	39.977
Mass of Bottle & Dry Sample, w2	50.238	50.494
Mass of Bottle, Sample & Water, w3	95.630	95.541
Mass of Bottle & Water, w4	91.863	91.762
Specific Gravity, Gs	1.58	1.57
Average Specific Gravity, Gs	1.58	

3. Grain-size Analysis- Mechanical Method

The grain-size distribution data of the coal sample was obtained using standard soil classification methods and procedure.

The mass of pan & dry material before washing= 428.6 g
The mass of pan & dry material after washing= 388.4 g. The mass of pan= 189.6 g

Table A16 Particle Size Distribution

Sieve No.	Sieve Size (mm)	Retained by Sieve			Cumulative (%) Passing Sieve
		Mass (g)	% Of Total Mass	Cumulative % of Total Mass	
8	2.360	0	0	0	100.0
16	1.180	7.8	1.01	1.01	96.08
28	0.600	34.3	4.45	5.46	82.75
40	0.425	78.1	10.14	15.60	60.71
50	0.300	101.6	13.20	28.80	48.89
100	0.150	153.5	19.94	48.74	22.79
200	0.075	196.4	25.51	74.25	1.21
Pan	--	198.3	225.75	100.0	--
TOTAL	--	770.0	100.0	--	--

To detect any loss of coal tailings in the mechanical sieving operation:

Total $\sum$ weight retained= 198.3 g
Original weight of sample + weight of pan – weight of pan= 388.4 – 189.6= 198.8 g
198.3 / 198.8 * 100= 99.75 %
Therefore 0.25 % of sample is lost. Less than 2 % of sample is lost and sieving process is validated. More than 2 % of sample loss is unacceptable and the test should be repeated.

Less than 10% passes the # 200 sieve, a hydrometer analysis will not be performed. Since less than 10% is -#200 material, this completes the particle size analysis.

E. Sample Identification: GG1 THICKENER UNDERFLOW

1. Atterberg Limits

The coal samples in containers no. 4, 5 and 15 were subjected to 10, 25 and 48 number of blows respectively.

Table A17 Liquid limit

Container no.	4	5	15
No. Of Blows	10	25	48
Moisture Content (%)	32.0	29.4	27.1
Average Moisture Content Of Sample (%)	29.5		

Table A18 Plastic limit

Container no.	13	19
Moisture Content (%)	22.7	22.1
Average Moisture Content Of Sample (%)	22.4	

Plasticity Index

The plastic index is calculated as the difference between the liquid and plastic limits.

PI = LL – PL
= 29.5 – 22.4 = 7.1 ~ 7

Trough no. A was used to determine linear shrinkage:

Length of dry sample = 146.9. Total shrinkage is 3.1 and the Linear shrinkage become 2.1.

2. Specific Gravity

The standard test was undertaken using two sample bottles to obtain the average specific gravity.

Table A19 Specific Gravity

Bottle Number	9	11
Mass of Bottle, w1	39.078	39.977
Mass of Bottle & Dry Sample, w2	50.023	50.839
Mass of Bottle, Sample & Water, w3	95.561	95.701
Mass of Bottle & Water, w4	91.522	91.631
Specific Gravity, Gs	1.58	1.59
Average Specific Gravity, Gs	1.59	

3. Grain-size Analysis- Mechanical Method

The grain-size distribution data of the coal sample was obtained using standard soil classification methods and procedure.

The mass of pan & dry material before washing= 442.5 g
The mass of pan & dry material after washing= 390.1 g. Mass of pan= 189.8 g

Table A20 Particle Size Distribution

Sieve No.	**Sieve Size (mm)**	**Retained by Sieve**			**Cumulative (%) Passing Sieve**
		Mass (g)	**% Of Total Mass**	**Cumulative % of Total Mass**	
8	2.360	0	0	0	100.0
16	1.180	7.8	1.01	1.01	96.11
28	0.600	28.6	3.7	4.71	85.72
40	0.425	69.5	8.98	13.69	65.30
50	0.300	122.6	15.84	29.53	38.79
100	0.150	148.4	19.18	48.71	25.91
200	0.075	197.3	25.49	74.20	1.50
Pan	--	199.7	25.80	100.0	--
TOTAL	--	773.9	100.0	--	--

<u>To detect any loss of coal tailings in the mechanical sieving operation</u>:

Total ∑ weight retained= 102.1 g. Original weight of sample + weight of pan – weight of pan= 291.7 – 189.4= 102.3 g
199.7 / 200.3 * 100= 99.70 %
Therefore 0.3 % 0f sample is lost. Less than 2 % of sample is lost and sieving process is validated. Less than 10% passes the # 200 sieve, a hydrometer analysis will not be performed. Since less than 10% is -#200 material, this completes the particle size analysis.

APPENDIX B

MINERALOGICAL INVESTIGATIONS: RESULTS AND EQUIPMENT SETTINGS (Philips Analytical X-Ray B. V. + PC-APD, Diffraction Software)

A. SAMPLE IDENTIFICATION:	**GG 1 DELKOR**
Data measured at:	18 October 2004 9: 19: 00
Diffractometer type:	PW1710 BASED
Tube anode:	Cu
Generator tension [kV]:	40
Generator current [mA]:	20
Wavelength Alpha 1 [Å]:	1.54056
Wavelength Alpha 2 [Å]:	1.54439
Intensity ratio (alpha 2/ alpha 1):	0.500
Divergence slit:	1 °
Receiving slit:	0.1
Monochromator used:	YES
Start angle [° 2 θ]:	3.000
End angle [° 2 θ]:	70.000
Step size [° 2 θ]:	0.020
Maximum intensity:	449.4400
Time per step [s]:	0.800
Type of scan:	CONTINUOUS
Peak positions defined by:	Top of smoothed peak
Minimum peak tip width:	0.01
Maximum peak tip width:	1.00
Peak base width:	2.00
Minimum significance:	0.75
Number of peaks:	27

Angle [° 2 θ]	d-value α1 [Å]	d-value α2 [Å]	Peak width [° 2 θ]	Peak int. [counts]	Back. int. [%]	Rel. int. [%]	Signif.
3.200	27.5872	27.6558	0.400	6	34	1.3	1.04
12.440	7.1094	7.1271	0.200	100	35	22.2	3.27
19.970	4.4425	4.4535	0.200	49	37	10.9	1.24
20.450	4.3393	4.3500	0.200	58	37	12.9	1.13
20.970	4.2328	4.2433	0.140	121	36	26.9	2.29
21.330	4.1622	4.1725	0.240	48	36	10.6	1.40
23.185	3.8332	3.8427	0.240	42	34	9.4	1.39
24.985	3.5610	3.5698	0.080	119	30	26.4	1.23
26.730	3.3323	3.3406	0.160	449	28	100.0	9.88
29.515	3.0239	3.0314	0.200	55	24	12.2	2.94
30.910	2.8906	2.8977	0.240	28	22	6.2	1.63
32.065	2.7890	2.7960	0.240	10	20	2.3	1.37
35.105	2.5542	2.5605	0.240	27	18	6.0	2.28
36.085	2.4870	2.4932	0.240	23	19	5.1	2.05
36.650	2.4500	2.4560	0.160	29	20	6.5	1.32
37.760	2.3804	2.3864	0.120	15	21	3.4	0.75
38.490	2.3370	2.3428	0.200	37	22	8.3	1.52
39.525	2.2781	2.2838	0.160	40	23	8.8	0.79
42.705	2.1155	2.1208	0.060	46	19	10.3	1.45
44.915	2.0165	2.0215	0.400	6	18	1.4	0.90
45.885	1.9761	1.9810	0.280	18	19	4.1	1.62
50.225	1.8150	1.8195	0.200	41	16	9.1	1.99
55.160	1.6637	1.6679	0.960	13	17	2.9	3.65
60.015	1.5402	1.5440	0.160	37	12	8.3	1.25
62.415	1.4866	1.4903	0.400	21	12	4.7	2.71
64.140	1.4507	1.4544	0.320	8	12	1.7	0.75
68.250	1.3730	1.3765	0.480	22	11	4.9	3.06

Table B1 Quantification of Sample GG 1 DELKOR

R. M. S.: 0.000	
Sum before normalization: 49.1 %	
Normalized to: 100.0 %	
Sample type: Pressed powder	
Correction applied for medium: No	
Correction applied for film: None	
Used compound list: Sharon	

B. SAMPLE IDENTIFICATION: GG1 THICKENER UNDERFLOW

Data measured at:	15 October 2004 10: 59: 00
Diffractometer type:	PW1710 BASED
Tube anode:	Cu
Generator tension [kV]:	40
Generator current [mA]:	20
Wavelength Alpha 1 [Å]:	1.54056
Wavelength Alpha 2 [Å]:	1.54439
Intensity ratio (alpha 2/ alpha 1):	0.500
Divergence slit:	1 °
Receiving slit:	0.1
Monochromator used:	YES
Start angle [° 2 θ]:	3.000
End angle [° 2 θ]:	70.000
Step size [° 2 θ]:	0.020
Maximum intensity:	396. 0100
Time per step [s]:	0.800
Type of scan:	CONTINUOUS
Peak positions defined by:	Top of smoothed peak
Minimum peak tip width:	0.01
Maximum peak tip width:	1.00
Peak base width:	2.00
Minimum significance:	0.75
Number of peaks:	25

Angle [° 2 θ]	d-value α1 [Å]	d-value α2 [Å]	Peak width [° 2 θ]	Peak int. [counts]	Back. int. [%]	Rel. int. [%]	Signif.
3.380	26.1185	26.1834	0.640	9	28	2.3	1.79
12.405	7.1294	7.1471	0.200	72	35	18.2	1.66
19.935	4.4502	4.4612	0.240	29	53	7.4	1.09
20.445	4.3403	4.3411	0.160	37	55	9.4	0.95
20.905	4.2458	4.2564	0.200	81	55	20.5	2.41
24.970	3.5631	3.5719	0.240	66	56	16.6	1.84
26.745	3.3305	3.3388	0.200	396	45	100.0	12.20
29.565	3.0189	3.0264	0.160	37	30	9.4	1.60
30.975	2.8846	2.8918	0.200	28	26	7.1	1.33
32.050	2.7903	2.7972	0.280	8	24	2.1	1.63
35.515	2.5256	2.5319	0.120	32	19	8.2	1.00
36.660	2.4493	2.4554	0.120	29	19	7.4	1.18
38.510	2.3358	2.3416	0.240	27	20	6.8	3.73
39.555	2.2765	2.2821	0.160	35	20	8.8	0.76
40.400	2.2308	2.2363	0.320	15	20	3.8	1.01
42.550	2.1229	2.1282	0.160	25	21	6.3	1.10
45.835	1.9781	1.9830	0.320	15	18	3.8	1.04
47.605	1.9086	1.9133	0.480	9	18	2.3	1.40
50.260	1.8138	1.8183	0.100	48	17	12.0	0.81
55.145	1.6641	1.6683	0.480	14	17	3.6	3.72
60.030	1.5399	1.5437	0.320	27	10	6.8	1.95
62.465	1.4856	1.4893	0.480	15	10	3.8	2.30
64.085	1.4519	1.4555	0.320	9	10	2.3	0.82
65.620	1.4216	1.4251	0.800	1	10	0.3	0.92
68.285	1.3724	1.3758	0.240	24	11	6.1	0.76

Table B2 Quantification of Sample GG 1 Thickener Underflow

R. M. S.: 0.000
Sum before normalization: 52.1 %
Normalized to: 100.0 %
Sample type: Pressed powder
Correction applied for medium: No
Correction applied for film: None
Used compound list: Sharon

C. SAMPLE IDENTIFICATION:	**GG2 DELKOR**
Data measured at:	15 October 2004 12:05:00
Diffractometer type:	PW1710 BASED
Tube anode:	Cu
Generator tension [kV]:	40
Generator current [mA]:	20
Wavelength Alpha 1 [Å]:	1.54056
Wavelength Alpha 2 [Å]:	1.54439
Intensity ratio (alpha 2/ alpha 1):	0.500
Divergence slit:	1 °
Receiving slit:	0.1
Monochromator used:	YES
Start angle [° 2 θ]:	3.000
End angle [° 2 θ]:	70.000
Step size [° 2 θ]:	0.020

Maximum intensity:	466.5600
Time per step [s]:	0.800
Type of scan:	CONTINUOUS
Peak positions defined by:	Top of smoothed peak
Minimum peak tip width:	0.01
Maximum peak tip width:	1.00
Peak base width:	2.00
Minimum significance:	0.75
Number of peaks:	31

Angle [° 2 θ]	d-value α1 [Å]	d-value α2 [Å]	Peak width [° 2 θ]	Peak int. [counts]	Back. int. [%]	Rel. int. [%]	Signif.
12.350	7.1610	7.1788	0.100	102	35	21.9	1.15
19.890	4.4602	4.4712	0.200	44	36	9.3	1.46
20.335	4.3635	4.3744	0.200	58	36	12.4	1.61
20.860	4.2549	4.2655	0.160	88	35	18.9	1.61
23.080	3.8504	3.8600	0.320	30	31	6.5	1.44
24.895	3.5736	3.5825	0.200	112	29	24.1	2.50
26.660	3.3409	3.3492	0.180	467	27	100.0	12.88
29.455	3.0300	3.0375	0.160	24	23	5.1	1.00
30.835	2.8974	2.9046	0.240	36	21	7.7	2.37
32.005	2.7941	2.8011	0.480	10	19	2.2	1.90
33.050	2.7081	2.7149	0.240	9	18	1.9	0.77
34.990	2.5623	2.5687	0.160	37	18	8.0	0.87
35.435	2.5311	2.5374	0.160	29	18	6.2	0.75
35.965	2.4950	2.5012	0.280	19	18	4.1	1.14
36.515	2.4587	2.4648	0.060	37	18	8.0	0.88
37.705	2.3838	2.3897	0.240	17	18	3.6	1.05
38.405	2.3419	2.3478	0.240	38	18	8.2	1.14
39.435	2.2831	2.2888	0.120	38	18	8.2	1.12
40.245	2.2390	2.2446	0.240	15	18	3.3	0.77
41.045	2.1972	2.2027	0.200	16	18	3.4	0.88
42.395	2.1303	2.1356	0.200	25	18	5.4	1.39
43.125	2.0959	2.1011	0.240	12	18	2.5	1.55
45.730	1.9824	1.9873	0.240	15	19	3.3	1.04
50.050	1.8209	1.8255	0.060	45	16	9.6	0.80
54.545	1.6810	1.6862	0.060	22	15	4.7	0.82
54.905	1.6708	1.6750	0.480	17	16	3.6	1.53
59.910	1.5427	1.5465	0.160	34	11	7.2	0.78
62.240	1.4904	1.4941	0.320	18	11	3.8	1.07
63.995	1.4537	1.4573	0.480	7	11	1.4	1.44
67.700	1.3829	1.3863	0.080	19	10	4.1	0.89
68.180	1.3743	1.3777	0.320	25	10	5.4	1.54

Table B3 Quantification of Sample GG2 Delkor

R. M. S.: 0.000
Sum before normalization: 53.0 %
Normalized to: 100.0 %
Sample type: Pressed powder
Correction applied for medium: No
Correction applied for film: None
Used compound list: Sharon

D. SAMPLE IDENTIFICATION: **DELKOR 1**

Data measured at:	15 October 2004 13: 01: 00
Diffractometer type:	PW1710 BASED
Tube anode:	Cu
Generator tension [kV]:	40
Generator current [mA]:	20
Wavelength Alpha 1 [Å]:	1.54056
Wavelength Alpha 2 [Å]:	1.54439
Intensity ratio (alpha 2/ alpha 1):	0.500
Divergence slit:	1 °
Receiving slit:	0.1
Monochromator used:	YES
Start angle [° 2 θ]:	3.000
End angle [° 2 θ]:	70.000
Step size [° 2 θ]:	0.020
Maximum intensity:	449.4400
Time per step [s]:	0.800
Type of scan:	CONTINUOUS
Peak positions defined by:	Top of smoothed peak
Minimum peak tip width:	0.01
Maximum peak tip width:	1.00
Peak base width:	2.00
Minimum significance:	0.75
Number of peaks:	28

Angle [° 2 θ]	d-value α1 [Å]	d-value α2 [Å]	Peak width [° 2 θ]	Peak int. [counts]	Back. int. [%]	Rel. int. [%]	Signif.
11.205	7.8901	7.9097	0.060	0	31	0.0	0.86
12.435	7.1123	7.1300	0.240	90	32	20.1	3.95
19.930	4.4513	4.4624	0.060	83	38	18.4	1.07
20.435	4.3424	4.3532	0.120	61	38	13.5	1.15
20.955	4.2358	4.2463	0.120	112	37	25.0	2.08
23.170	3.8357	3.8452	0.240	41	34	9.1	0.90
24.980	3.5617	3.5705	0.200	119	31	26.4	3.16
26.740	3.3311	3.3394	0.180	449	28	100.0	12.42
29.530	3.0224	3.0299	0.120	31	24	7.0	1.07
30.950	2.8869	2.8941	0.320	36	22	8.0	2.37
33.105	2.7037	2.7105	0.240	12	19	2.7	1.53
35.050	2.5580	2.5644	0.320	22	18	4.9	1.14
36.045	2.4897	2.4959	0.060	71	18	15.7	1.36
36.610	2.4525	2.4586	0.240	22	18	4.9	2.35
38.500	2.3364	2.3422	0.160	44	18	9.7	0.77
39.570	2.2756	2.2813	0.060	41	18	9.1	1.09
41.165	2.1911	2.1965	0.400	14	18	3.2	1.35
42.550	2.1229	2.1282	0.120	24	18	5.3	1.46
44.890	2.0175	2.0225	0.240	10	18	2.1	0.98
45.780	1.9803	1.9853	0.480	16	18	3.6	2.53
50.235	1.8147	1.8192	0.080	42	16	9.4	0.94
55.175	1.6633	1.6674	0.640	19	14	4.3	2.01
56.625	1.6241	1.6281	0.800	5	13	1.2	0.78
60.055	1.5393	1.5431	0.120	66	11	14.6	4.06
60.215	1.5356	1.5394	0.060	42	11	9.4	0.98
62.450	1.4859	1.4896	0.120	26	11	5.8	0.78

64.125	1.4510	1.4547	0.480	7	10	1.6	1.21
68.260	1.3729	1.3763	0.320	26	11	5.8	1.82

Table B4 Quantification of Sample Delkor 1

R. M. S.: 0.000
Sum before normalization: 54.7 %
Normalized to: 100.0 %
Sample type: Pressed powder
Correction applied for medium: No
Correction applied for film: None
Used compound list: Sharon

E. SAMPLE IDENTIFICATION:	**DELKOR 2**
Data measured at:	15 October 2004 14: 30: 00
Diffractometer type:	PW1710 BASED
Tube anode:	Cu
Generator tension [kV]:	40
Generator current [mA]:	20
Wavelength Alpha 1 [Å]:	1.54056
Wavelength Alpha 2 [Å]:	1.54439
Intensity ratio (alpha 2/ alpha 1):	0.500
Divergence slit:	1 °
Receiving slit:	0.1
Monochromator used:	YES
Start angle [° 2 θ]:	3.000
End angle [° 2 θ]:	70.000
Step size [° 2 θ]:	0.020
Maximum intensity:	441.0000
Time per step [s]:	0.800
Type of scan:	CONTINUOUS
Peak positions defined by:	Top of smoothed peak
Minimum peak tip width:	0.01
Maximum peak tip width:	1.00
Peak base width:	2.00
Minimum significance:	0.75
Number of peaks:	29

Angle [° 2 θ]	d-value α1 [Å]	d-value α2 [Å]	Peak width [° 2 θ]	Peak int. [counts]	Back. int. [%]	Rel. int. [%]	Signif. L
12.420	7.1208	7.1385	0.080	108	31	24.5	0.94
19.890	4.4602	4.4712	0.160	44	36	9.9	1.84
20.390	4.3519	4.3627	0.160	62	36	14.2	0.96
20.925	4.2418	4.2524	0.140	100	35	22.7	2.03
21.350	4.1583	4.1687	0.240	58	35	13.1	1.19
23.165	3.8365	3.8460	0.240	45	31	10.2	1.07
24.920	3.5701	3.5790	0.200	117	29	26.4	2.45
26.700	3.3360	3.3443	0.220	441	27	100.0	18.84
29.555	3.0199	3.0274	0.080	56	23	12.8	0.85
30.940	2.8878	2.8950	0.320	34	21	7.6	3.38
32.065	2.7890	1.7960	0.240	14	19	3.1	0.93
33.090	2.7049	2.7117	0.240	8	18	1.8	1.04
35.070	2.5566	2.5630	0.320	26	17	5.9	1.02
36.030	2.4907	2.4969	0.160	34	17	7.6	1.03
36.585	2.4542	2.4603	0.160	36	18	8.2	1.04
38.480	2.3375	2.3434	0.280	46	18	10.5	2.82
39.490	2.2801	2.2857	0.160	42	18	9.6	0.94
40.340	2.2339	2.2395	0.400	10	18	2.3	0.99
42.470	2.2167	2.1320	0.240	17	18	3.8	1.73
45.670	1.9849	1.9898	0.480	13	18	2.9	1.70
50.185	1.8164	1.8209	0.240	41	15	9.3	2.33
52.725	1.7347	1.7390	0.480	3	13	0.7	0.86
54.995	1.6683	1.6725	0.240	22	13	5.0	0.95
56.425	1.6294	1.6334	0.480	10	13	2.2	0.92
59.980	1.5410	1.5449	0.120	46	12	10.5	0.88
62.370	1.4876	1.4913	0.320	23	11	5.2	1.70
64.145	1.4506	1.4542	0.400	7	11	1.5	1.02
67.750	1.3820	1.3854	0.120	19	10	4.4	0.78
68.190	1.3741	1.3775	0.240	24	10	5.4	2.11

Table B5 Quantification of Sample Delkor 2

R. M. S.: 0.000
Sum before normalization: 52.5 %
Normalized to: 100.0 %
Sample type: Pressed powder
Correction applied for medium: No
Correction applied for film: None
Used compound list: Sharon

APPENDIX C

EXPERIMENTAL RESULTS: EFFECT OF DIFFERENCE IN INITIAL WATER CONTENT

TEST 3

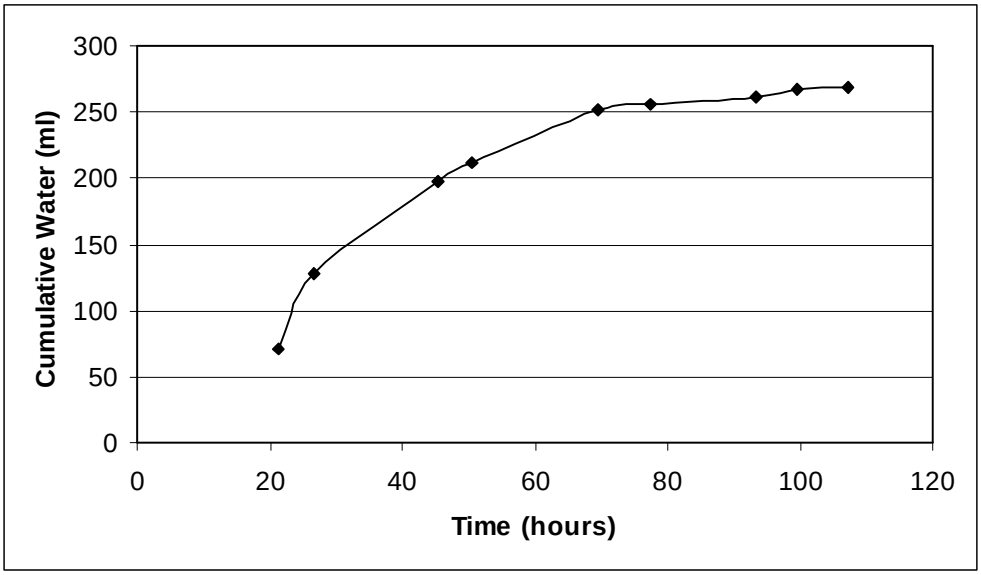


Figure C1 Cumulative Water versus Time

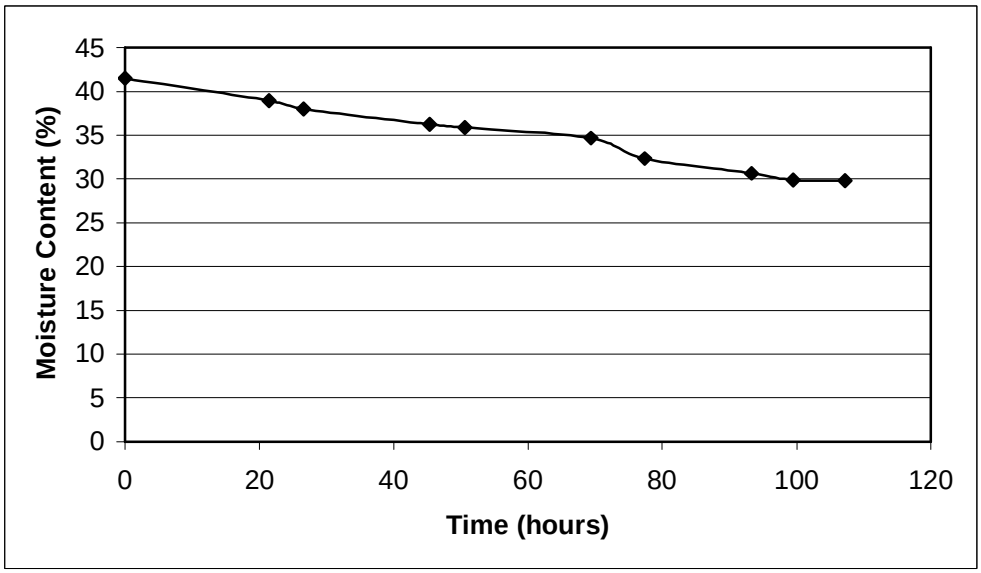


Figure C2 Variation in Moisture Content versus Time

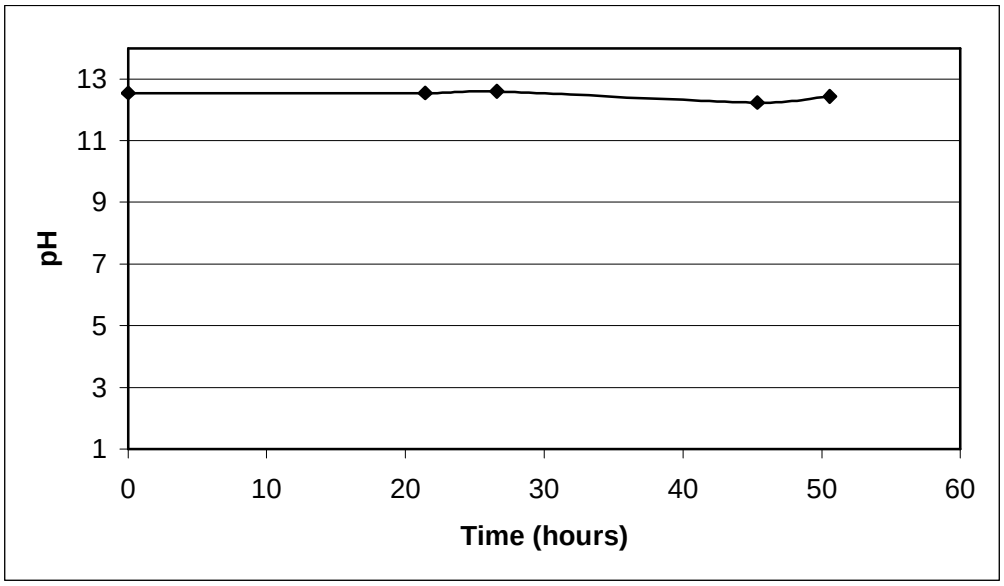


Figure C3 pH versus Time

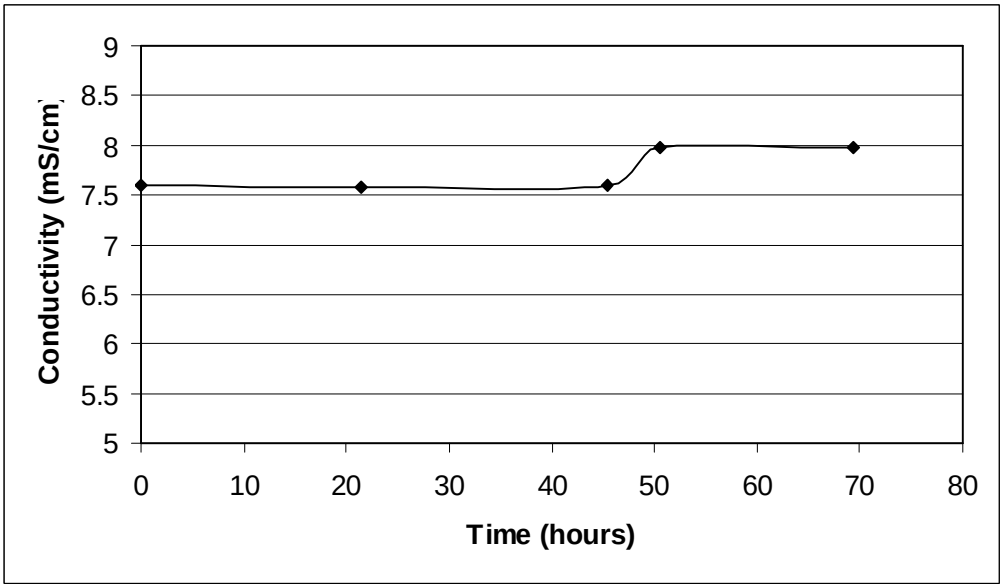


Figure C4 Conductivity versus Time

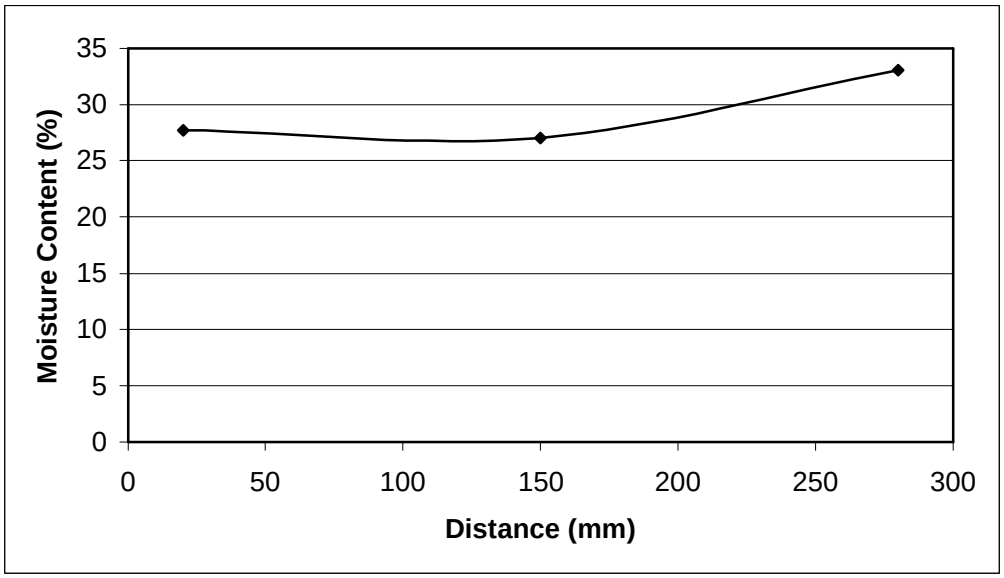


Figure C5 Variation in Final moisture content from Anode to Cathode

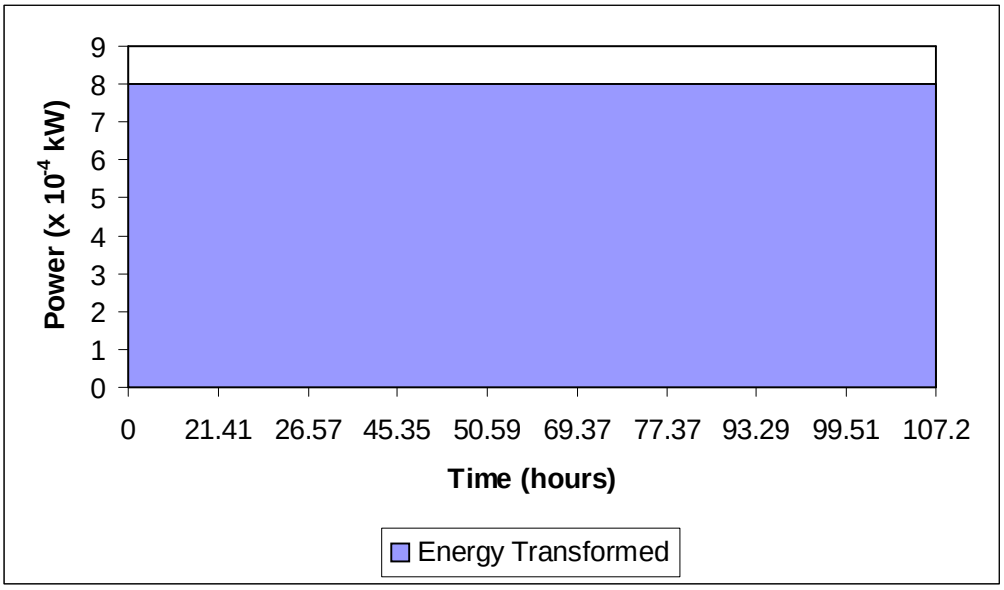


Figure C6 Power versus Time

TEST 4

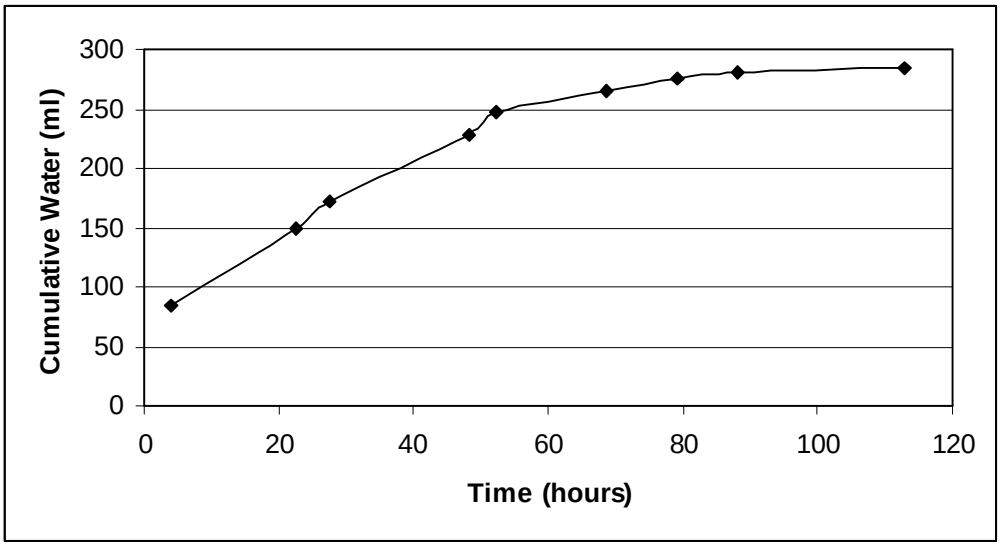


Figure C7 Cumulative Water versus Time

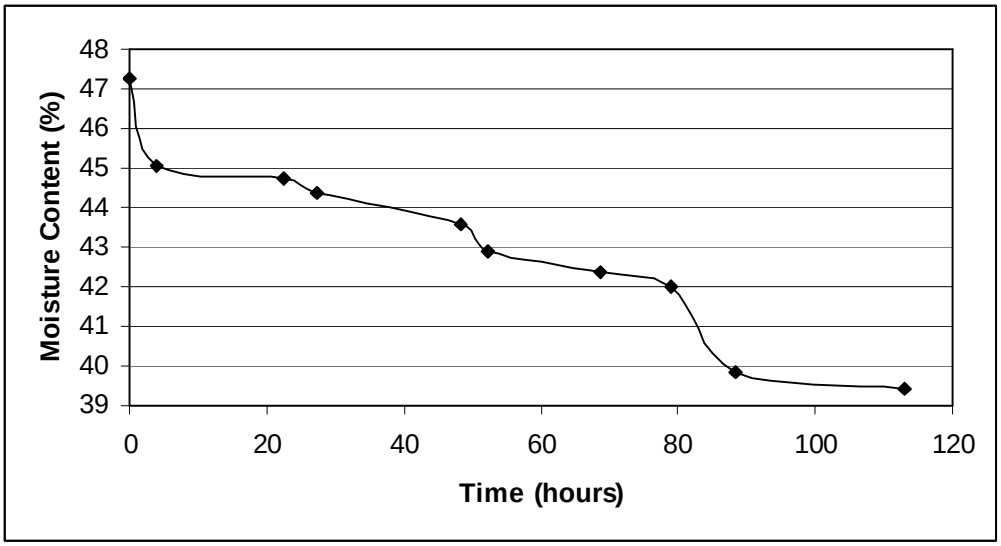


Figure C8 Variation in Moisture Content versus Time

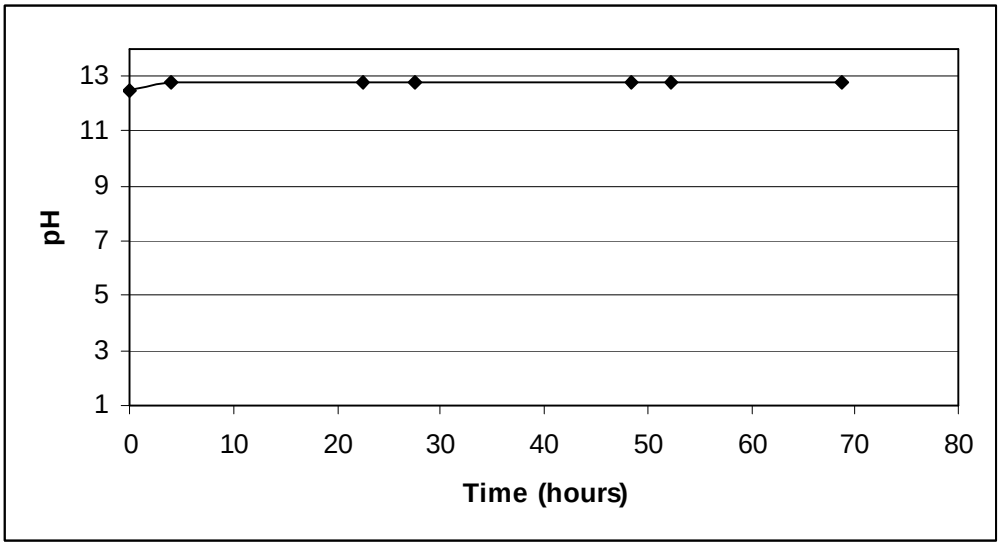


Figure C9 pH versus Time

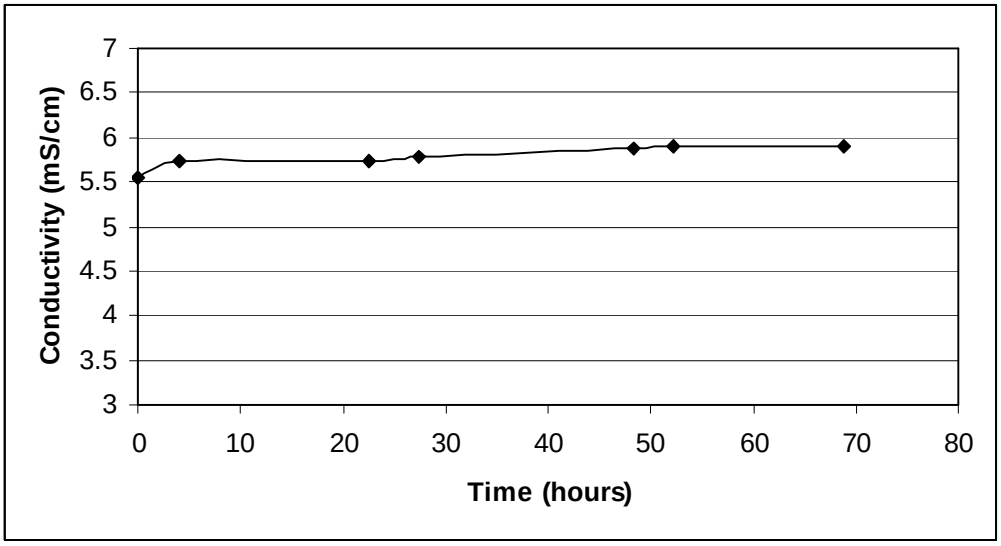


Figure C10 Conductivity versus Time

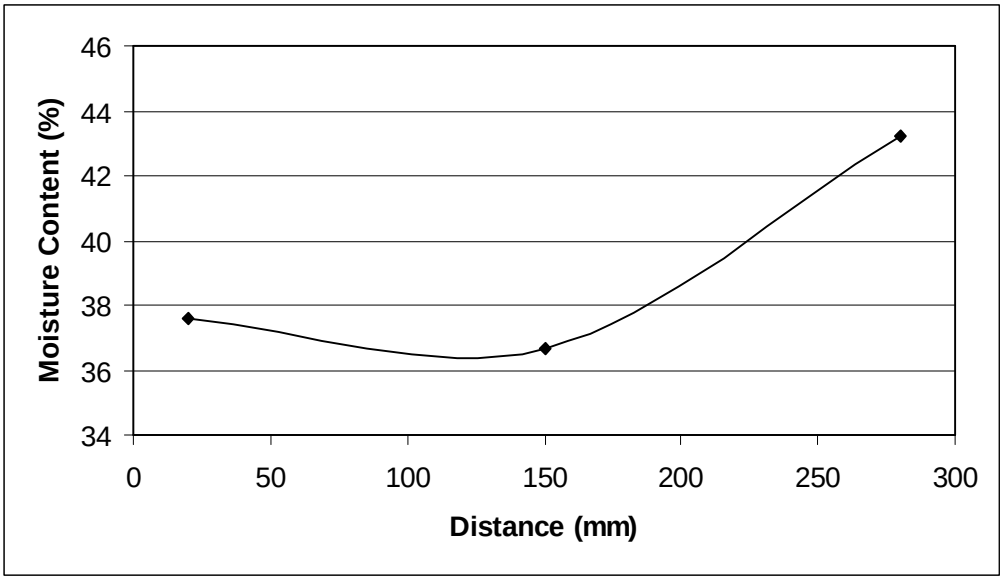


Figure C11 Variation in final Moisture Content from Anode to Cathode

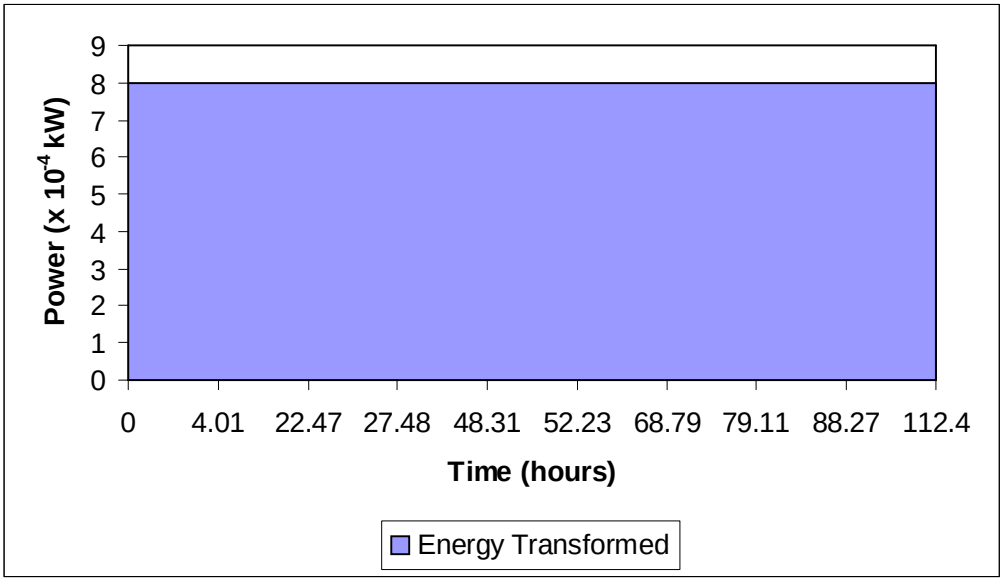


Figure C12 Power versus Time

TEST 5

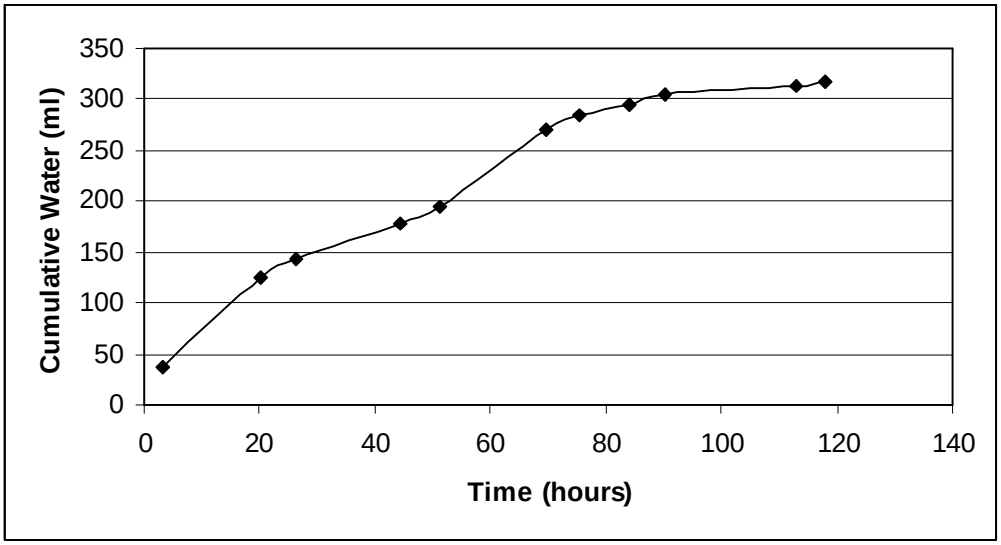


Figure C13 Cumulative Water versus Time

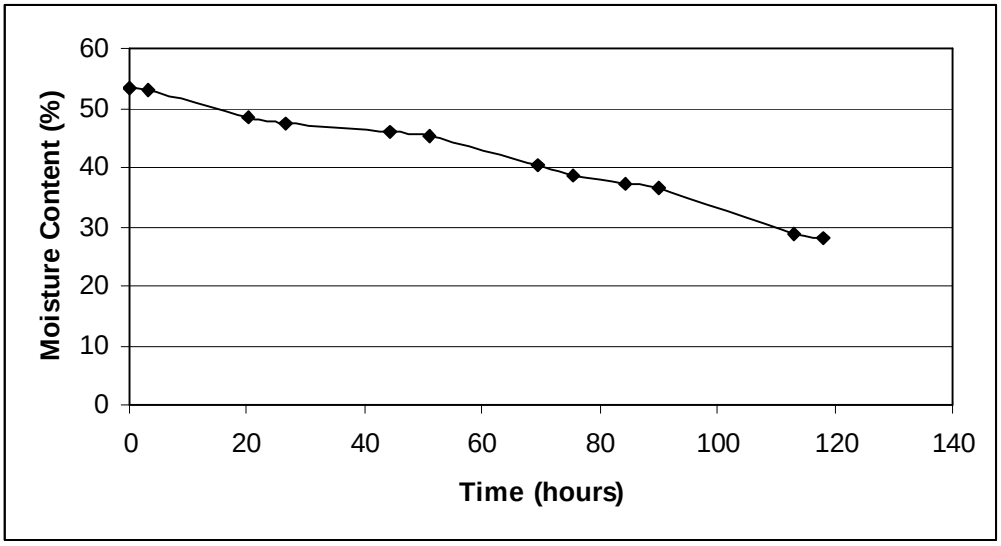


Figure C14 Variation of Moisture Content versus Time

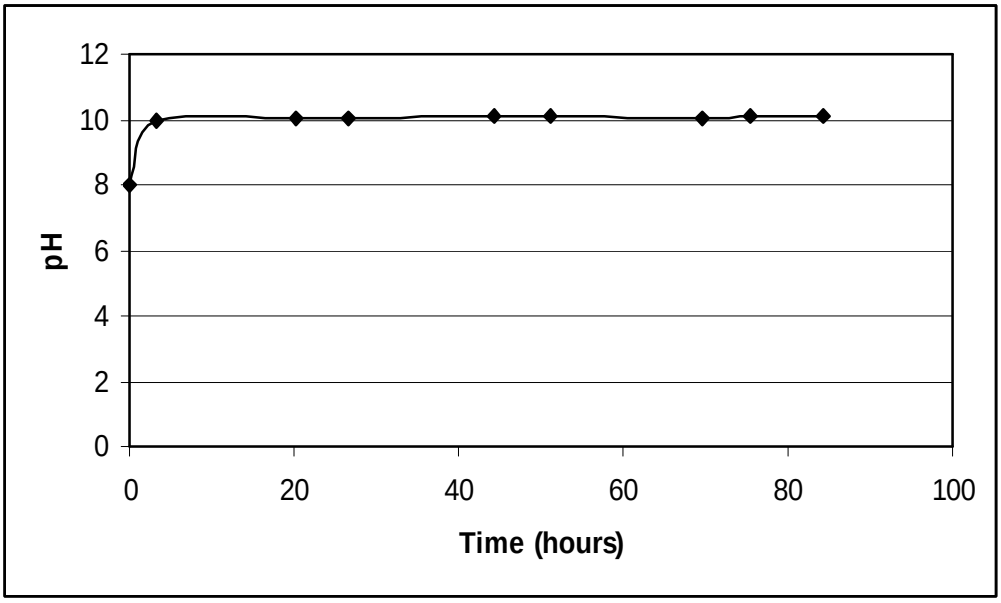


Figure C15 pH versus Time

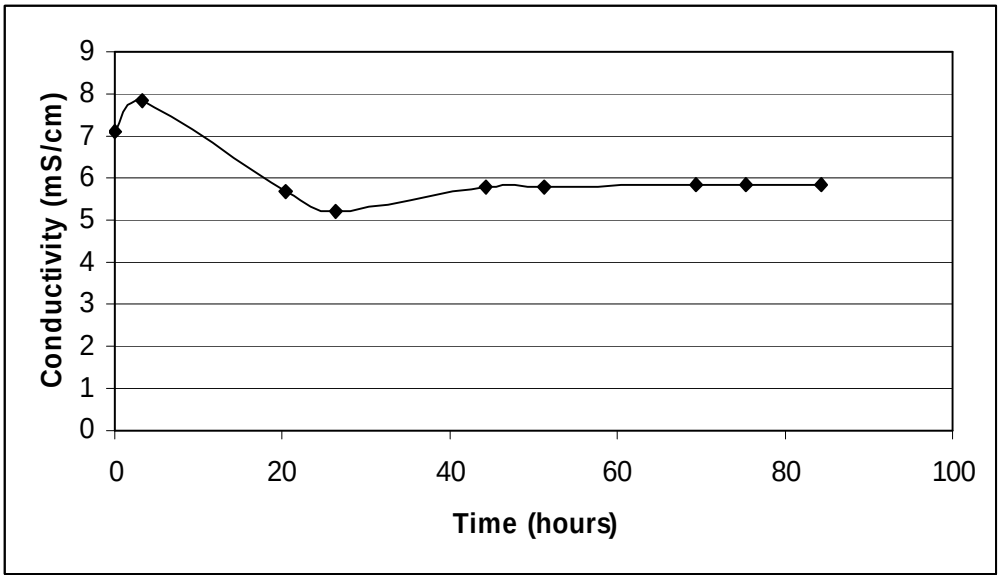


Figure C16 Conductivity versus Time

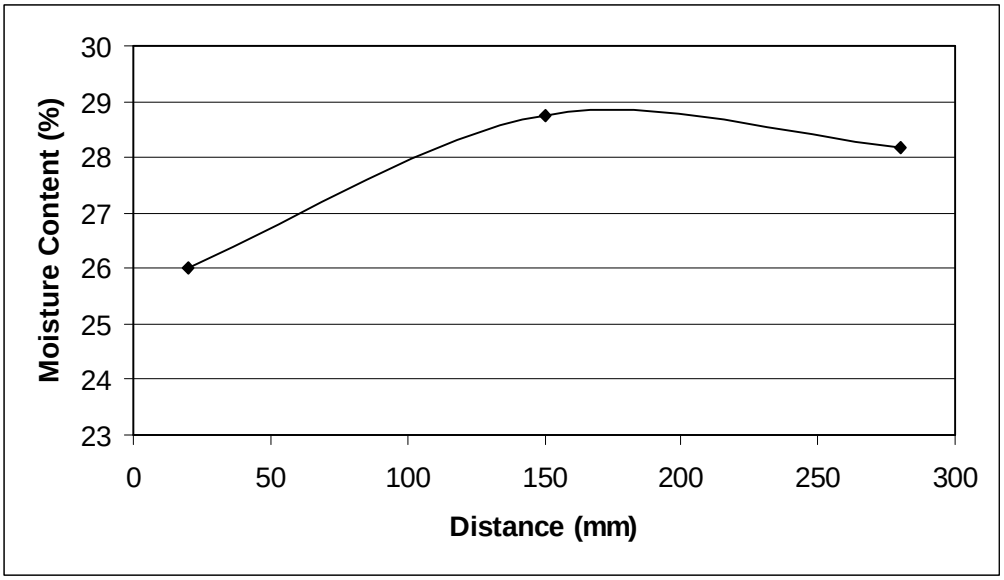


Figure C17 Variation in Final Moisture Content from Anode to Cathode

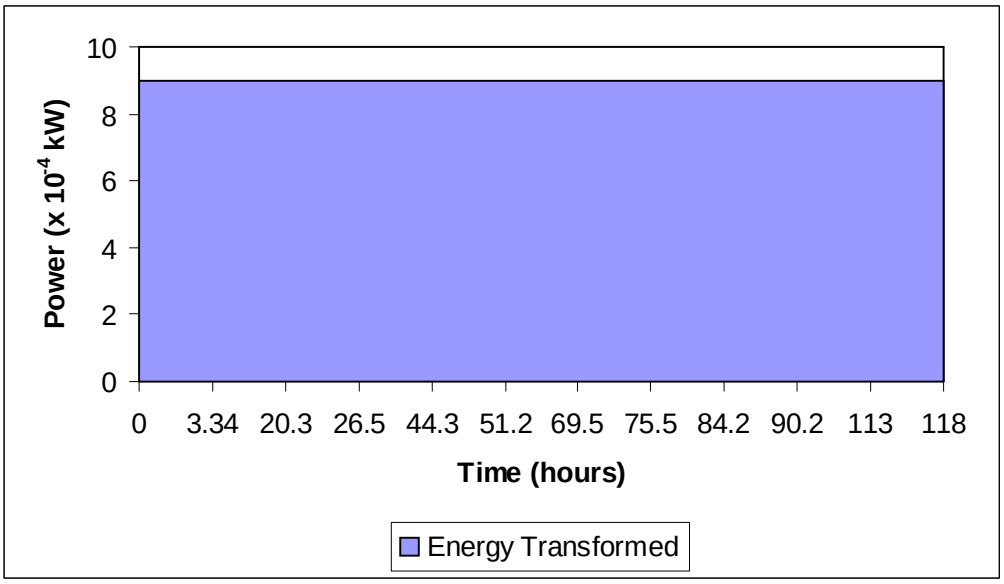


Figure C18 Power versus Time

TEST 6

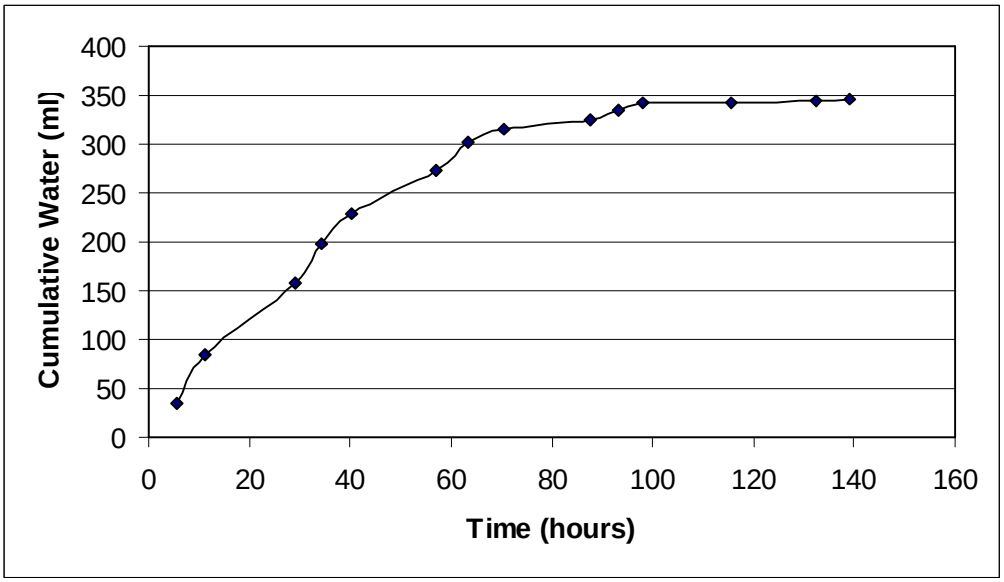


Figure C19 Cumulative Water vs. Time

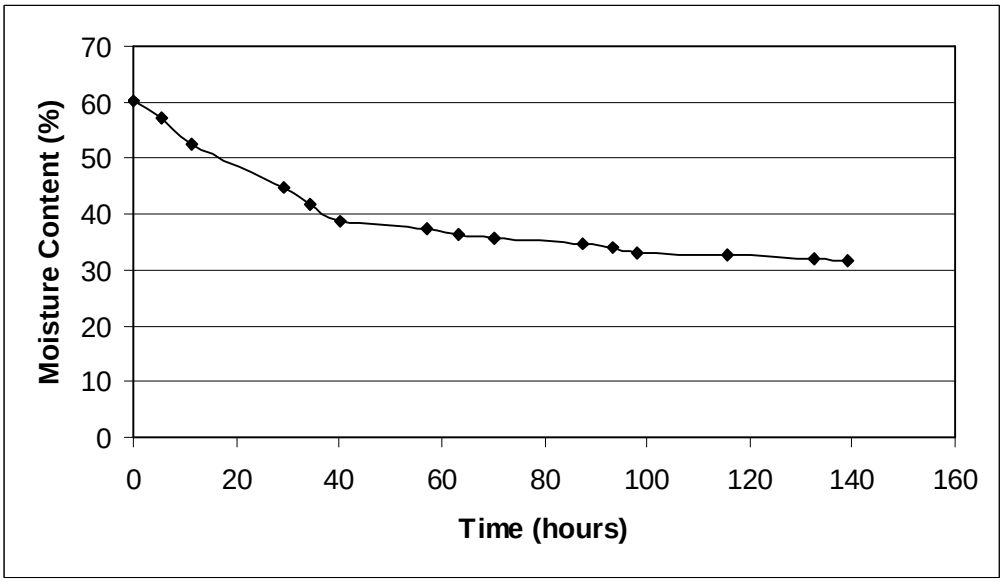


Figure C20 Variation of Moisture Content with Time

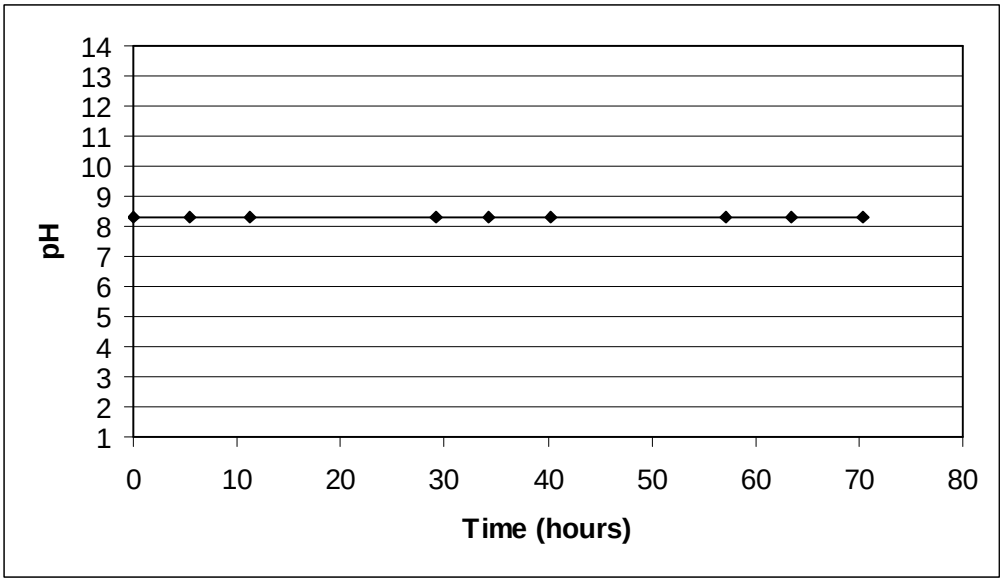


Figure C21 pH vs. Time

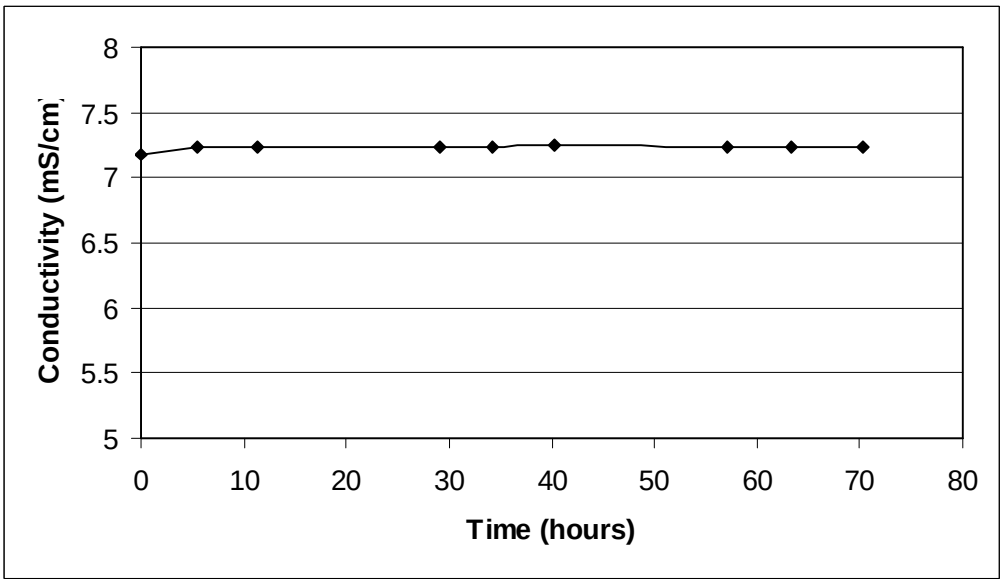


Figure C22 Conductivity vs. Time

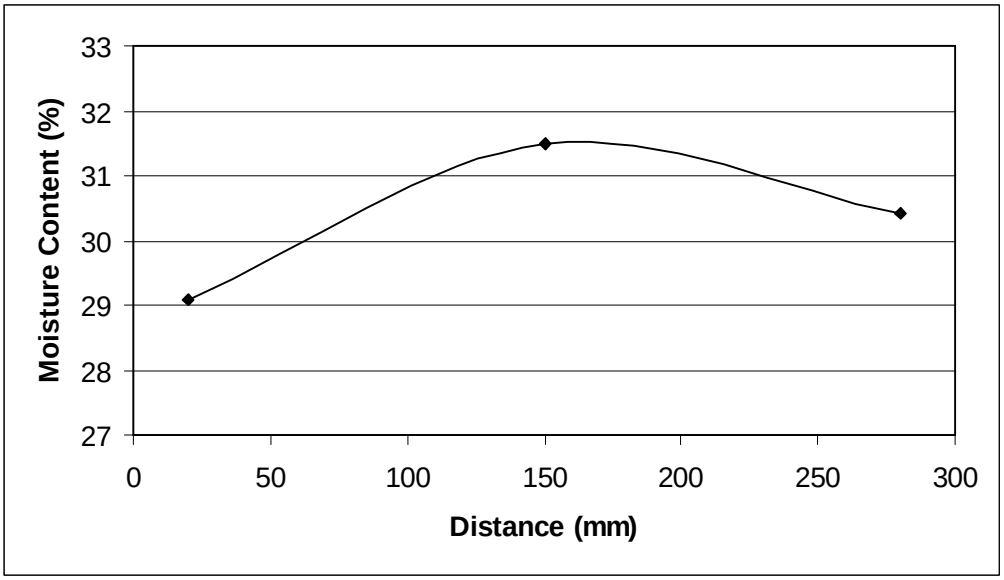


Figure C23 Variation in Moisture Content from Anode to Cathode

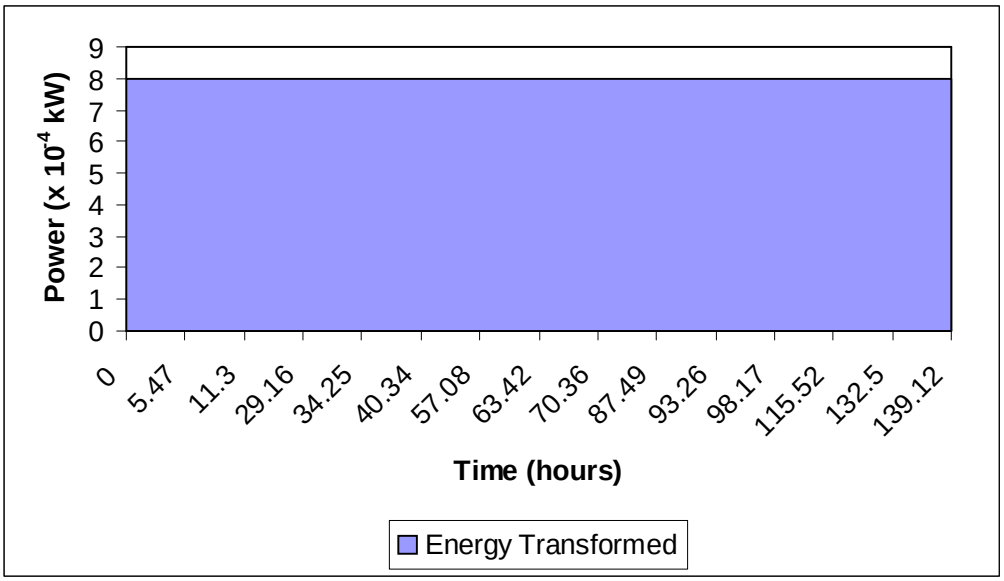


Figure C24 Power versus Time

TEST 7

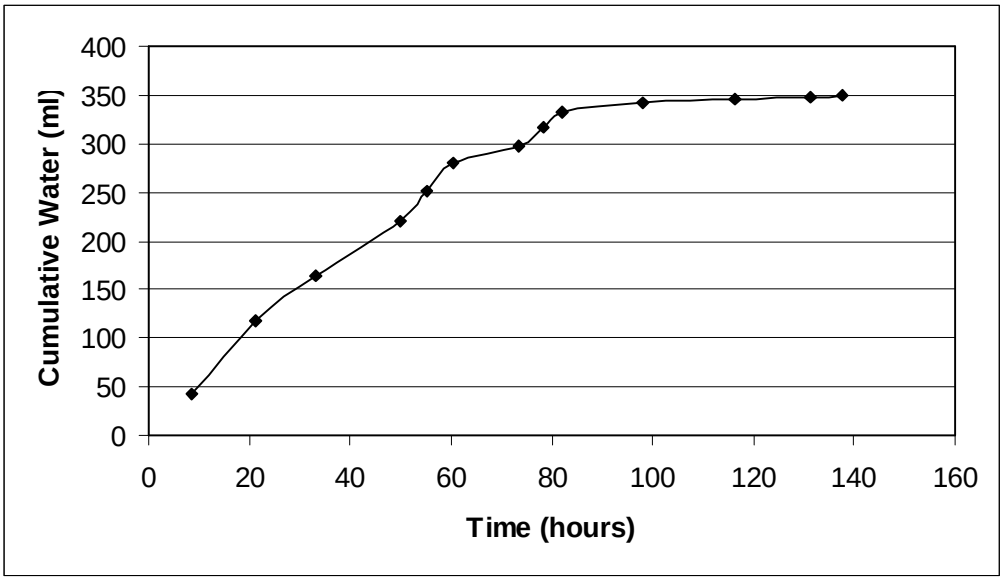


Figure C25 Cumulative Water vs. Time

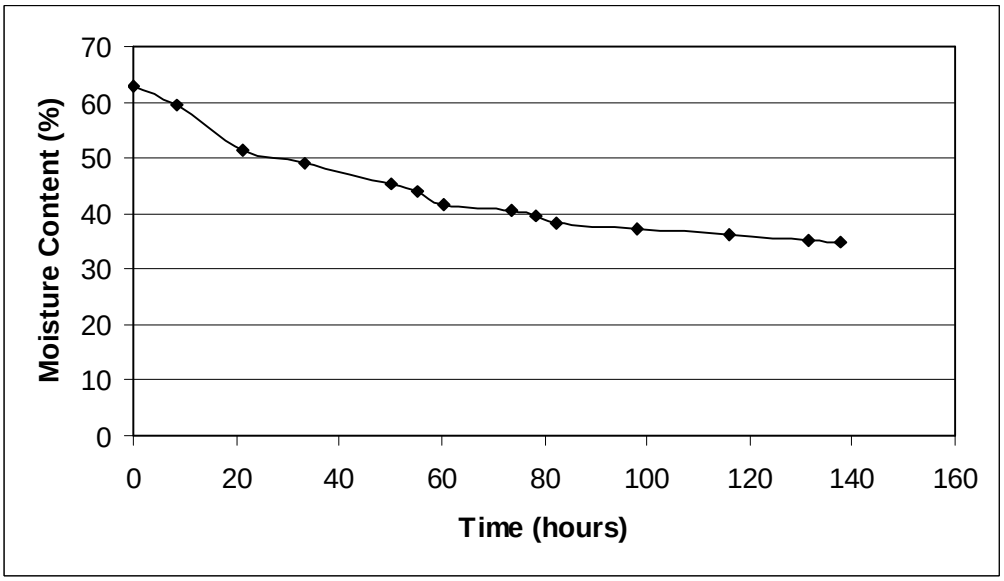


Figure C26 Variation of Moisture Content with Time

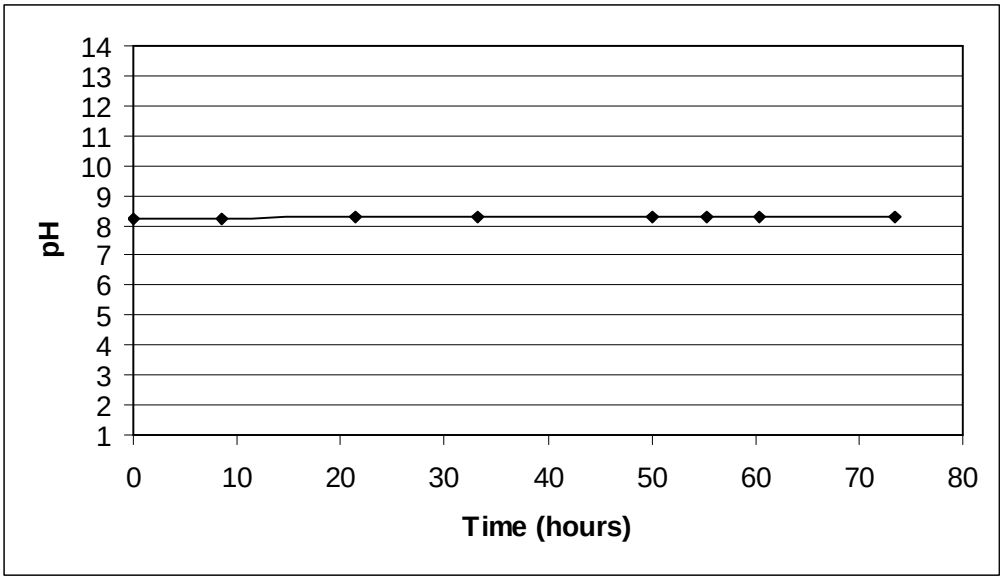


Figure C27 pH vs. Time

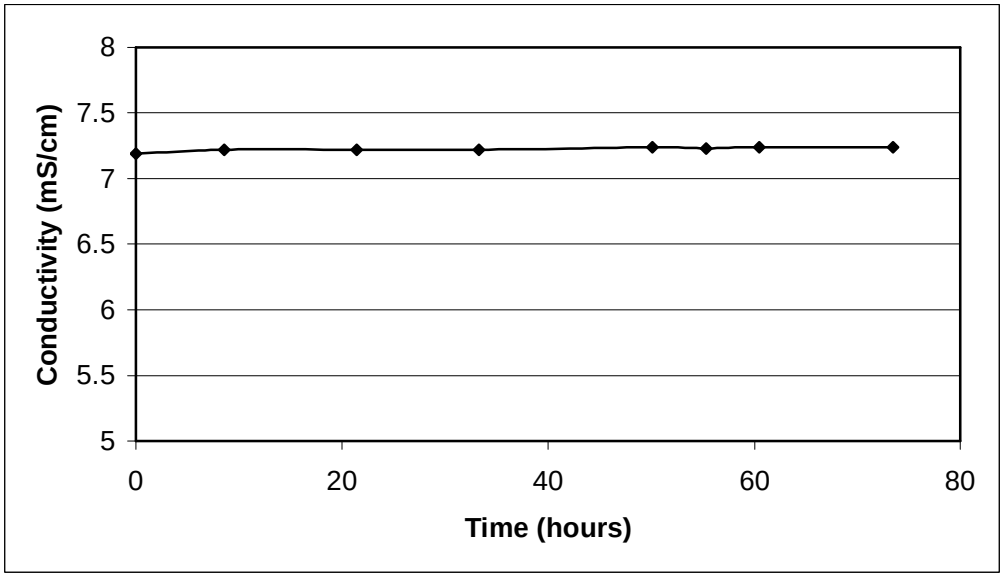


Figure C28 Conductivity vs. Time

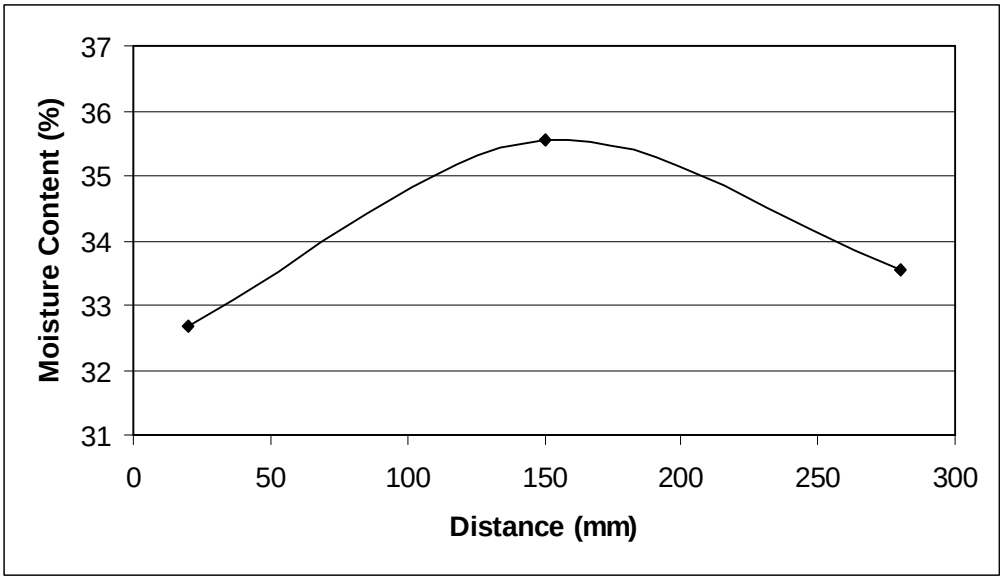


Figure C29 Variation in Moisture Content from Anode to Cathode

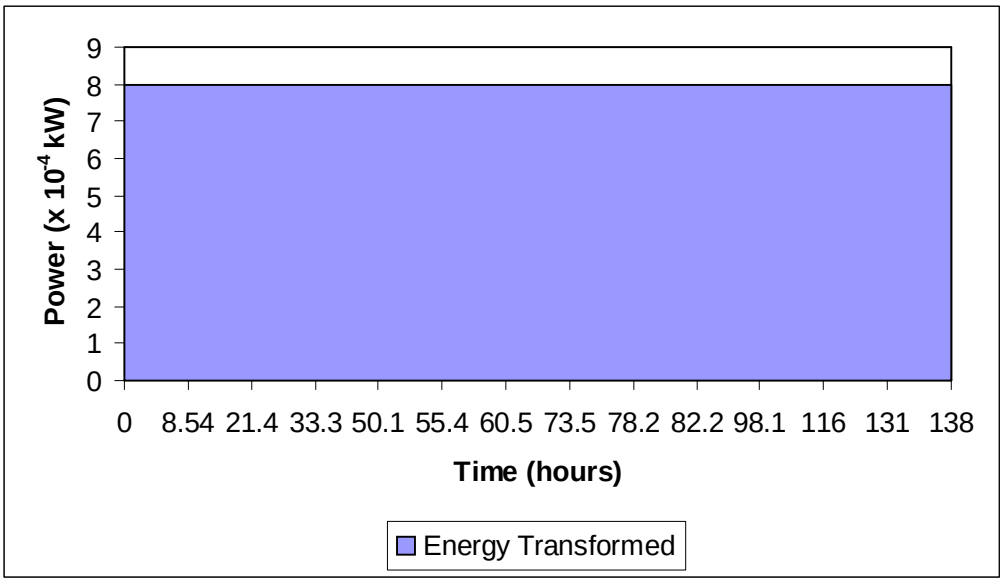


Figure C30 Power versus Time

TEST 8

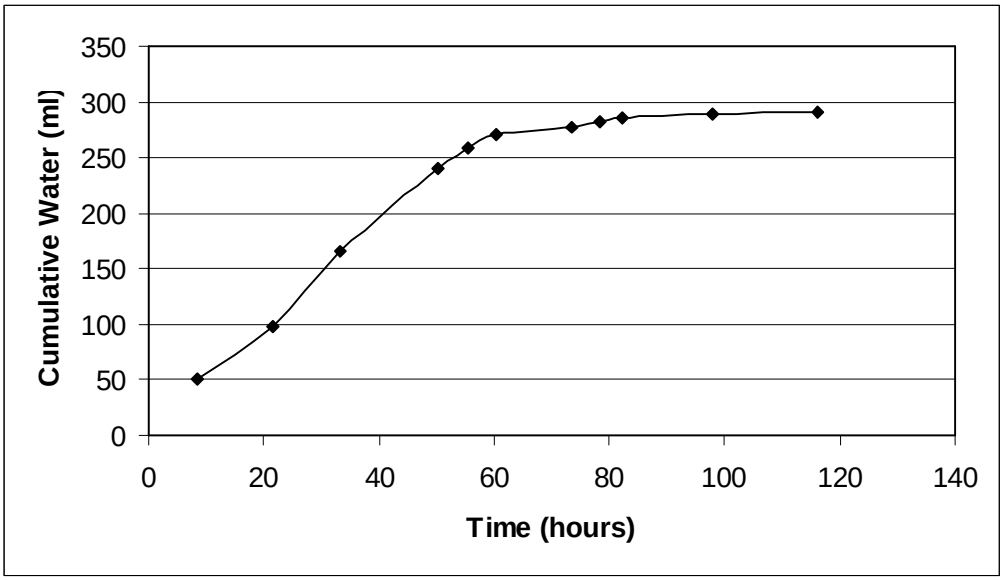


Figure C31 Cumulative Water vs. Time

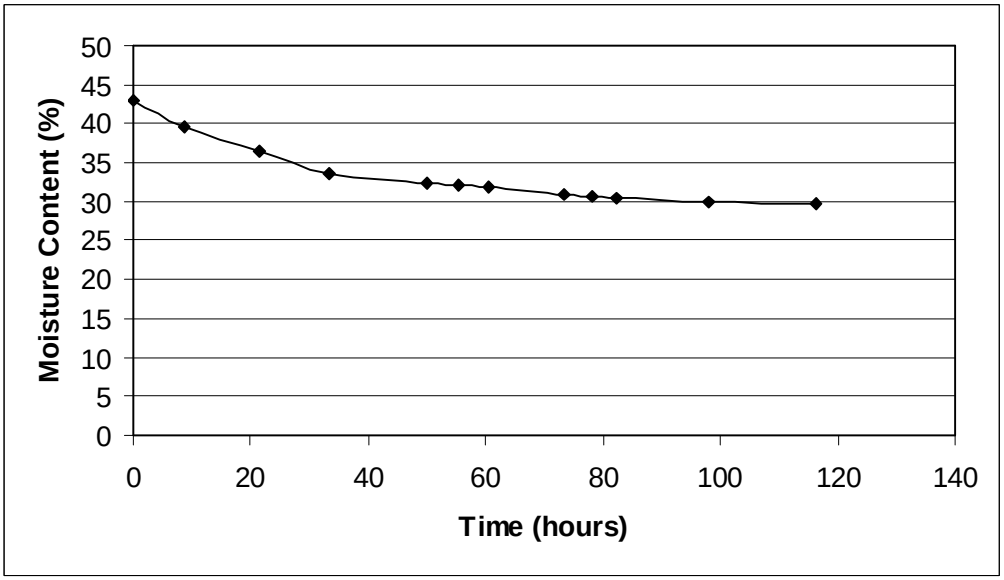


Figure C32 Variation of Moisture Content with Time

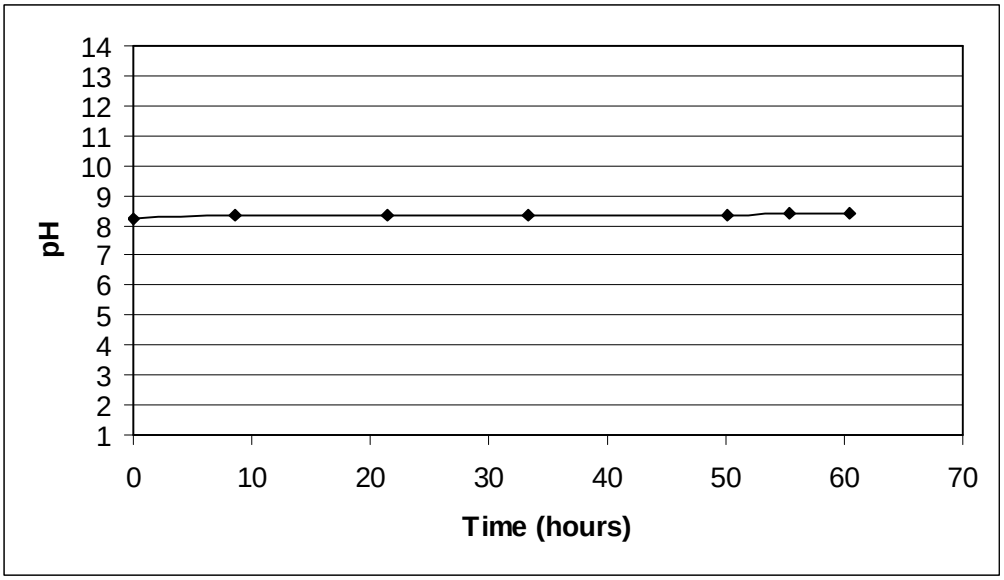


Figure C33 pH vs. Time

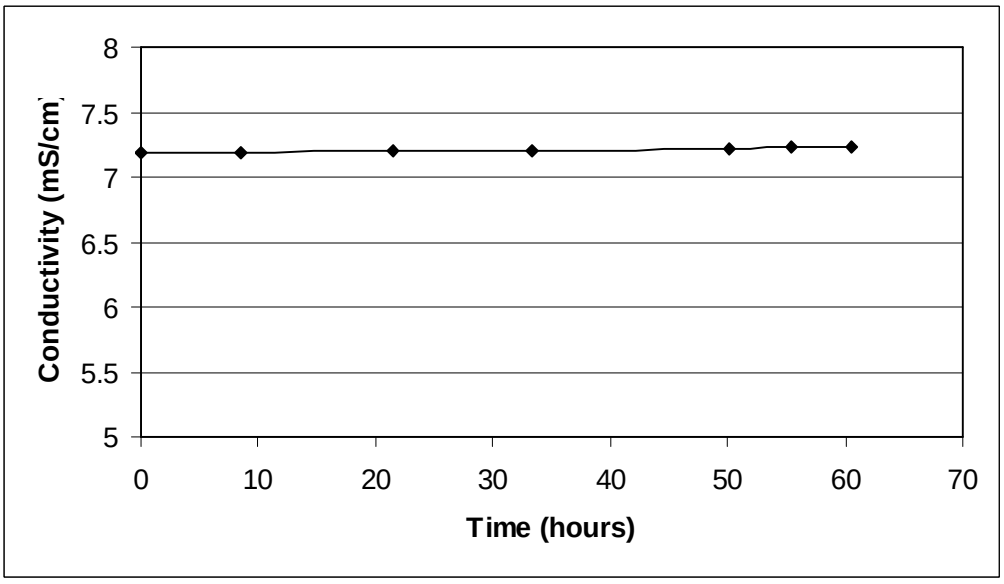


Figure C34 Conductivity vs. Time

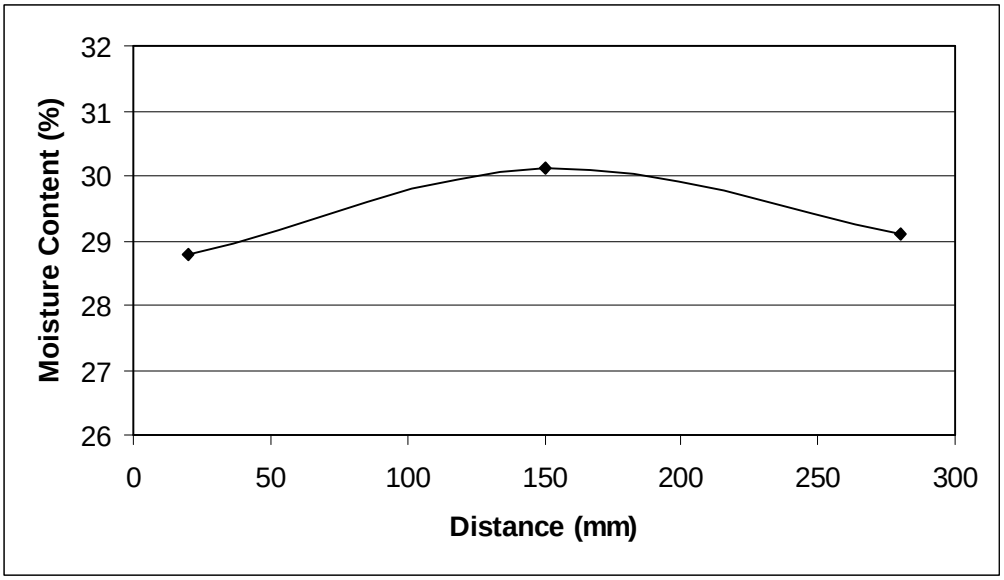


Figure C35 Variation in Moisture Content from Anode to Cathode

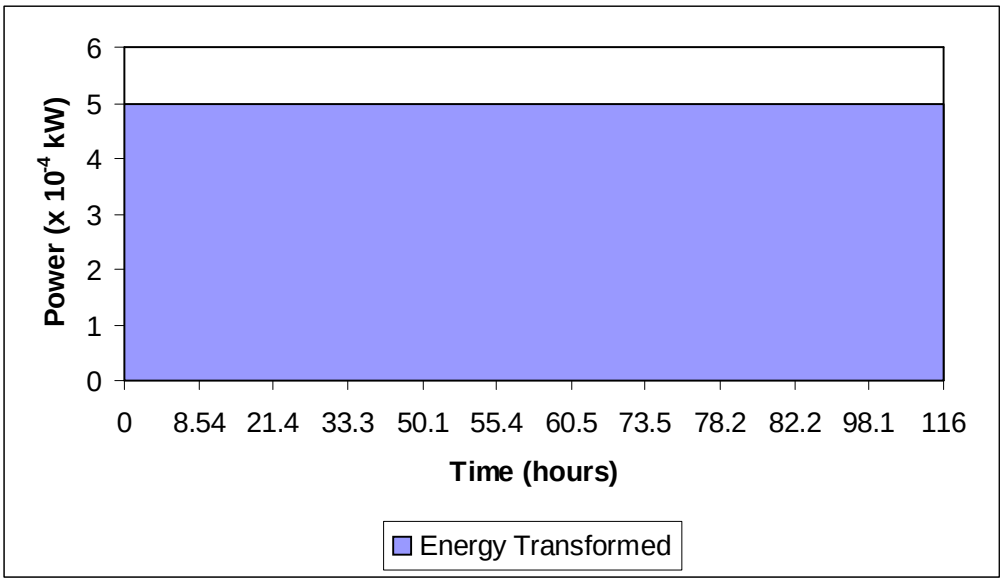


Figure C36 Power versus Time

TEST 9

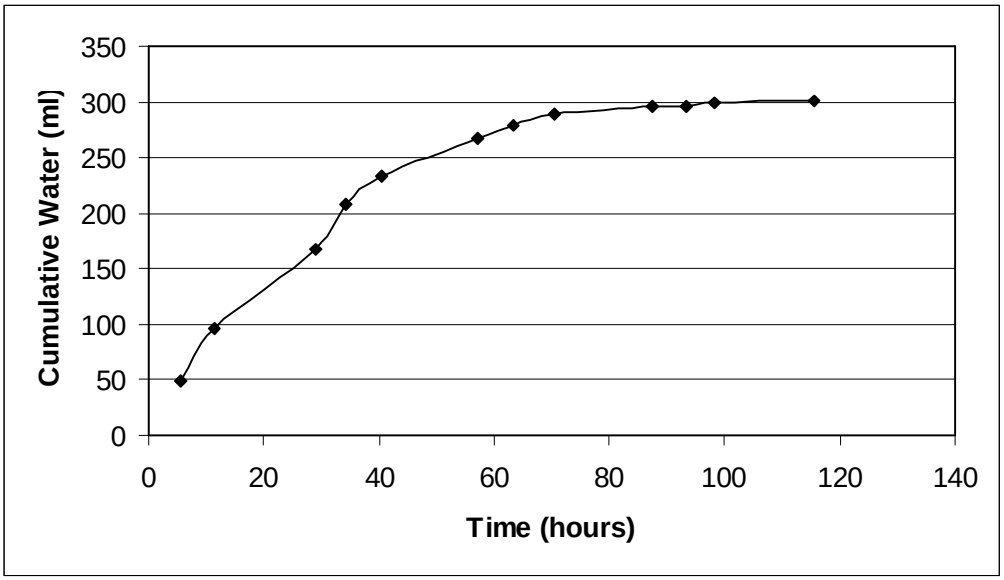


Figure C37 Cumulative Water vs. Time

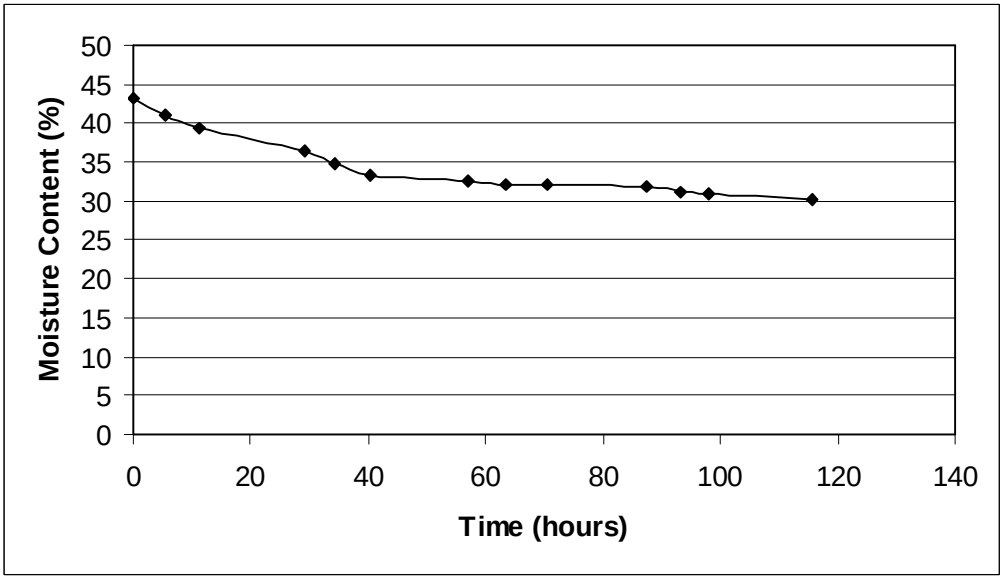


Figure C38 Variation of Moisture Content with Time

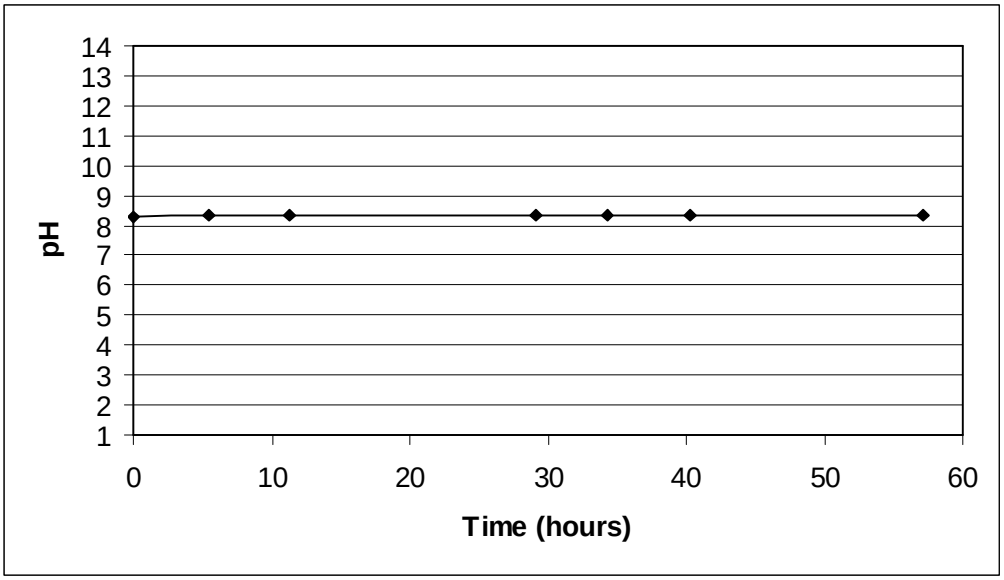


Figure C39 Conductivity vs. Time

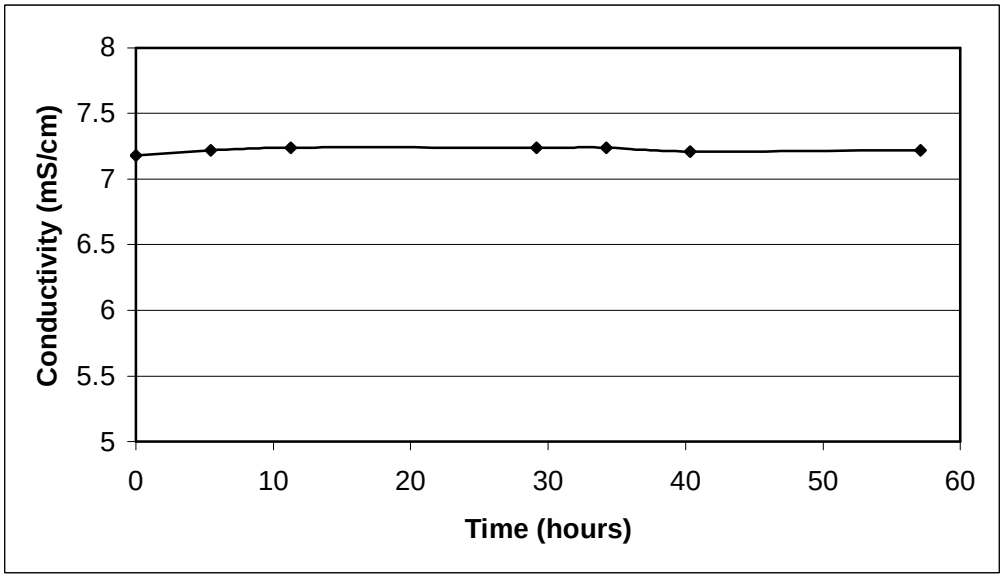


Figure C40 Conductivity vs. Time

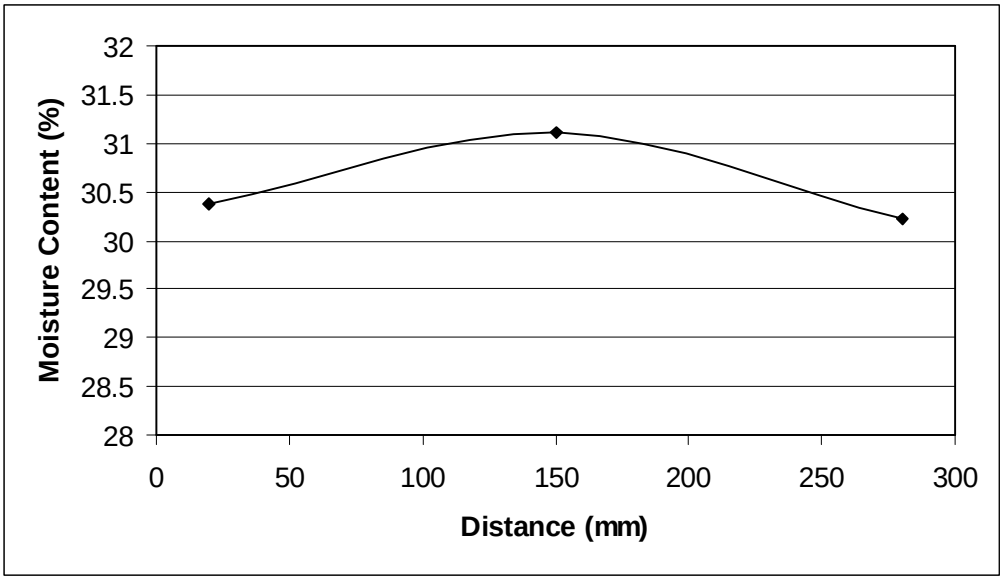


Figure C41 Variation in Moisture Content from Anode to Cathode

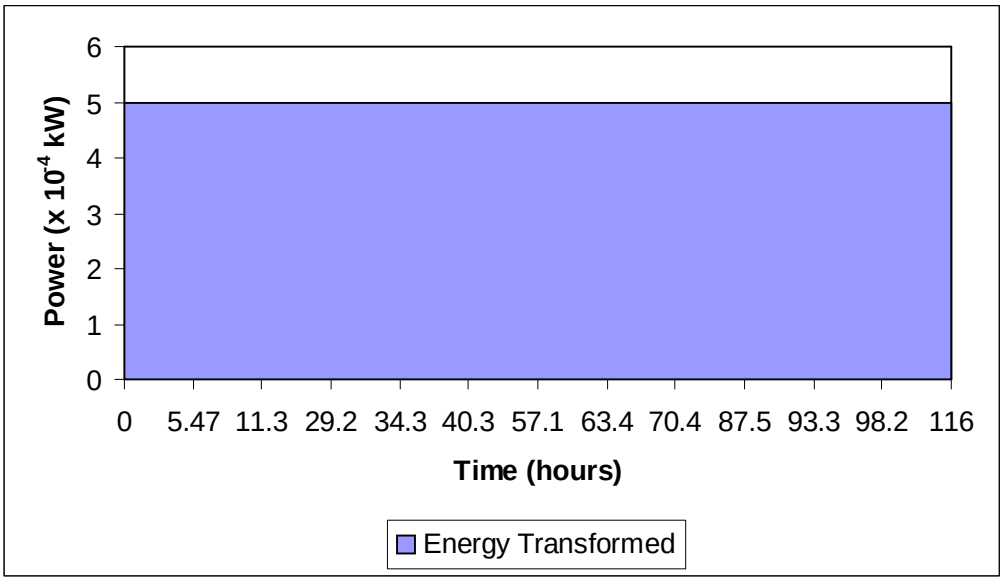


Figure C42 Power versus Time

TEST 10

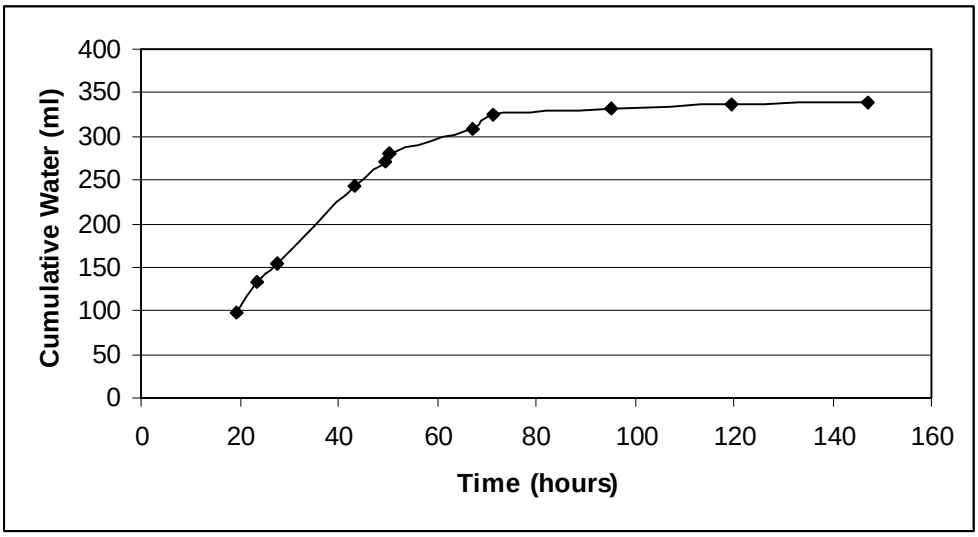


Figure C43 Cumulative Water versus Time

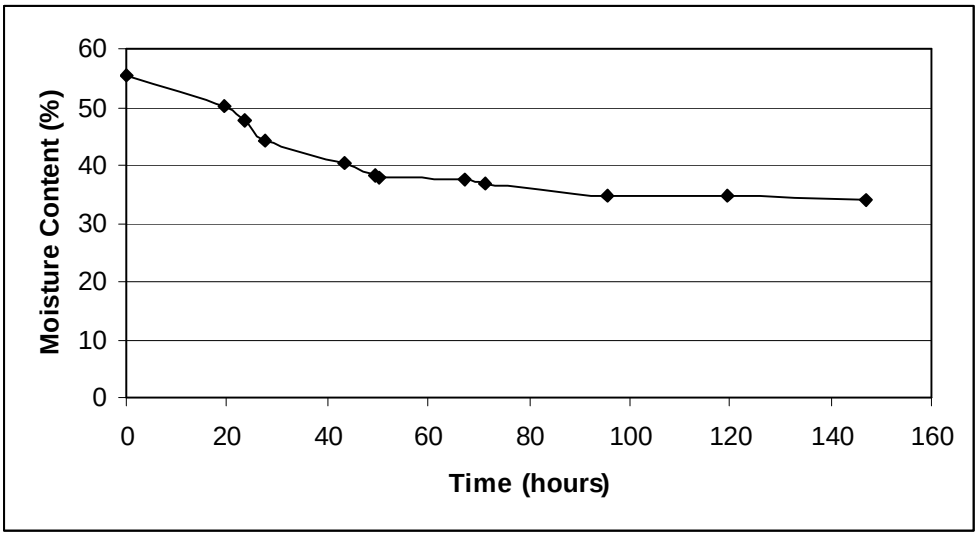


Figure C44 Variation in Moisture Content versus Time

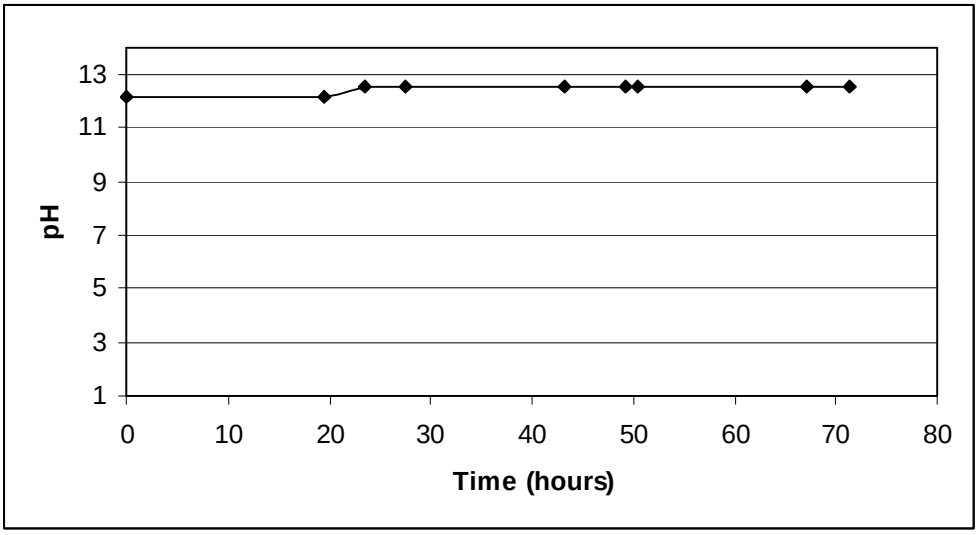


Figure C45 pH versus Time

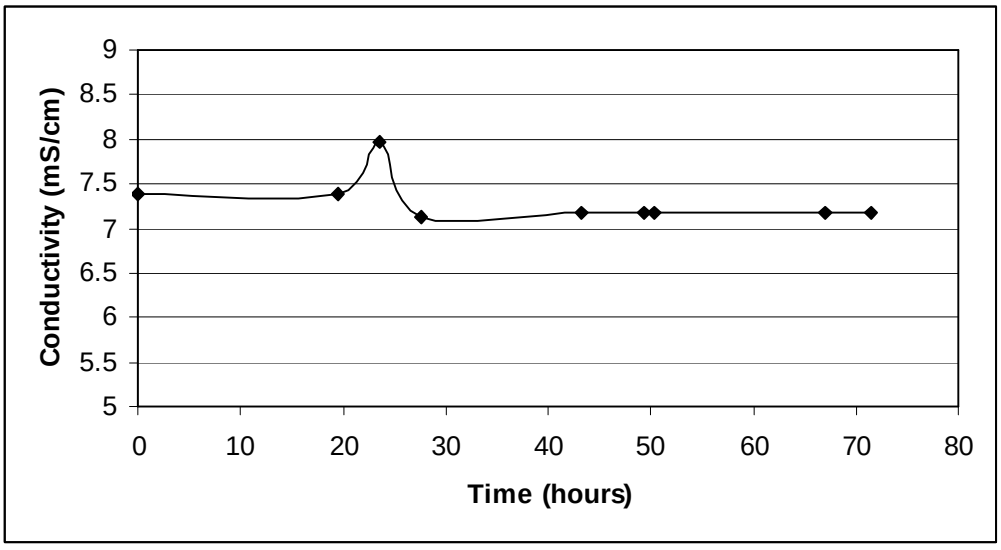


Figure C46 Conductivity versus Time

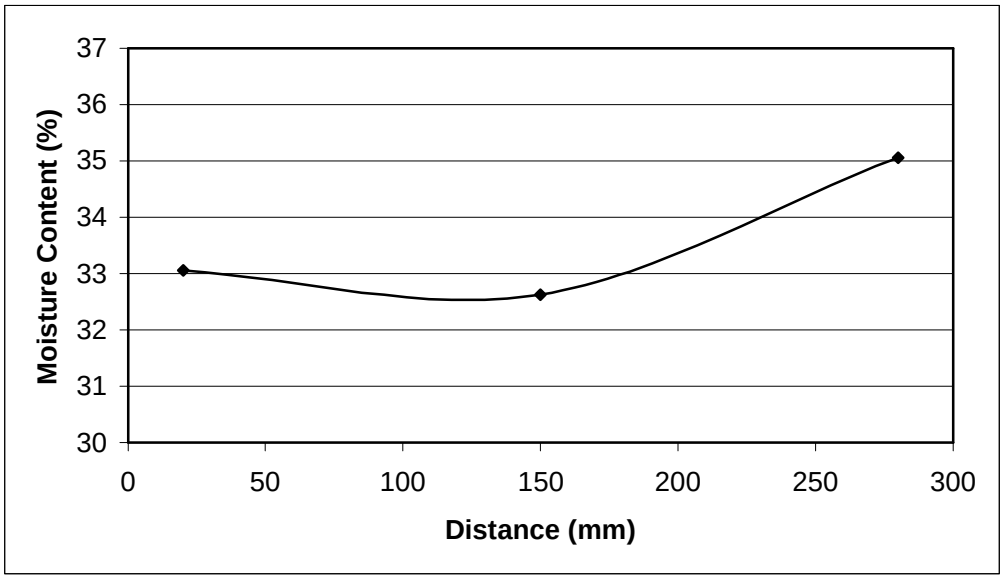


Figure C47 Variation in Final moisture content from Anode to Cathode

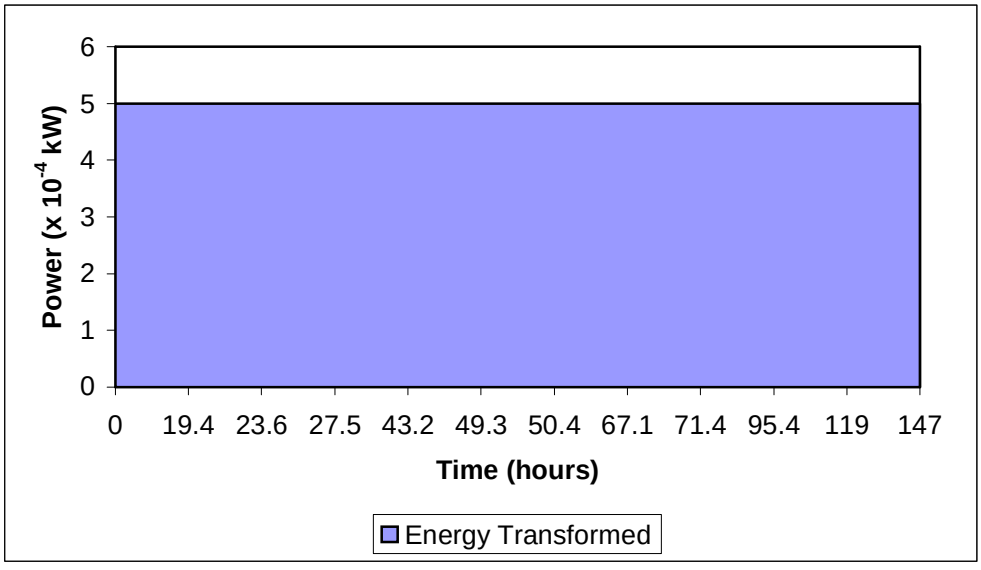


Figure C48 Power versus Time

TEST 11

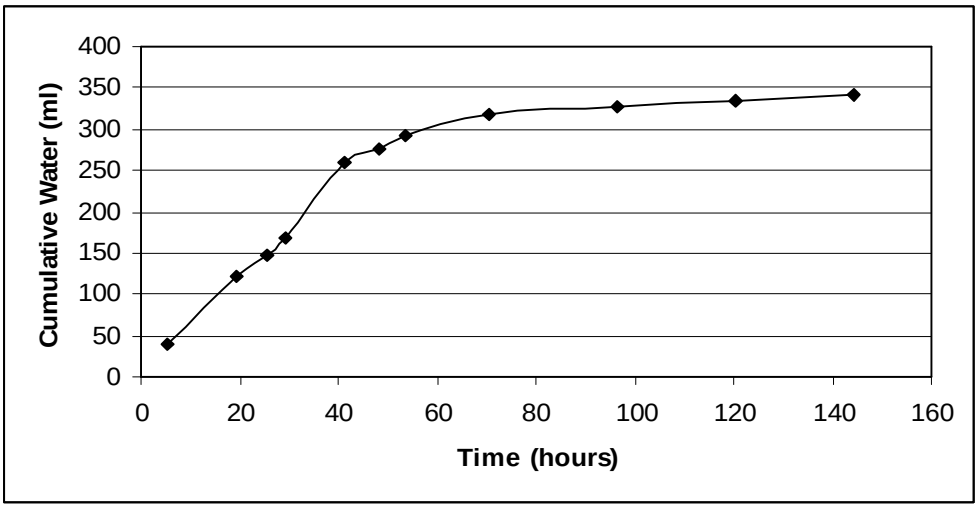


Figure C49 Cumulative Water versus Time

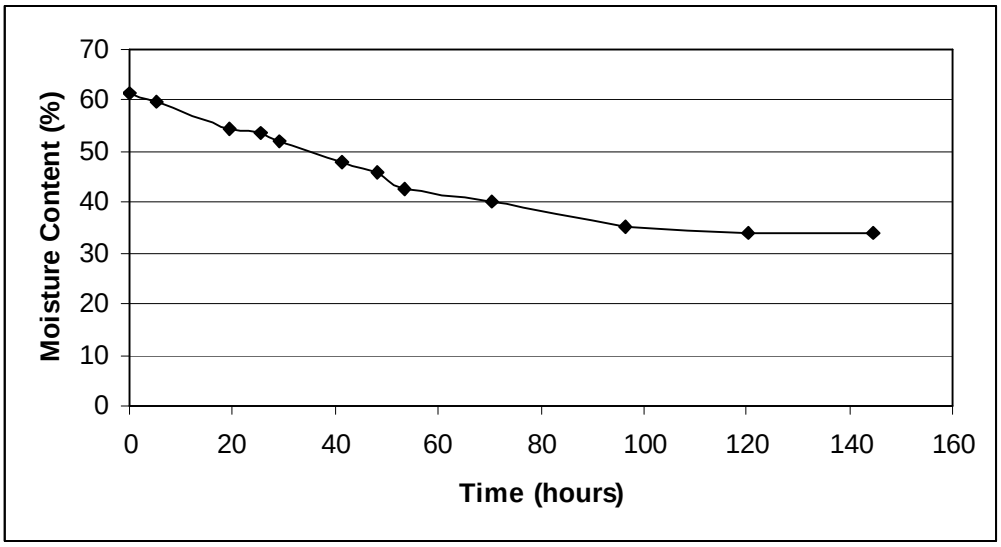


Figure C50 Variation in Moisture Content versus Time

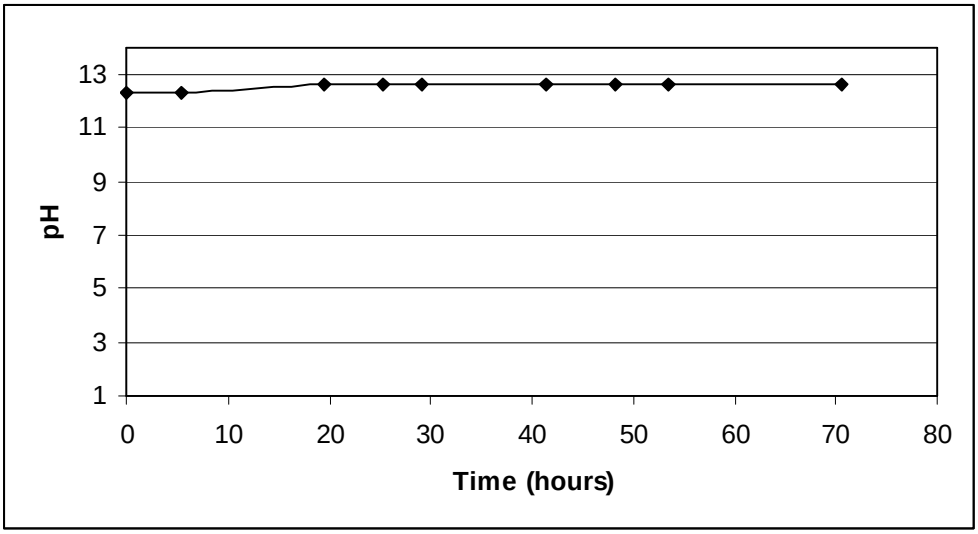


Figure C51 pH versus Time

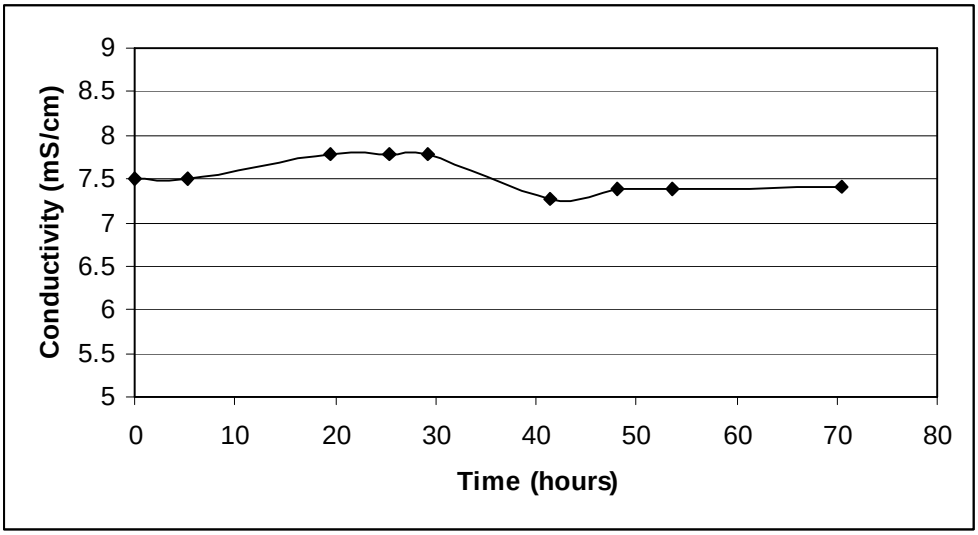


Figure C52 Conductivity versus Time

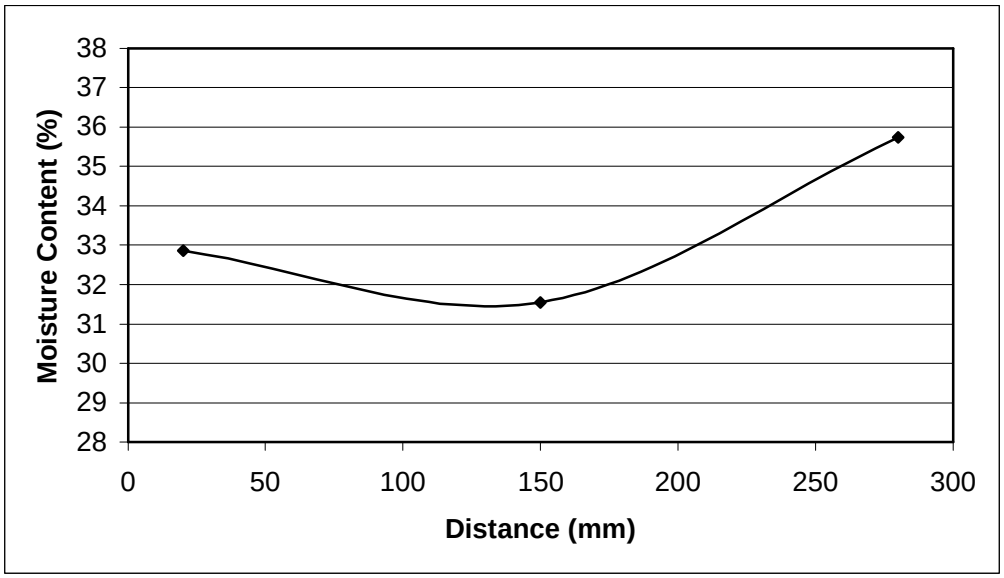


Figure C53 Variation in Final moisture content from Anode to Cathode

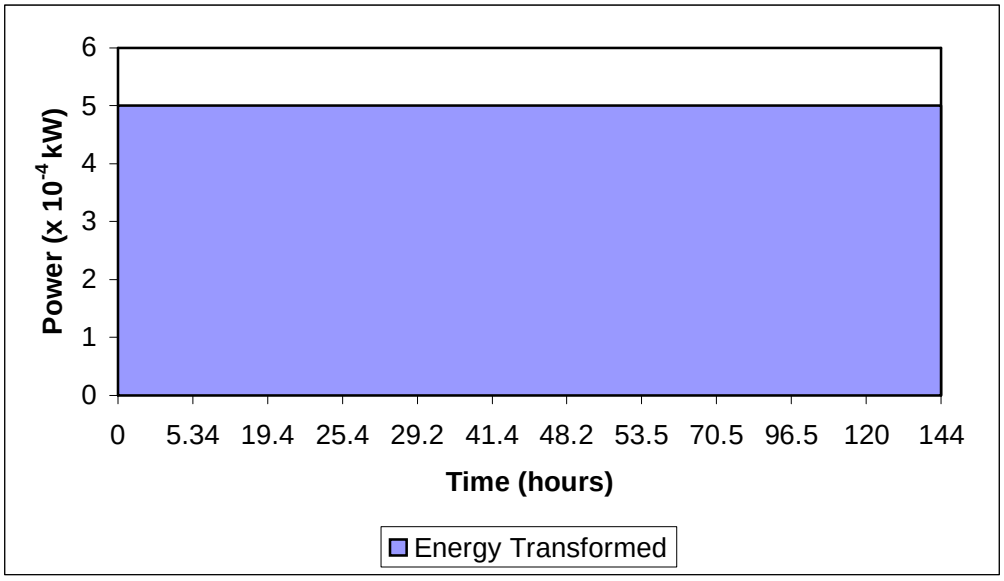


Figure C54 Power versus Time

TEST 12

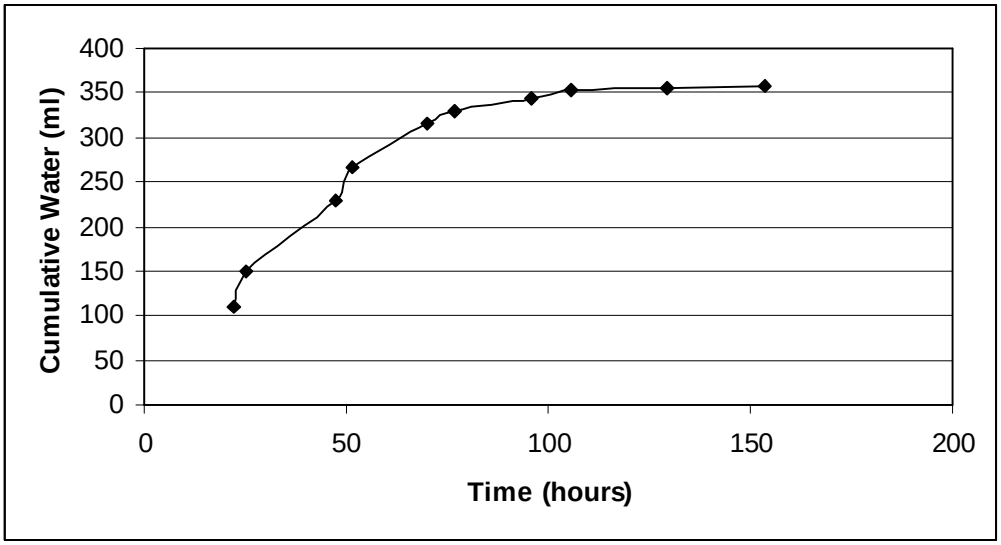


Figure C55 Cumulative Water versus Time

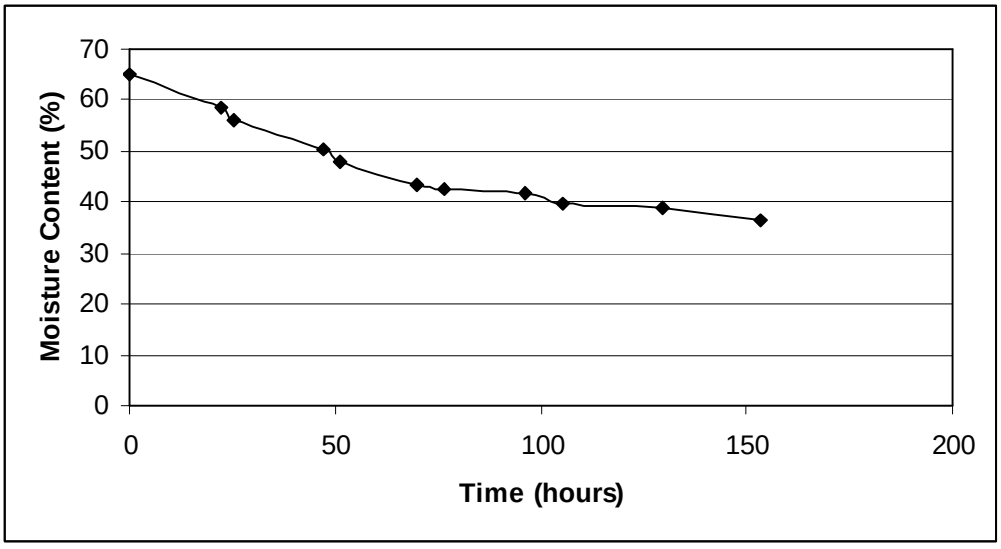


Figure C56 Variation in Moisture Content versus Time

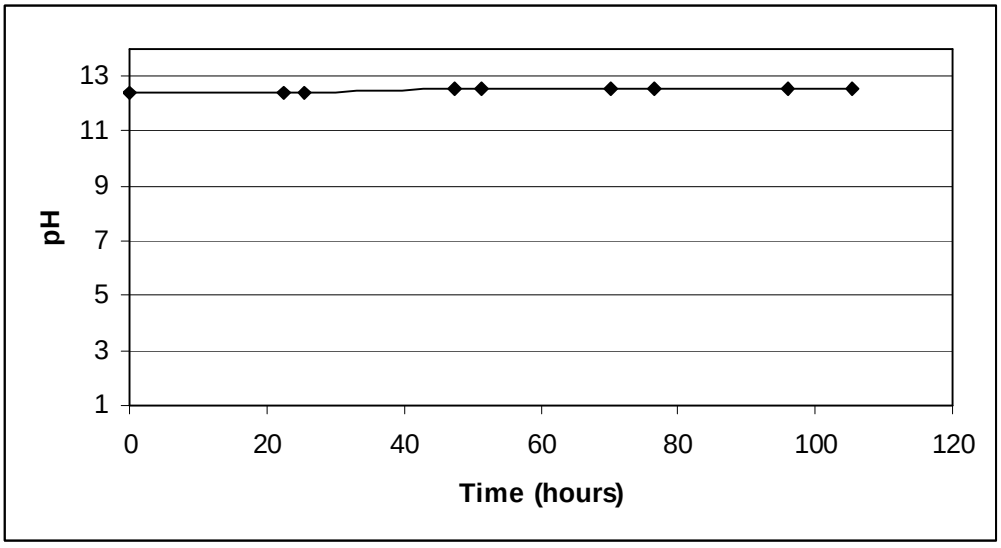


Figure C57 pH versus Time

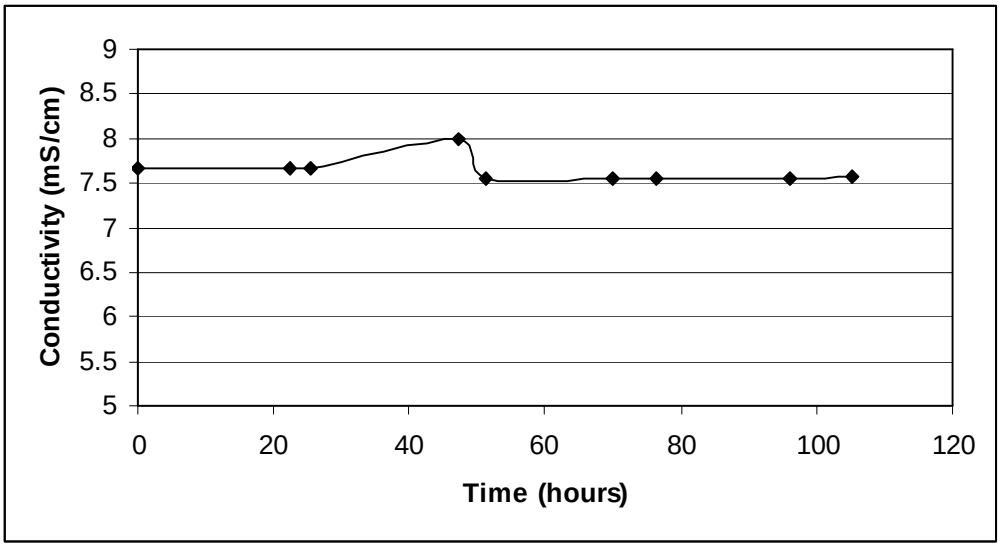


Figure C58 Conductivity versus Time

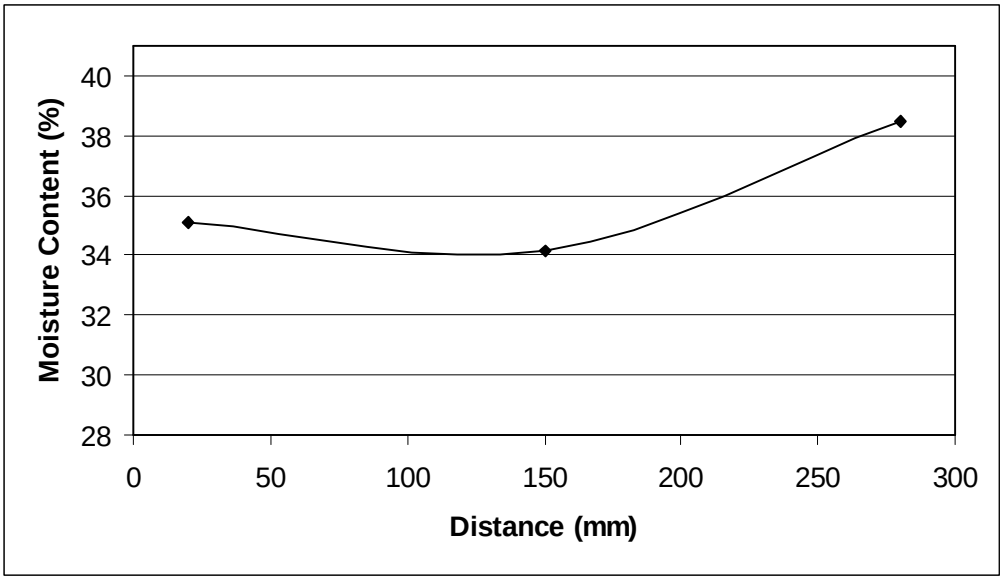


Figure C59 Variation in Final moisture content from Anode to Cathode

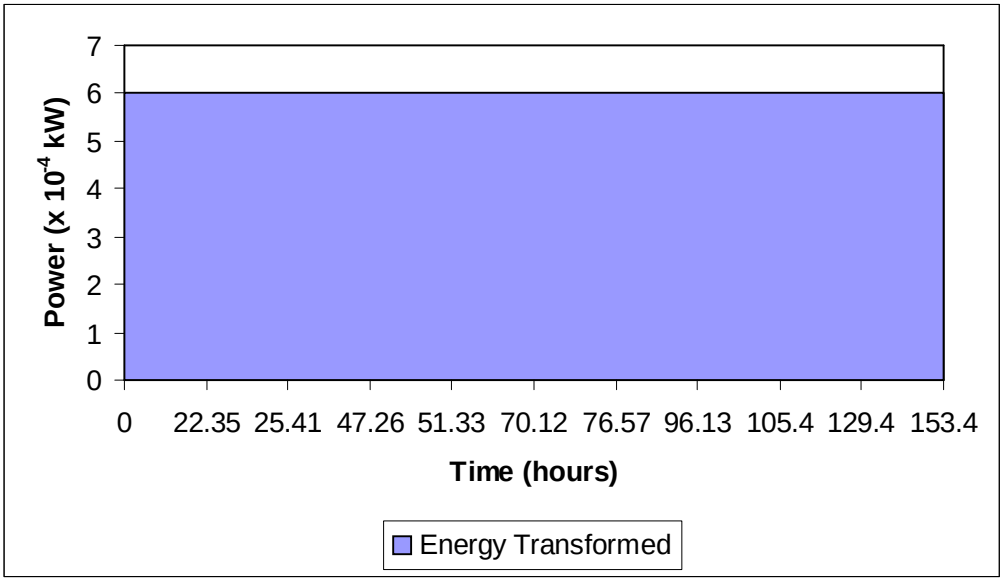


Figure C60 Power versus Time

APPENDIX D

CUMULATIVE WATER, CONDUCTIVITY, pH AND MOISTURE CONTENT DATA.

TEST 1

- Details of Electrodes

The mass of the anode and cathode is 611.0 g and 609.5 g respectively.

- Test and Control Box

The test box has a length of 30 cm and width of 20 cm. Its mass is 3 019.0 g
Mass of the test box + mass of electrodes = 4 233.7 g. Mass of the test box + mass of electrodes + wet mass of sample = 15 469.4 g. Mass of control box = 55 g. Mass of control box + wet mass of sample = 2 391.2 g

- Volume of Sample

The total volume of sample used in the test box is 77.816 x 10^{-4} m^3.

- Voltage and Current

10 volts were applied to the test and the DC source read 0.08 amperes for current.

Table D1 Initial Water Content

Container No.	**Mass of Container (g)**	**Mass of Container + Mass of Wet Sample (g)**	**Mass of Container + Dry Mass of Sample (g)**	**Individual Water Content (%)**
8	24.739	50.407	41.025	57.61
3	25.234	50.100	41.108	56.65
10	24.646	50.304	40.896	57.90
11	25.083	50.876	41.530	56.82
Average Initial Water Content (%) for the Sample				**57.25**

Table D2 Amount of Water Removed from Sample

Time Elapsed (hours)	**Water Removed (ml)**	**Cumulative Water (ml)**
9.24	98.4	98.4
23.02	103.8	202.2
32.46	90.8	293.0
47.05	71.2	364.2
52.00	65.0	429.2
56.46	65.5	494.7
71.09	39.3	534.0
77.46	1.6	535.6
101.00	0.1	535.7
125.00	0.3	536.0

Table D3 Variation in Moisture Content

Time Elapsed (hours)	Moisture Content (%)
0	57.25 (initial moisture content)
9.24	50.37
23.02	42.28
32.46	37.41
47.05	34.26
52.00	31.47
56.46	29.48
71.09	27.45
77.46	26.23
101.00	25.92
125.00	25.39

Table D4 Changes in pH and Conductivity Measurements during Test

Time (hours)	pH	Conductivity (mS/cm)
0	12.01	7.54
9.24	12.01	7.56
23.02	12.12	7.67
32.46	12.93	7.83
47.05	13.15	7.99
52.00	13.18	8.10
56.46	13.16	8.14
71.09	13.15	8.14

Table D5 Variation in Final Moisture Content

Container No.	Mass of Container (g)	Wet Mass + Mass of Container (g)	Dry Mass + Mass of Container (g)	Final Moisture Content (%)
5 (anode)	24.582	33.516	31.804	23.71
12 (anode)	24.730	33.710	31.966	24.10
15 (center)	24.919	33.825	32.256	21.38
20 (center)	25.102	33.938	32.340	22.08
19 (cathode)	24.670	33.767	31.865	26.44
22 (cathode)	24.421	33.696	31.739	26.74

Energy Consumption and Dewatering Efficiency

The energy consumption and dewatering efficiency data for Test 1 is calculated as follows:

$P = VI = 10 \times 0.08 = 8 \times 10^{-4}$ kW

$E_u = (\int VI\, dt) / V_s = VI\,(t_2 - t_1) / V_s = 8 \times 10^{-4}\,(125) / 77.816 \times 10^{-4} = 12.85$ kWh/m^3

Dewatering Efficiency = Total amount of water / It
= 536 / 0.08 x 125 = 53.60 ml/Ah

TEST 2

- Test and Control Box

The test box has a length of 30 cm and width of 20 cm. Its mass is 3 014.1 g. Mass of the test box + mass of electrodes = 3 121.5 g. Mass of the test box + mass of electrodes + wet mass of sample = 13 550.9 g
Mass of control box = 55 g. Mass of control box + wet mass of sample = 2 391.2 g

- Volume of Sample

The total volume of sample used in the test box is 74.014 x 10^{-4} m^3.

- Voltage and Current

10 volts were applied to the test and the DC source read 0.05 amperes for current.

Table D6 Initial Water Content

Container N0.	**Mass of Container (g)**	**Mass of Container + Mass of Wet Sample (g)**	**Mass of Container + Dry Mass of Sample (g)**	**Individual Water Content (%)**
8	24.739	50.407	41.025	57.61
3	25.234	50.100	41.108	56.65
10	24.646	50.304	40.896	57.90
11	25.083	50.876	41.530	56.82
Average Initial Water Content (%) for the Sample				**57.25**

Table D7 Amount of Water Removed from Sample

Time Elapsed (hours)	**Water Removed (ml)**	**Cumulative Water (ml)**
9.24	148.1	148.1
23.02	185.1	333.2
32.46	77.9	411.1
47.05	7.1	418.2
52.00	3.6	421.8
56.46	3.0	424.8
71.09	0.5	425.3
77.46	0.1	425.4

Table D8 Variation in Moisture Content

Time Elapsed (hours)	**Moisture Content (%)**
0	57.25 (initial moisture content)
9.24	44.76
23.02	38.20
32.46	35.31
47.05	34.25
52.00	33.78
56.46	32.74
71.09	31.26
77.46	30.43

Table D9 Changes in pH and Conductivity Measurements during Test

Time (hours)	pH	Conductivity (mS/cm)
0	12.01	7.55
9.24	12.02	7.56
23.02	12.04	7.55
32.46	12.08	7.60
47.05	12.07	7.60

Table D10 Variation in Final Moisture Content

Container No.	Mass of Container (g)	Wet Mass + Mass of Container (g)	Dry Mass + Mass of Container (g)	Final Moisture Content (%)
4 (anode)	23.856	32.564	30.599	29.14
23 (anode)	24.767	33.837	31.799	28.98
9 (center)	23.769	33.779	31.386	31.42
18 (center)	25.008	33.615	31.555	31.46
21 (cathode)	24.769	33.936	31.874	29.02
25 (cathode)	24.360	33.338	31.301	29.35

Energy Consumption and Dewatering Efficiency

The energy consumption and dewatering efficiency data for Test 2 is calculated as follows:

$P = VI = 10 \times 0.05 = 5 \times 10^{-4}$ kW

$E_u = (\int VI\, dt) / V_s = VI (t_2 - t_1) / V_s = 5 \times 10^{-4} (77.46) / 74.014 \times 10^{-4}$
$= 5.23$ kWh/m^3

Dewatering Efficiency = Total amount of water / It
= 425.4 / 0.05 x 77.46 = 109.84 ml/Ah

TEST 3

- Details of Electrodes

The same brass electrodes used in Test 2 were used for Test 3. The mass of the anode and cathode is 600.4 g and 609.4 g respectively.

- Test and Control Box

The test box has a length of 30 cm and width of 20 cm. Its mass is 3 035.3 g. Mass of the test box + mass of electrodes = 3 142.9 g. Mass of the test box + mass of electrodes + wet mass of sample = 14 047.6 g
Mass of control box = 62.9 g. Mass of control box + wet mass of sample = 1 663.7 g

- Volume of Sample

The total volume of sample used in the test box is 75.238×10^{-4} m^3.

- Voltage and Current

10 volts were applied to the test and the DC source read 0.08 amperes for current.

Table D11 Initial Water Content

Container N0.	Mass of Container (g)	Mass of Container + Mass of Wet Sample (g)	Mass of Container + Dry Mass of Sample (g)	Individual Water Content (%)
19	24.680	44.598	36.373	41.55
8	24.738	42.706	35.183	41.31
11	25.101	51.026	41.584	41.59
15	24.928	41.536	32.538	41.56
Average Initial Water Content (%) for the Sample				**41.50**

Table D12 Amount Of water Removed from Sample

Time Elapsed (hours)	Water Removed (ml)	Cumulative Water (ml)
21.41	71.1	71.1
26.57	56.2	127.3
45.35	70.1	197.4
50.59	14.7	212.1
69.37	39.8	251.9
77.37	3.9	255.8
93.29	6.0	261.8
99.51	5.3	267.1
107.22	2.1	269.2

Table D13 Variation in Moisture Content

Time Elapsed (hours)	Moisture content (%)
0 (Initial)	41.50
21.41	38.98
26.57	38.00
45.35	36.27
50.59	35.87
69.37	34.68
77.37	32.33
93.29	30.66
99.51	29.87
107.22	29.80

Table D14 Changes in pH and Conductivity Measurements during Test

Time (hours)	pH	Conductivity (mS/cm)
0	12.55	7.59
21.41	12.55	7.58
45.35	12.60	7.89
50.59	12.24	7.97
69.37	12.44	7.98

Table D15 Variation in Final Moisture Content

Container No.	Mass of Container (g)	Wet Mass + Mass of Container (g)	Dry Mass + Mass of Container (g)	Final Moisture Content (%)
59 (anode)	24.648	82.552	69.778	28.30
13 (anode)	25.341	73.990	63.603	27.15
25 (center)	24.360	77.138	65.949	26.90
58 (center)	24.486	79.092	67.423	27.18
23 (cathode)	24.767	81.132	66.581	34.80
18 (cathode)	25.009	78.245	65.539	31.35

Energy Consumption and Dewatering Efficiency

The energy consumption and dewatering efficiency data for Test 3 is calculated as follows:

$P = VI$
$= 10 \times 0.08 = 8 \times 10^{-4}$ kW

$E_u = (\int VI\, dt) / V_s$
$= VI (t_2 - t_1) / V_s = 8 \times 10^{-4} (107.22) / 75.238 \times 10^{-4} = 11.40$ kWh/m^3

Dewatering Efficiency = Total amount of water / It
= 269.2 / 0.08 x 107.22 = 31.38 ml/Ah

TEST 4

- Details of Electrodes

The same two brass tubing used in Test 2 and 3 were used here. The mass of the anode and cathode is 593.7 g and 610.0 g respectively.

- Test and Control Box

The test box has a length of 30 cm and width of 30 cm. Its mass is 3 018.3 g. Mass of the test box + mass of electrodes = 4 222 g. Mass of the test box + mass of electrodes + wet mass of sample = 15 705.3 g
Mass of control box = 55 g. Mass of control box + wet mass of sample = 1 856.4 g

- Volume of Sample

The total volume of sample used in the test box is 78.621 x 10^{-4} m^3.

- Voltage and Current

10 volts were applied to the test and the DC source read 0.08 amperes for current.

Table D16 Initial Water Content

Container No.	Mass of Container (g)	Mass of Container + Mass of Wet Sample (g)	Mass of Container + Dry Mass of Sample (g)	Individual Water Content (%)
11	25.103	49.469	41.791	46.01
13	25.340	49.548	40.732	47.68
15	24.928	49.537	40.554	48.02
19	24.683	49.572	40.578	47.32
Average Initial Water Content (%) for the Sample				**47.26**

Table D17 Amount Of Water Removed from Sample

Time Elapsed (hours)	Water Removed (ml)	Cumulative Water (ml)
4.07	83.41	83.41
22.47	65.89	149.30
27.48	23.17	172.47
48.39	56.23	228.70
52.23	17.92	146.62
68.79	18.84	265.46
79.11	9.35	274.81
88.27	6.58	281.39
112.96	3.38	284.77

Table D18 Variation in Moisture Content

Time Elapsed (hours)	Moisture Content (%)
0 (Initial)	47.26
4.07	45.03
22.47	44.72
27.48	44.38
48.39	43.56
52.23	42.91
68.79	42.37
79.11	42.02
88.27	39.83
112.96	39.44

Table D19 Changes in pH and Conductivity Measurements during Test

Time (hours)	pH	Conductivity (mS/cm)
0	12.47	5.55
4.07	12.75	5.73
22.47	12.76	5.74
27.48	12.76	5.79
48.39	12.77	5.88
52.23	12.76	5.89
68.79	12.75	5.91

Table D20 Variation in Final Moisture Content

Container No.	Mass of Container (g)	Wet Mass + Mass of Container (g)	Dry Mass + Mass of Container (g)	Final Moisture Content (%)
11 (anode)	25.100	38.782	35.060	37.37
13 (anode)	25.340	38.866	35.151	37.87
15 (center)	24.924	38.786	35.055	36.83
17 (center)	25.235	38.994	35.317	36.47
19 (cathode)	24.681	38.851	34.598	42.89
21 (cathode)	24.773	38.222	34.143	43.53

Energy Consumption and Dewatering Efficiency

The energy consumption and dewatering efficiency data for Test 4 is calculated as follows:

$P = VI$
$= 10 \times 0.08 = 8 \times 10^{-4}$ kW

$E_u = (\int VI\, dt) / V_s$
$= VI (t_2 - t_1) / V_s = 8 \times 10^{-4} (112.96) / 78.621 \times 10^{-4} = 11.49$ kWh/m^3

Dewatering Efficiency = Total amount of water / It
= 284.77 / 0.08 x 112.96 = 31.51 ml/Ah

TEST 5

- Details of Electrodes

The same sets of brass tubing used in previous tests are being used here. The mass of the anode and cathode is 591.4 g and 610.2 g respectively.

- Test and Control Box

The test box has a length of 30 cm and width of 20 cm. Its mass is 4 175.2 g. Mass of the test box + mass of electrodes = 5 397.5 g. Mass of the test box + mass of electrodes + wet mass of sample = 14 945.2 g
Mass of control box =62.8 g. Mass of control box + wet mass of sample = 1 456.2 g

- Volume of Sample

The total volume of sample used in the test box is 76.639 x 10^{-4} m^3.

- Voltage and Current

Ten volts were applied to the test and the DC source read 0.09 amperes for current.

Table D21 Initial Water Content

Container N0.	Mass of Container (g)	Mass of Container + Mass of Wet Sample (g)	Mass of Container + Dry Mass of Sample (g)	Individual Water Content (%)
59	24.648	43.608	37.031	53.11
64	25.772	43.966	37.614	53.64
152	24.187	42.145	35.897	53.36
58	24.486	43.632	36.983	53.20
Average Initial Water Content (%) for the Sample				**53.33**

Table D22 Amount of Water Removed from Sample

Time Elapsed (hours)	Water removed (ml)	Cumulative Water (ml)
3.34	36.10	36.10
20.30	89.71	125.81
26.46	17.29	143.10
44.29	34.67	177.77
51.17	16.33	194.10
69.51	75.28	267.38
75.47	15.17	284.55
84.22	11.21	295.76
90.17	9.76	305.52
113.04	8.53	314.05
117.95	3.09	317.14

Table D23 Variation in Moisture Content

Time Elapsed (hours)	Moisture Content (%)
0	53.33 (initial moisture content)
3.34	52.89
20.30	48.29
26.46	47.36
44.29	46.09
51.17	45.24
69.51	40.25
75.47	38.56
84.22	37.24
90.17	36.52
113.04	30.66
117.95	27.92

Table D24 Changes in pH and Conductivity Measurements during Test

Time (hours)	pH	Conductivity (mS/cm)
0	8.00	7.11
3.34	9.98	7.82
20.30	10.06	5.68
26.46	10.06	5.23
44.29	10.12	5.80
51.17	10.08	5.81
69.51	10.07	5.82
75.47	10.08	5.86
84.22	10.10	5.83

Table D25 Variation in Final Moisture Content

Container No.	Mass of Container (g)	Wet Mass + Mass of Container (g)	Dry Mass + Mass of Container (g)	Final Moisture Content (%)
5 (anode)	24.591	40.593	37.288	26.03
10 (anode)	24.665	40.847	37.508	25.99
13 (center)	25.334	40.556	37.159	28.73
18 (center)	25.011	40.836	37.300	28.78
11 (cathode)	25.100	40.502	37.130	28.03
12 (cathode)	24.733	40.711	37.189	28.28

Energy Consumption and Dewatering Efficiency

The energy consumption and dewatering efficiency data for Test 5 is calculated as follows:

$P = VI$
$= 10 \times 0.09 = 9 \times 10^{-4}$ kW

$E_u = (\int VI\, dt) / V_s = VI (t_2 - t_1) / V_s$
$= 9 \times 10^{-4} (117.95) / 76.639 \times 10^{-4} = 13.85$ kWh/m^3

Dewatering Efficiency = Total amount of water / It
= 317.14 / 0.09 x 117.95 = 29.86 ml/Ah

TEST 6

- Details of Electrodes

The mass of the anode and cathode is 590.2 g and 610.4 g respectively.

- Test and Control Box

The test box has a length of 30 cm and width of 20 cm. Its mass is 2 915.1 g. Mass of the test box + mass of electrodes = 4 231.6 g. Mass of the test box + mass of electrodes + wet mass of sample = 12 109.4 g
Mass of control box = 55 g. Mass of control box + wet mass of sample = 2 090.3 g

- Volume of Sample

The total volume of sample used in the test box is 79.337 x 10^{-4} m^3.

§ Voltage and Current

10 volts were applied to the test and the DC source read 0.08 amperes for current.

Table D26 Initial Water Content

Container N0.	Mass of Container (g)	Mass of Container + Mass of Wet Sample (g)	Mass of Container + Dry Mass of Sample (g)	Individual Water Content (%)
59	24.647	51.861	41.573	60.78
4	24.505	51.763	41.681	58.70
19	24.680	51.904	41.524	61.62
15	24.928	51.752	41.698	59.26
Average Initial Water Content (%) for the Sample				**60.26**

Table D27 Amount of Water Removed from Sample

Time Elapsed (hours)	Water Removed (ml)	Cumulative Water (ml)
5.47	35.36	35.36
11.30	48.32	83.68
29.16	74.87	158.55
34.25	38.57	197.14
40.34	32.64	229.78
57.08	43.19	272.97
63.42	28.77	301.74
70.36	13.38	315.12
87.49	10.24	325.36
93.26	9.96	335.32
98.17	6.69	342.01
115.52	1.02	343.03
132.50	1.65	344.68
139.12	1.43	346.11

Table D28 Variation in Moisture Content

Time Elapsed (hours)	Moisture Content (%)
0	60.26
5.47	57.30
11.30	52.61
29.16	44.78
34.25	41.68
40.34	38.57
57.08	37.27
63.42	36.33
70.36	35.80
87.49	34.67
93.26	33.83
98.17	33.12
115.52	32.55
132.50	31.92
139.12	31.49

Table D29 Changes in pH and Conductivity Measurements during Test

Time (hours)	pH	Conductivity (mS/cm)
0	8.30	7.18
5.47	8.32	7.23
11.30	8.32	7.24
29.16	8.33	7.24
34.25	8.33	7.24
40.34	8.32	7.25
57.08	8.33	7.24
63.42	8.33	7.24
70.36	8.33	7.24

Table D30 Variation in Final Moisture Content

Container No.	Mass of Container (g)	Wet Mass + Mass of Container (g)	Dry Mass + Mass of Container (g)	Final Moisture Content (%)
19 (anode)	24.683	50.426	44.612	29.17
21 (anode)	24.774	50.538	44.741	29.03
25 (center)	24.360	50.517	44.323	31.03
59 (center)	24.648	50.550	44.278	31.95
15 (cathode)	24.928	50.700	44.713	30.26
8 (cathode)	24.736	50.721	44.639	30.56

The average final moisture content is 30.33 %.

Energy Consumption and Dewatering Efficiency

The energy consumption and dewatering efficiency data for Test 6 is calculated as follows:

$P = VI = 10 \times 0.08 = 8 \times 10^{-4}$ kW

$E_u = (\int VI\, dt) / V_s = VI (t_2 - t_1) / V_s = 8 \times 10^{-4} (139.12) / 79.337 \times 10^{-4} = 14.03$ kWh/m^3

Dewatering Efficiency = Total amount of water / It
= 346.11 / 0.08 x 139.12 = 13.13 ml/Ah

TEST 7

- Details of Electrodes

The mass of the anode and cathode is 589.8 g and 610.5 g respectively.

- Test and Control Box

The test box has a length of 30 cm and width of 20 cm. Its mass is 3 226.5 g
Mass of the test box + mass of electrodes = 4 569.6 g
Mass of the test box + mass of electrodes + wet mass of sample = 12 615.7 g
Mass of control box = 55 g
Mass of control box + wet mass of sample = 2 180.3 g

- Volume of Sample

The total volume of sample used in the test box is 79.610 x 10^{-4} m^3.

- Voltage and Current

10 volts were applied to the test and the DC source read 0.08 amperes for current.

Table D31 Initial Water Content

Container No.	Mass of Container (g)	Mass of Container + Mass of Wet Sample (g)	Mass of Container + Dry Mass of Sample (g)	Individual Water Content (%)
8	24.912	51.927	41.398	63.86
10	24.639	51.819	41.233	63.79
15	24.737	51.676	41.126	64.37
25	24.356	51.438	41.264	60.17
Average Initial Water Content (%) for the Sample				**63.05**

Table D32 Amount of Water Removed from Sample

Time (hours)	Water Removed (ml)	Cumulative Water (ml)
8.54	41.56	41.56
21.41	76.39	117.95
33.27	45.84	163.79
50.12	56.18	219.97
55.36	31.26	251.23
60.48	28.90	280.13
73.45	18.01	298.14
78.19	19.38	317.52
82.23	14.28	331.80
98.06	9.44	341.24
116.18	4.97	346.21
131.31	2.53	348.74
137.53	1.67	350.41

Table D33 Variation in Moisture Content

Time (hours)	Moisture Content (%)
0	63.05
8.54	59.47
21.41	51.25
33.27	48.92
50.12	45.36
55.36	43.83
60.48	41.49
73.45	40.56
78.19	39.66
82.23	38.29
98.06	37.17
116.18	36.31
131.31	35.14
137.53	34.98

Table D34 Changes in pH and Conductivity Measurements during Test

Time (hours)	pH	Conductivity (mS/cm)
0	8.24	7.19
8.54	8.25	7.22
21.41	8.28	7.22
33.27	8.28	7.22
50.12	8.29	7.24
55.36	8.29	7.25
60.48	8.30	7.24
73.45	8.30	7.24

Table D35 Variation in Final Moisture Content

Container No.	Mass of Container (g)	Wet Mass + Mass of Container (g)	Dry Mass + Mass of Container (g)	Final Moisture Content (%)
7(anode)	25.218	50.487	44.336	32.17
12 (anode)	24.733	50.505	44.081	33.20
13 (center)	25.340	50.544	43.882	35.92
18 (center)	25.014	50.619	43.957	35.17
64 (cathode)	25.772	50.523	44.136	33.86
11 (cathode)	25.103	50.607	44.241	33.26

The average final moisture content for Test 7 is 33.93 %.

Energy Consumption and Dewatering Efficiency

The energy consumption and dewatering efficiency data for Test 7 is calculated as follows:

$P = VI = 10 \times 0.08 = 8 \times 10^{-4}$ kW

$E_u = (\int VI\, dt) / V_s = VI (t_2 - t_1) / V_s = 8 \times 10^{-4} (137.53) / 79.610 \times 10^{-4} = 13.82$ kWh/m^3

Dewatering Efficiency = Total amount of water / It
= 350.41 / 0.08 x 137.53 = 31.86 ml/Ah

TEST 8

- Test and Control Box

The test box has a length of 30 cm and width of 20 cm. Its mass is 2 915.2 g. Mass of the test box + mass of electrodes = 4 245.7 g. Mass of the test box + mass of electrodes + wet mass of sample = 12 833.0 g
Mass of control box = 55 g. Mass of control box + wet mass of sample = 2 367.2 g

- Volume of Sample

The total volume of sample used in the test box is 80.925×10^{-4} m^3.

- Voltage and Current

10 volts were applied to the test and the DC source read 0.05 amperes for current.

Table D36 Initial Water Content

Container N0.	Mass of Container (g)	Mass of Container + Mass of Wet Sample (g)	Mass of Container + Dry Mass of Sample (g)	Individual Water Content (%)
19	24.651	49.146	41.994	41.24
4	23.849	49.400	41.797	42.36
6	24.527	49.106	41.326	46.31
22	24.414	49.611	41.177	41.85
Average Initial Water Content (%) for the Sample				**42.94**

Table D37 Amount of Water Removed from Sample

Time Elapsed (hours)	Water Removed (ml)	Cumulative Water (ml)
8.54	50.28	50.28
21.41	47.39	97.67
33.27	67.38	165.05
50.12	75.67	240.72
55.36	17.30	258.02
60.48	12.4	270.42
73.45	6.1	276.52
78.19	5.2	281.72
82.23	4.3	286.02
98.06	2.6	288.62
116.18	1.9	290.52

Table D38 Variation in Moisture Content

Time (hours)	Moisture Content (%)
0	42.94
8.54	39.51
21.41	36.47
33.27	33.52
50.12	32.46
55.36	32.12
60.48	31.88
73.45	30.90
78.19	30.72
82.23	30.48
98.06	30.02
116.18	29.64

Table D39 Changes in pH and Conductivity Measurements during Test

Time (hours)	pH	Conductivity (mS/cm)
0	8.25	7.19
8.54	8.35	7.19
21.41	8.36	7.21
33.27	8.37	7.21
50.12	8.37	7.22
55.36	8.38	7.23
60.48	8.38	7.23

Table D40 Variation in Final Moisture Content

Container No.	Mass of Container (g)	Wet Mass + Mass of Container (g)	Dry Mass + Mass of Container (g)	Final Moisture Content (%)
4 (anode)	24.505	82.928	69.862	28.81
21 (anode)	24.774	82.629	69.699	28.76
59 (center)	24.648	82.667	69.261	30.05
10 (center)	24.639	82.538	69.121	30.16
25 (cathode)	24.356	82.723	69.654	29.50
22 (cathode)	24.414	82.697	69.703	28.69

The average final moisture content is 29.33 %.

Energy Consumption and Dewatering Efficiency

The energy consumption and dewatering efficiency data for Test 8 is calculated as follows:

$P = VI = 10 \times 0.05 = 5 \times 10^{-4}$ kW

$E_u = (\int VI\, dt) / V_s = VI (t_2 - t_1) / V_s = 5 \times 10^{-4} (115.18) / 80.925 \times 10^{-4}$
$= 7.12$ kWh/m^3

Dewatering Efficiency = Total amount of water / It
= 290.52 / 0.05 x 115.18 = 50.45 ml/Ah

TEST 9

- Test and Control Box

The test box has a length of 30 cm and width of 20 cm. Its mass is 3 226.5 g
Mass of the test box + mass of electrodes = 4 448.2 g
Mass of the test box + mass of electrodes + wet mass of sample = 12 291.3 g
Mass of control box = 55 g. Mass of control box + wet mass of sample = 2 129.3 g

- Volume of Sample

The total volume of sample used in the test box is 79.180×10^{-4} m^3.

- Voltage and Current

10 volts were applied to the test and the DC source read 0.05 amperes for current.

Table D41 Initial Water Content

Container N0.	Mass of Container (g)	Mass of Container + Mass of Wet Sample (g)	Mass of Container + Dry Mass of Sample (g)	Individual Water Content (%)
15	24.927	49.956	42.362	43.56
5	24.582	49.865	42.258	43.04
19	24.670	49.924	42.445	43.08
22	24.421	49.981	42.137	44.28
Average Initial Water Content (%) for the Sample				**43.24**

Table D42 Amount of Water Removed from Sample

Time (hours)	Water Removed (ml)	Cumulative Water (ml)
5.47	48.39	48.39
11.30	48.27	96.66
29.16	70.61	167.27
34.25	40.53	207.80
40.34	25.18	232.98
57.08	34.33	267.31
63.42	12.01	279.32
70.36	10.40	289.72
87.49	7.00	296.72
93.26	6.58	303.30
98.17	3.49	306.79
115.52	1.61	308.40

Table D43 Variation in Moisture Content

Time (hours)	Moisture Content (%)
0	43.24
5.47	41.12
11.30	39.38
29.16	36.49
34.25	34.68
40.34	33.22
57.08	32.51
63.42	32.24
70.36	32.05
87.49	31.78
93.26	31.26
98.17	30.98
115.52	30.22

Table D44 Changes in pH and Conductivity Measurements during Test

Time (hours)	pH	Conductivity (mS/cm)
0	8.31	7.18
5.47	8.32	7.22
11.30	8.34	7.24
29.16	8.36	7.24
34.25	8.36	7.24
40.34	8.36	7.21
57.08	8.36	7.22

Table D45 Variation in Final Moisture Content

Container No.	Mass of Container (g)	Wet Mass + Mass of Container (g)	Dry Mass + Mass of Container (g)	Final Moisture Content (%)
58 (anode)	24.486	80.731	67.503	30.73
5 (anode)	24.591	80.642	67.710	29.99
6 (center)	24.527	80.868	67.537	31.00
2 (center)	24.506	80.905	67.491	31.21
152 (cathode)	24.187	80.658	67.610	30.05
19 (cathode)	24.683	80.682	67.625	30.41

Energy Consumption and Dewatering Efficiency

The energy consumption and dewatering efficiency data for Test 9 is calculated as follows:

$P = VI = 10 \times 0.05 = 5 \times 10^{-4}$ kW

$E_u = (\int VI\, dt) / V_s = VI (t_2 - t_1) / V_s = 5 \times 10^{-4} (115.52) / 79.180 \times 10^{-4}$
$= 7.29$ kWh/m^3

Dewatering Efficiency = Total amount of water / It
= 308.40 / 0.05 x 115.52 = 53.36 ml/Ah

TEST 10

- Test and Control Box

The test box has a length of 30 cm and width of 20 cm. Its mass is 2 935.3 g. Mass of the test box + mass of electrodes = 4 155.2 g. Mass of the test box + mass of electrodes + wet mass of sample = 12 244.4 g. Mass of control box = 62.8 g. Mass of control box + wet mass of sample = 629.7 g.

- Volume of Sample

The total volume of sample used in the test box is 69.593×10^{-4} m^3.

- Voltage and Current

Ten volts were applied to the test and the DC source read 0.05 amperes for current.

Table D46 Initial Water Content

Container N0.	Mass of Container (g)	Mass of Container + Mass of Wet Sample (g)	Mass of Container + Dry Mass of Sample (g)	Individual Water Content (%)
5	24.591	50.523	41.223	55.92
64	25.772	50.510	41.701	55.30
15	24.928	50.456	41.307	55.86
152	24.187	50.817	41.334	55.30

The average initial water content for this sample is 55.60 %.

Table D47 Amount of Water Removed from Sample

Time Elapsed (hours)	Water removed (ml)	Cumulative Water (ml)
19.40	98.34	98.34
23.59	35.81	134.15
27.53	21.05	155.20
43.16	88.76	243.96
49.34	26.38	270.34
50.40	10.33	280.67
67.07	28.97	309.64
71.44	15.28	324.92
95.44	8.39	333.31
119.44	3.22	336.53
147.16	1.56	338.09

Table D48 Variation in Moisture Content

Time Elapsed (hours)	Moisture Content (%)
0	55.60 (initial water content)
19.40	50.34
23.59	47.67
27.53	44.28
43.16	40.37
49.34	38.26
50.40	37.87
67.07	37.58
71.44	36.96
95.44	34.91
119.44	34.72
147.16	33.86

Table D49 Changes in pH and Conductivity Measurements during Test

Time (hours)	pH	Conductivity
0	12.21	7.38
19.40	12.21	7.38
23.59	12.53	7.96
27.53	12.54	7.12
43.16	12.55	7.17
49.34	12.55	7.17
50.40	12.56	7.18
67.07	12.55	7.18
71.44	12.56	7.18

Table D50 Variation in Final Moisture Content

Container No.	Mass of Container (g)	Wet Mass + Mass of Container (g)	Dry Mass + Mass of Container (g)	Final Moisture Content (%)
18 (anode)	25.008	50.216	44.027	32.78
13 (anode)	25.341	50.911	44.522	33.31
11 (center)	25.103	50.381	44.228	32.17
64 (center)	25.772	50.227	44.147	33.09
7 (cathode)	25.218	50.367	43.952	35.25
15 (cathode)	24.928	50.288	43.836	34.87

Energy Consumption and Dewatering Efficiency

The energy consumption and dewatering efficiency data for Test 10 is calculated as follows:

$P = VI$
$= 10 \times 0.05 = 5 \times 10^{-4}$ kW

$E_u = (\int VI\, dt) / V_s = VI (t_2 - t_1) / V_s$
$= 5 \times 10^{-4} (147.16) / 69.593 \times 10^{-4} = 10.57$ kWh/m^3

Dewatering Efficiency = Total amount of water / It
= 338.37 / 0.05 x 147.16 = 45.95 ml/Ah

TEST 11

- Test and Control Box

The test box has a length of 30 cm and width of 20 cm. Its mass is 2 935.3 g. Mass of the test box + mass of electrodes = 4 177.0 g. Mass of the test box + mass of electrodes + wet mass of sample = 13 848.1 g.
Mass of control box = 62.8 g. Mass of control box + wet mass of sample = 1 461.6 g

- Volume of Sample

The total volume of sample used in the test box is 74.485 x 10^{-4} m^3.

- Voltage and Current

Ten volts were applied to the test and the DC source read 0.05 amperes for current.

Table D51 Initial Water Content

Container N0.	Mass of Container (g)	Mass of Container + Mass of Wet Sample (g)	Mass of Container + Dry Mass of Sample (g)	Individual Water Content (%)
4	24.505	50.445	40.618	60.98
10	24.665	50.427	40.603	61.64
11	25.100	50.451	40.789	61.58
19	24.683	50.448	40.620	61.67
Average Initial Water Content (%) for the Sample				**61.47**

Table D52 Amount of Water Removed from Sample

Time Elapsed (hours)	Water removed (ml)	Cumulative Water (ml)
5.34	39.57	39.57
19.41	82.34	121.91
25.37	25.67	147.58
29.21	20.83	168.41
41.36	91.71	260.12
48.19	15.27	275.39
53.52	18.16	293.55
70.46	25.64	319.19
96.46	7.91	327.10
120.46	8.39	335.49
144.46	5.88	341.37

Table D53 Variation in Moisture Content

Time Elapsed (hours)	Moisture Content (%)
0	61.47 (initial water content)
5.34	59.62
19.41	54.39
25.37	53.71
29.21	51.83
41.36	47.75
48.19	45.66
53.52	42.71
70.46	40.23
96.46	35.18
120.46	34.15
144.46	33.97

Table D54 Changes in pH and Conductivity Measurements during Test

Time (hours)	pH	Conductivity (mS/cm)
0	12.35	7.50
5.34	12.36	7.51
19.41	12.61	7.78
25.37	12.61	7.78
29.21	12.62	7.79
41.36	12.61	7.26
48.19	12.63	7.39
53.52	12.62	7.39
70.46	12.62	7.40

Table D55 Variation in Final Moisture Content

Container No.	Mass of Container (g)	Wet Mass + Mass of Container (g)	Dry Mass + Mass of Container (g)	Final Moisture Content (%)
8 (anode)	24.738	50.415	44.138	32.36
15 (anode)	24.928	50.763	44.302	33.35
19 (center)	24.680	50.815	44.539	31.60
59 (center)	24.648	50.719	44.475	31.49
152 (cathode)	24.187	50.926	43.927	35.46
21 (cathode)	24.774	50.734	43.860	36.02

Energy Consumption and Dewatering Efficiency

The energy consumption and dewatering efficiency data for Test 11 is as follows:

$P = VI$
$= 10 \times 0.05 = 5 \times 10^{-4}$ kW

$E_u = (\int VI\, dt) / V_s = VI (t_2 - t_1) / V_s$
$= 5 \times 10^{-4} (144.46) / 74.485 \times 10^{-4} = 9.70$ kWh/m^3

Dewatering Efficiency = Total amount of water / It
= 341.37 / 0.05 x 144.46 = 47.26 ml/Ah

TEST 12

- Test and Control Box

The test box has a length of 30 cm and width of 20 cm. Its mass is 2 935.4 g. Mass of the test box + mass of electrodes = 4 236.5 g. Mass of the test box + mass of electrodes + wet mass of sample = 14 754.3 g
Mass of control box = 62.8 g. Mass of control box + wet mass of sample = 2 126.9 g

- Volume of Sample

The total volume of sample used in the test box is 75.897 x 10^{-4} m^3.

- Voltage and Current

Again 10 volts were applied to the test and the DC source read 0.06 amperes for current.

Table D56 Initial Water Content

Container N0.	Mass of Container (g)	Mass of Container + Mass of Wet Sample (g)	Mass of Container + Dry Mass of Sample (g)	Individual Water Content (%)
2	24.506	50.921	40.604	64.09
7	25.218	50.879	40.593	66.90
12	24.733	50.725	40.569	64.13
18	25.014	50.738	40.651	64.51
Average Initial Water Content (%) for the Sample				**64.91**

Table D57 Amount of Water Removed from Sample

Time Elapsed (hours)	Water Removed (ml)	Cumulative Water (ml)
22.35	110.27	110.27
25.41	38.95	149.22
47.26	79.38	228.60
51.33	37.11	265.71
70.12	49.12	314.83
76.57	15.24	330.07
96.13	14.38	344.45
105.42	7.87	352.32
129.42	3.21	355.53
153.42	1.25	356.78

Table D58 Variation in Moisture Content

Time Elapsed (hours)	Moisture Content (%)
0	64.91 (initial water content)
22.35	58.68
25.41	56.27
47.26	50.39
51.33	47.95
70.12	43.38
76.57	42.67
96.13	41.59
105.42	39.64
129.42	38.96
153.42	36.51

Table D59 Changes in pH and Conductivity Measurements during Test

Time (hours)	pH	Conductivity (mS/cm)
0	12.40	7.66
22.35	12.41	7.66
25.41	12.42	7.67
47.26	12.56	7.99
51.33	12.56	7.56
70.12	12.57	7.55
76.57	12.57	7.55
96.13	12.56	7.56
105.42	12.56	7.57

Table D60 Variation in Final Moisture Content

Container No.	Mass of Container (g)	Wet Mass + Mass of Container (g)	Dry Mass + Mass of Container (g)	Final Moisture Content (%)
58 (anode)	24.486	50.238	43.623	34.57
15 (anode)	24.928	50.854	44.041	35.65
21 (center)	24.774	50.654	44.012	34.53
19 (center)	24.680	50.396	43.896	33.83
59 (cathode)	24.648	50.137	43.101	38.13
8 (cathode)	24.738	50.269	43.127	38.84

Energy Consumption and Dewatering Efficiency

The energy consumption and dewatering efficiency data for Test 12 is calculated as follows:

$P = VI$
$= 10 \times 0.06 = 6 \times 10^{-4}$ kW

$E_u = (\int VI\, dt) / V_s = VI (t_2 - t_1) / V_s$
$= 6 \times 10^{-4} (153.42) / 75.897 \times 10^{-4} = 12.13$ kWh/m^3

Dewatering Efficiency = Total amount of water / It
= 356.78 / 0.06 x 153.42 = 38.76 ml/Ah

8 REFERENCES

1. Adams, R. A. and Bollinger, J. M. (1983) In: K. Osseo-Asare and J. D. Miller (eds.), *Proceedings of the 3rd International Symposium Hydrometallurgy, AIME,* Atlanta, pp. 449.

2. Balkau, F. (1998) Environmental Issues In Tailings Management. *United Nations Environment Programme, Industry and Environment* (UNEP IE).

3. Dentel, S. K., Abu-Orf, M. M. and Walker, C.A. (2000) Optimization of Slurry Flocculation and Dewatering based on Electrokinetic and Rheological Phenomena. *Chemical Engineering Journal*. Vol. 80, Issues 1 – 3, pp. 65- 72.

4. Environmental Mining Council of British Columbia, (2004). Acid Mine Drainage: Mining and Water Pollution Issues In BC. INTERNET. (http://www.miningwatch.org/emcbc/publications/amd_water.htm) Cited 12 November 2004.

5. Fowler, J. and Trainer, E. (1997). Dewatering sewage sludge with geotextile tubes. *Geotechnical Fabrics Report.*

6. Freeman, M. P. (1982) Chemical Engineering Programme, no. 78, pp. 74.

7. Financial Post, November 17, 1994

8. Gawu, S. K. Y. (2003). PhD Thesis. Characterizing high-density thickened tailings for sound environmental surface placement. Johannesburg.

9. Gilles, C. (1996) *Canadian Minerals Yearbook 1995*, Natural Resources Canada, Ottawa, pp. 28

10. Huerta, A., Kriegsmann, G. A., and Kriezek, R.J. (1988) Permeability and compression of slurries from seepage induced consolidation. *Journal of Geotechnical Engineering*, ASCE, vol. 114, pp. 614- 627.

11. Johns, D.G. (2005) Electroosmotic Dewatering of Mine Tailings. *Jones & Wagener Consulting Civil Engineers.*

12. Jones, C.J.F.P. and Shim, G.S.C. Consolidation trial using Electrokinetic Geosynthetic Electrodes. University of Newcastle upon Tyne. *Research Report No. 010/01*

13. Kanda, H. (1997) Based on "The Institute of Applied Energy, *New Energy Perspective Lowgrade Coal Reforming Technology*." Chemical Engineering Department, Yokusuka Research Laboratory.

14. Lindsay, W. L. (1979) Chemical equilibria in soils. John Wiley & Sons, New York.

15. Lockhart, N. C. (1981). Clays Clay Minerals, vol. 29, pp. 413 and 423

16. Lockhart, N.C. and Stickland, R. E. (1984) Dewatering Coal Washery Tailings Ponds by Electro-osmosis. CSIRO Institute of Energy and Earth Resources, *Physical Technology Unit. Powder Technology*, vol. 40, pp. 215 – 221

17. Lockhart, N. C. (1983). *Powder Technology*, 35, pp 17

18. Lockhart, N. C., (1986) Electro-dewatering of fine suspensions. *Advances in Solid-Liquid Separation*, pp. 241- 274.

19. McVay, M., Townsend, F., and Bloomquist, D. (1986) Quiscent consolidation of phosphate waste clays. *Journal of Geotechnical Engineering*, ASCE, vol. 112, Issue 11, pp. 1033- 1049.

20. Newman, P. (2003). Geotextile bags for the containment, filtering and decontamination of slurries. In: *Geosynthetics: Protecting the Environment*, Thomas Telford, London.

21. Newman, P., Hodgson, M., and Rosselot, E. (2003). The disposal of tailings and mine water sludge using geotextile dewatering techniques. *Processing and disposal of Minerals Industry waste*. Minerals Engineering. Volume 17, Issue 2, pp. 115 - 121.

22. Pearse, T.D. (1996) Pearse Resource Consulting, "*Mining and the Environment*," pp. 14.

23. Price, B. and Errington, J. (1997) Draft Guidelines for Metal Leaching and Acid Rock Drainage at Mine Sites in BC, MEI, Victoria

24. Raats, M. H. M., van Diemen, A. J. G., Laven, J. and Stein, H. N. (2002). Full Scale electrokinetic dewatering of waste sludge. *Colloids and Surfaces: A Physicochemical and Engineering Aspects*. vol. 210, Issue 2-3, pp. 231 – 241.

25. Shang, J.Q. (1997). Electrokinetic dewatering of clay slurries as engineered soil covers. The University of Western Ontario, London, ON N6A 5B9, *Canadian Geotechnical Journal*, vol. 34, pp. 78 - 86.

26. Shang, J.Q., Lo, K.Y. and Huang, K.M. (1996) Effects of voltage gradient and polarity reversal on Electro-osmotic consolidation. *Proceedings, 2nd International conference on Soft Soil Engineering*, Nanjing, China

27. Shang, J. Q. and Lo, K. Y. (1998). Electrokinetic dewatering of a phosphate clay. Faculty of Engineering Science, The University of Western Ontario, London, Ont., Canada N6A 5B9

28. Sunderland, J. G. and Ellis, D. (1976). *NTIS PB Report 276411*.

29. Sunderland, J. G. and Ellis, D. (1977). *NTIS PB Report 276412*.

30. Sprute, R. H., and Kelsh, D. J. (1980) Dewatering of fine-particle suspensions with direct current. *Proceedings of the International Symposium of fine Particle Processing*, Las Vegas, Nev., vol. 2, pp. 1828- 1844.

31. Sprute, R. H., and Kelsh, D. J. (1975) Electrokinetic densification of hydraulic backfill- a field test. *United States Bureau of Mines, Report of Investigations 8075*.

32. The Energy Conservation Center (ECC) 1993. Output of a Seminar on Energy Conservation in Paper and Pulp Industry: Japan. Handy Manual.

33. Yoshida, H. I. (2000). Electro-Osmotic Dewatering under Intermittent Power Application by Rectification of A.C. Electric Field. *Research Paper. Department of Materials Chemistry and Bioengineering, Oyama National College of Technology, Oyama 323-0806, Japan.* Journal of Chemical Engineering of Japan, Vol. 33, No. 1, pp. 134–140.

34. Yuan, C. and Weng, C. (2002) Sludge dewatering by electrokinetic technique: effect of processing time and potential gradient. Taiwan, ROC.

35. Yuan, C., and Weng, C. (2003). Sludge dewatering by electrokinetic technique: effect of processing time and potential gradient. *Advances in Environmental Research*, May 2003, vol. 7, no. 3, pp. 727-732(6). Elsevier Science.